Vascular abnormalities of cerebral arteries and penetrating arterioles during hypertension and heart failure

by

Crystal May R. Acosta

A Thesis submitted to the Faculty of Graduate Studies of

The University of Manitoba

in partial fulfillment of the requirements for the degree of

DOCTOR OF PHILOSOPHY

Department of Pharmacology & Therapeutics

University of Manitoba

Winnipeg

ABSTRACT

Hypertension increases resistance to blood flow and compromises the vasculature. Chronically elevated blood pressure is antecedent to heart failure and both are associated with the development of cognitive decline and dementia. Thus, we sought to examine the cerebrovascular effects of hypertension alone and with predisposition for heart failure. Using pressurized cerebral vessels isolated from animals with genetic hypertension, we investigated structural, mechanical and functional properties by pressure myography. Structural and mechanical parameters were calculated using media and lumen dimensions measured at constant or incremental intraluminal pressures, respectively. Middle cerebral arteries (MCA) from spontaneously hypertensive heart failure (SHHF) rats underwent a combination of growth and remodeling, exhibited greater wall component stiffness and were less compliant. Studies suggest resveratrol may be beneficial for the treatment of hypertension. Therefore, we investigated the effects of resveratrol and two structural analogs on abnormal MCA. Vascular hypertrophy and wall component stiffness improved with oral doses (2.5 mg/kg/d) of resveratrol, pterostilbene and gnetol, albeit in the absence of blood pressure lowering. This indicates these stilbenoids act directly on the vascular wall. Findings in MCA led to further examination of downstream penetrating arterioles that regulate cerebral perfusion. SHHF penetrating arterioles exhibited eutrophic remodeling, increased stiffness and reduced compliance. Although eutrophic remodeling was similarly observed in spontaneously hypertensive rats (SHR), penetrating arterioles were less stiff and more compliant. Transmission electron microscopy revealed increased collagen deposition in arterioles from SHHF rats consistent with reduced compliance. Whereas, SHR arterioles had unchanged collagen/elastin ratio. Functional responses were evaluated using pharmacological agents that were bath applied to penetrating arterioles in increasing concentrations. Relaxation to glutamate/D-serine was reduced in SHHF rats but not in SHR. In contrast, acetylcholine-mediated

relaxation was potentiated in SHR but maintained in SHHF rats. Interestingly, endothelium-independent relaxation to nitric oxide donor, sodium nitroprusside, resulted in constriction in both hypertensive strains. These findings suggest penetrating arterioles undergo some adaptations in hypertension, which are absent when there is a propensity for developing heart failure. Altogether, this is the first to identify and characterize the cerebrovascular abnormalities in MCA and penetrating arterioles in models of hypertension alone and with risk for heart failure.

First and foremost, I thank my thesis advisor, Dr. Hope Anderson, and co-advisor, Dr. Chris Anderson. I am grateful for their various roles that have led to the successful completion of my PhD – thank you for your part in my journey. I wish to thank my Advisory Committee members, Dr. Sari Hannila and Dr. Grant Pierce for providing insightful suggestions and discussions about my research.

I'm thankful to my fellow graduate students, as well as past and present members of the Neuroscience Research Program at the Kleysen Institute for Advanced Medicine and the Canadian Centre for Agri-Food Research in Health and Medicine of St. Boniface Hospital Research for being a source of friendship, advice, training and collaboration.

This journey would not have been possible without a good support system. To my family, thank you for allowing me to carve out my own path and at my own pace. To my mentors, thank you for sharing your wisdom and making me a better trainee. To my friends, thank you for encouraging me in all my pursuits and keeping me sane throughout grad school.

This work was supported in part by the Manitoba Health Research Council (MHRC), University of Manitoba Graduate Fellowship (UMGF), JG Fletcher PhD Fellowship, JH Stewart Reid Memorial Fellowship, Smerchanski Endowed Studentship Grant, Leslie F. Buggey Award and the Dr. Mark Nickerson Graduate Entrance Scholarship in Pharmacology & Therapeutics. I gratefully acknowledge these funding sources among others for making my PhD possible.

LIST OF APPENDICES

ANG II	angiotensin II
AMPAR	α-amino-3-hydroxy-5-methyl-4-isoxazole propionate receptors
AMPK	AMP-activated protein kinase
BP	blood pressure
CBF	cerebral blood flow
cGMP	cyclic GMP
CSA	cross-sectional area
Cx	connexin
DAG	diacylglycerol
DOX	doxorubicin
EC	endothelial cells
ECM	extracellular matrix
EET	epoxyeicosatrienoic acids
eNOS	endothelial nitric oxide synthase
ERK	extracellular signal-regulated kinase
GPCR	G-protein coupled receptor
IP_3	inositol triphosphate
MMP	matrix metalloproteinases
MCA	middle cerebral arteries
M/L	media/lumen
NFκB	nuclear factor-kappa B
NMDAR	N-methyl-D-aspartate receptors
NO	nitric oxide

PDGF	platelet-derived growth factor
PKC	protein kinase C
PPAR	peroxisome proliferator-activated receptors
SIRT	sirtuin
sGC	soluble guanylyl cyclase
SD	Sprague Dawley
SHHF	spontaneously hypertensive heart failure rats
SHR	spontaneously hypertensive rats
SHRSP	stroke-prone spontaneously hypertensive rats
TGF-β	transforming growth factor-β
TIMP	tissue inhibitors of MMP
TNF-α	tumour necrosis factor-α
VSMC	vascular smooth muscle cells

1 Introduction

The brain is one of the most highly perfused bodily organs. While it represents only 2% of total body weight, it receives 15% of the total cardiac output and 10% of the total blood supply to the body.[1, 2] However, despite being one of the most important and complex organs, our understanding of the effects of hypertension on the cerebrovascular bed is lacking.

Hypertension is clinically diagnosed as chronic elevations in blood pressure (BP) above 140/90 mm Hg (i.e. systolic/diastolic).[3, 4] It increases vascular resistance[5, 6] and leads to changes in the heart and the systemic microcirculation over time. High BP increases the resistance against which the heart must pump, and the walls thicken to compensate for the increased workload. Indeed, one of the most common adaptations to hypertension is left ventricular hypertrophy, which is associated with an increase in cardiomyocyte size, hypertrophy and hyperplasia of fibroblasts, collagen accumulation, and infiltration of monocytes and lymphocytes.[7] However, ventricular hypertrophy is also regarded as a pathological hallmark of hypertension and a common example of hypertensive end-organ damage. Although the development of ventricular hypertrophy is for a time compensatory, eventually failure occurs resulting in decompensation and the onset of heart failure. Importantly, hypertension is antecedent in 75% of patients with heart failure;[8] the risk for heart failure in hypertensive patients is 2-fold in men and 3-fold in women, and is associated with low survival rates.[9] Hypertension also elicits structural modifications in the systemic microcirculation that lead to a smaller lumen diameter.[10, 11] Such alterations perpetuate elevated vascular resistance and contribute to the pathogenesis of hypertension.

Recently hypertension has been recognized as an important risk factor for the development of cognitive decline and dementia.[12-15] In turn, heart failure increases the risk of cognitive decline[16] and promotes the progression to dementia and Alzheimer disease.[17] Given that both hypertension and Alzheimer are highly prevalent in the general population, this emphasizes the importance of examining the cerebrovascular changes that develop in response to chronic elevations in BP. However, while our efforts to understand the impact of hypertension on the brain remains ongoing, the contribution of heart failure risk remains unknown.

This thesis addresses two major knowledge gaps: 1) what vascular transformations occur at different levels of the cerebrovasculature (resistance arteries vs. arterioles) in response to longstanding hypertension with risk for heart failure and 2) the effects of stilbenoid treatment on the vasculature. In this thesis two (2) brain vessel types were examined. Initial studies focused on superficial cerebral arteries, namely middle cerebral arteries (MCA). Structural and mechanical changes were characterized in MCA from spontaneously hypertensive heart failure (SHHF) rats using ex vivo analysis by pressure myography. These animals were treated with resveratrol and two structural analogs (gnetol and pterostilbene) to determine effects on BP and arterial properties. The focus then turned towards penetrating arterioles. Structural, mechanical, and functional properties were characterized in penetrating vessels from spontaneously hypertensive (SHR) and SHHF rats. Considering the deleterious effects of hypertension and heart failure on cognition, these studies provide valuable insight into the vascular mechanisms that may predispose hypertensive and heart failure patients to cognitive decline.

1.1 Background & literature overview

1.1.1 Resistance arteries determine vascular resistance and blood flow

Total peripheral resistance is the resistance against which blood is pushed through the entire systemic circulatory system to generate BP and flow. The greatest resistance to flow occurs at the level of the small arteries (lumen diameters of 150 – 300 μm) and arterioles (<150 μm in lumen diameter).[18] The latter are estimated to generate 45-50% of the total peripheral resistance.[18-22] By comparison the capillaries (~7 μm) account for 23 – 30% of total peripheral resistance.[22] Although an individual capillary has a smaller diameter, the total cross-sectional area of the capillary bed is greater than that of any other vessel type such that resistance is dissipated across the capillary network. Mean arterial pressure decreases as blood flows from arteries to veins, with the greatest drop in pressure occurring between arteries and arterioles. Small arteries contribute 40% of the pre-capillary pressure drop, while arterioles contribute 30%.[18] As the sites of the most precipitous pressure drop, small arteries and arterioles are the main regulators of vascular resistance and are given the term resistance arteries. These vessels are thought to be between 15 – 300 μm.[23]

If considered a closed system, the resistance of the circulatory system can be determined through the viscosity of blood and vessel dimension by way of **Poiseuille's law of resistance**:

$$\boldsymbol{R} \propto \frac{\boldsymbol{8L}\,\eta}{\boldsymbol{\pi r^4}}$$

- R is the resistance of blood flow
- L is the length of the vessel

- η is the viscosity of blood
- r is the radius of the blood vessel

This law describes the resistance ***R*** to the flow of blood having viscosity $\boldsymbol{\eta}$ through a lumen with radius ***r*** and length **L.** Viscosity is the inherent resistance of a fluid to flow. As such, the viscosity of blood represents an intrinsic resistance to blood flow and describes the consistency (stickiness and thickness) of blood. The major determinants of blood viscosity are hematocrit (percent volume of erythrocytes or red blood cells), plasma protein concentration, as well as the size, shape and deformability of erythrocytes.[24] These remain constant in a healthy individual; therefore, blood viscosity tends to also remain constant, but can change with respect to changes in flow velocity (shear rate) and lumen diameter. Since the length of a given vessel also remains constant, resistance is dependent mostly on the radius of the blood vessel. When pressure is considered, blood velocity or flow can be determined using **Poiseuille's equation**:

$$\boldsymbol{F} \propto \frac{\boldsymbol{\pi r^4 \Delta P}}{\boldsymbol{8L}\,\eta} = \frac{\boldsymbol{\Delta P}}{\boldsymbol{R}}$$

- F is the blood flow
- ΔP is the pressure difference

This equation describes the relationship between blood flow ***F,*** resistance ***R***, radius ***r***, and pressure ***P***. This relationship shows that the arterial radius plays an important role in determining resistance and blood flow. Accordingly, vascular resistance is inversely proportional to the arterial lumen radius and therefore increases as the lumen narrows. This equation also shows that slight changes

in the lumen radius of resistance arteries can have significant effects on total peripheral resistance and blood flow because as the vessel dilates (lumen radius increases) or constricts (lumen radius decreases) the resistance is divided by this change to the fourth power (Figure 1). Therefore, an artery constricting to half of its initial radius would increase resistance by sixteen-fold. In the brain, cerebral blood flow (CBF) remains the same with changes in blood viscosity if blood vessels are able to compensate for changes in viscosity by dilation (increased viscosity) and vasoconstriction (decreased viscosity).[25]

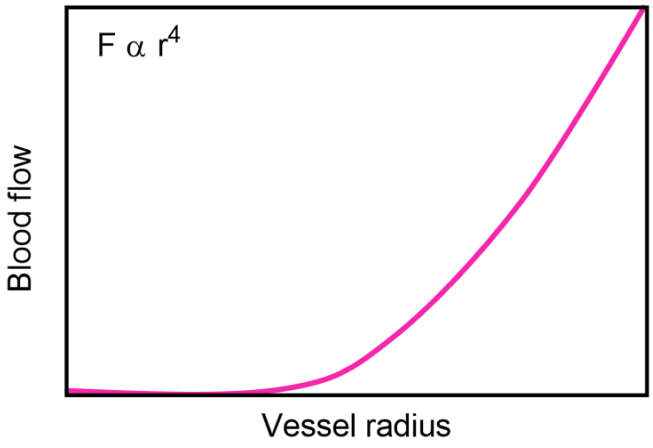

Figure 1. The relationship between blood flow and radius according to Poiseuille's equation. Slight changes in vessel diameter cause drastic changes in blood flow; the change is proportional to the change in radius to the fourth power. F, blood flow and r, radius. Adapted from *Determinants of Resistance to Flow (Poiseuille's Equation)* by R.E. Klabunde, 2017: [26] https://www.cvphysiology.com/Hemodynamics/H003

1.1.2 Hypertensive vascular modifications that contribute to a smaller lumen

There are three major vascular modifications that might reduce lumen diameter and contribute to the pathogenesis and maintenance of hypertension. These modifications are related to:

a) Structure and geometry

b) Biomechanical behaviour

c) Vascular function

In hypertensive patients and various experimental animal models of hypertension, peripheral resistance arteries and arterioles have been shown to exhibit varying forms of remodeling,[27-30] vascular stiffness,[31, 32] and vascular dysfunction.[33] Thus, characterization of the structural, mechanical (stiffness), and functional changes in the cerebrovasculature is crucial to better understand the vascular mechanisms that might leave the brain at risk for damage related to hypertension.

a) Vascular remodeling contributes to structural changes

The vascular wall is subjected to two major mechanical forces: shear stress due to blood flow and mechanical stretch (circumferential stress) due to BP. Shear stress is the force per unit area created when the frictional force of blood acts on to the vessel wall[34] and is experienced directly by the endothelium. Endothelial cells (EC) subjected to shear stress have been shown to align in the direction of flow.[35] Shear stress is directly proportional to blood flow velocity and blood viscosity, and inversely proportional to vessel radius.[34]

Blood distends the vessel wall by exerting a radial force perpendicular to its surface (mechanical stretch). In turn, the vessel opposes this force by applying circumferential and longitudinal forces, resulting in cellular elongation and alignment perpendicular to the applied force.[36] The Law of LaPlace states that wall tension ***T*** (force per unit length of the vessel wall) is directly proportional to pressure ***P*** across the wall that is due to the flow inside times the arterial radius ***r***:

$$\boldsymbol{T \propto P \times r}$$

- T is tension
- P is the pressure difference
- r is the radius

Thus, for a given pressure, a larger radius is required to withstand greater wall tension. Increased wall tension results from increasing the load on thin-walled arteries. This load is expressed as wall stress ∂, which is the wall tension divided by the wall thickness:

$$\boldsymbol{\sigma \propto \frac{P \times r}{\omega} = \frac{T}{\omega}}$$

- σ is the wall stress
- ω is the wall thickness

Accordingly, the radius and wall thickness are proportional; therefore, for any given pressure an increase in radius would require a proportional increase in wall thickness in order to keep wall

stress constant. Increasing the pressure would therefore require a thicker wall; as pressure increases wall stress would only be maintained or normalized by increasing the thickness of the wall or by reducing the diameter or both. Thus, persistent alterations in haemodynamic forces would invariably change the vessel wall in order to restore normal wall stress.

Structural modifications of resistance arteries are due to the process of *vascular remodeli*ng. Arterial remodeling is a normal physiological response and regarded as a compensatory mechanism, which acts to reduce the stress on the vessel wall.[37] However, in pathological states, such as hypertension, persistent transformations of the vessel wall can become maladaptive. Indeed, it is widely accepted that abnormal small artery structure contributes to hypertension.[38-40] Hence, remodeling is often considered a pathological hallmark of hypertension.

Vascular remodeling is a dynamic process involving different components of the vessel wall, which are divided into three distinct layers (Figure 2): (1) EC of the intima; (2) vascular smooth muscle cells (VSMC) of the media; and (3) fibroblasts and inflammatory cells of the adventitia. These elements are supported by underlying extracellular matrix (ECM) composed mostly of collagen, elastin, fibronectin, proteoglycan, and other macromolecules. The intima, which is the most interior layer, includes an endothelium that lines the lumen and is in direct contact with blood. EC release vasoactive factors, including vasodilators (ex. nitric oxide (NO), prostacyclin, endothelium-derived hyperpolarizing factor) and vasoconstrictors (ex. thromboxane and endothelin-1) that act on VSMC in the medial layer, making them important regulators of vascular tone.[41] The intima also has a subendothelial layer consisting of collagenous bundles, elastic fibrils,

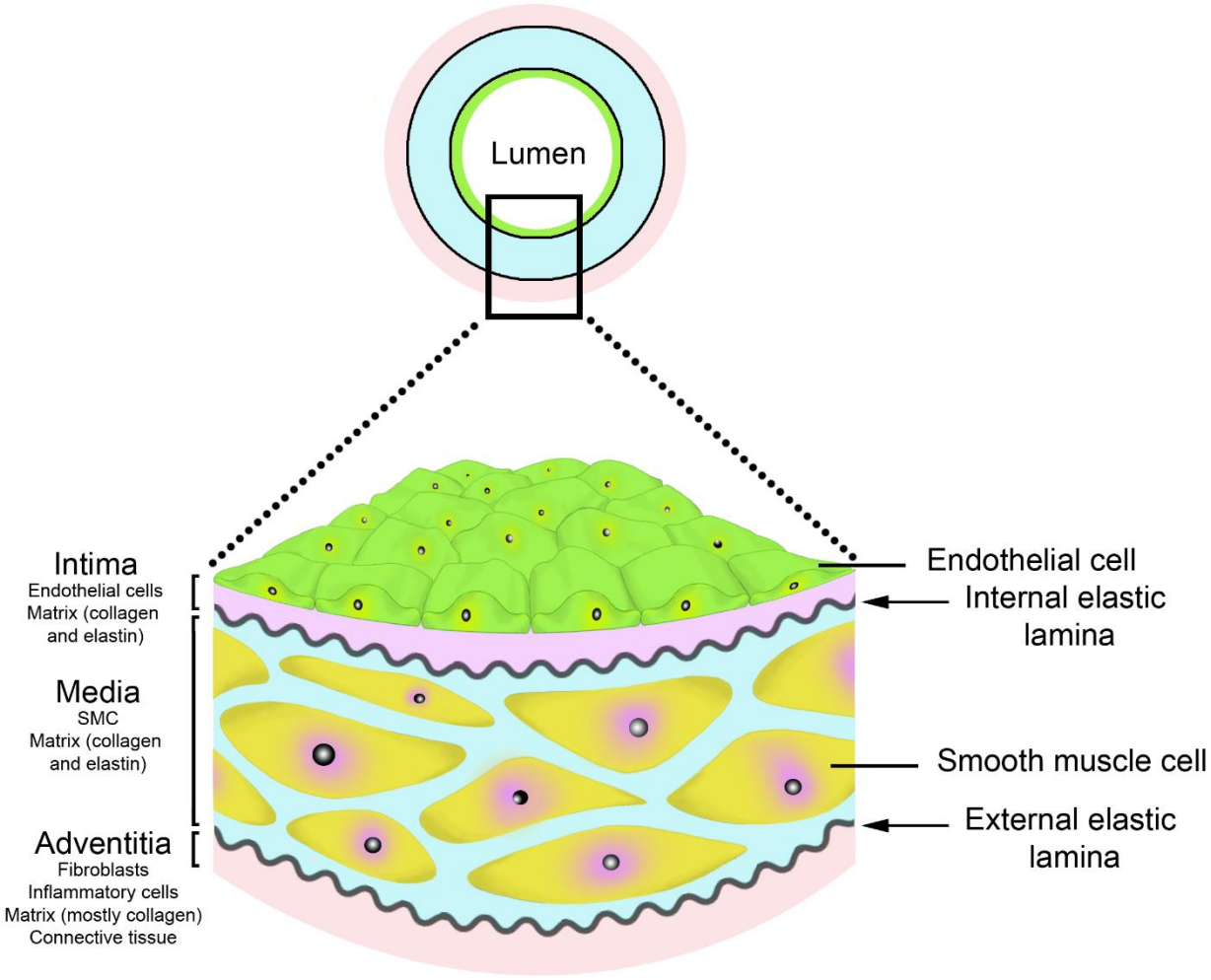

Figure 2. Arterial anatomy. The three distinct layers of the vascular wall are shown with associated cellular and matrix components.

VSMC, and an internal elastic lamina composed of elastic fibres. The media is the most prominent layer of the vessel wall and consists of layers of VSMC, elastic and collagenous fibres, and

external elastic lamina. Contraction and relaxation of VSMC allows vessels to constrict or dilate, respectively. Laminar units are arranged concentrically, are fenestrated and anchored to VSMC.[42] In small vessels, elastin is found mostly in the intimal region and are initially parallel and longitudinally aligned, but deform under pressure (30 mm Hg).[43] Indeed, arterioles have only subendothelial elastic fibres (internal elastic lamina).[44] Fibroblasts and inflammatory cells (mast cells and macrophages) occupy the adventitial layer which consists mostly of collagenous fibres but also elastin, fibroblasts, mast cells, and microphages.

Several processes contribute to vascular remodeling including: VSMC hypertrophy,[45, 46] apoptosis,[47] or a combination of both,[48] hyperplasia;[49, 50] EC dysfunction;[51] and ECM deposition and rearrangement.[31, 48, 52] The term remodeling was first applied to resistance arteries by Baumbach and Heistad, based on observations made in pial arterioles from stroke-prone spontaneously hypertensive rats (SHRSP), to indicate structural rearrangement of existing wall material around a smaller lumen.[53] Since then the nomenclature has changed, taking into account the notion that structural changes do not always involve net growth. As such, there are three major forms of remodeling used to describe structural changes of vessels **(**Figure 3**):**

1) hypertrophic growth

2) eutrophic remodeling

3) hypotrophic remodeling

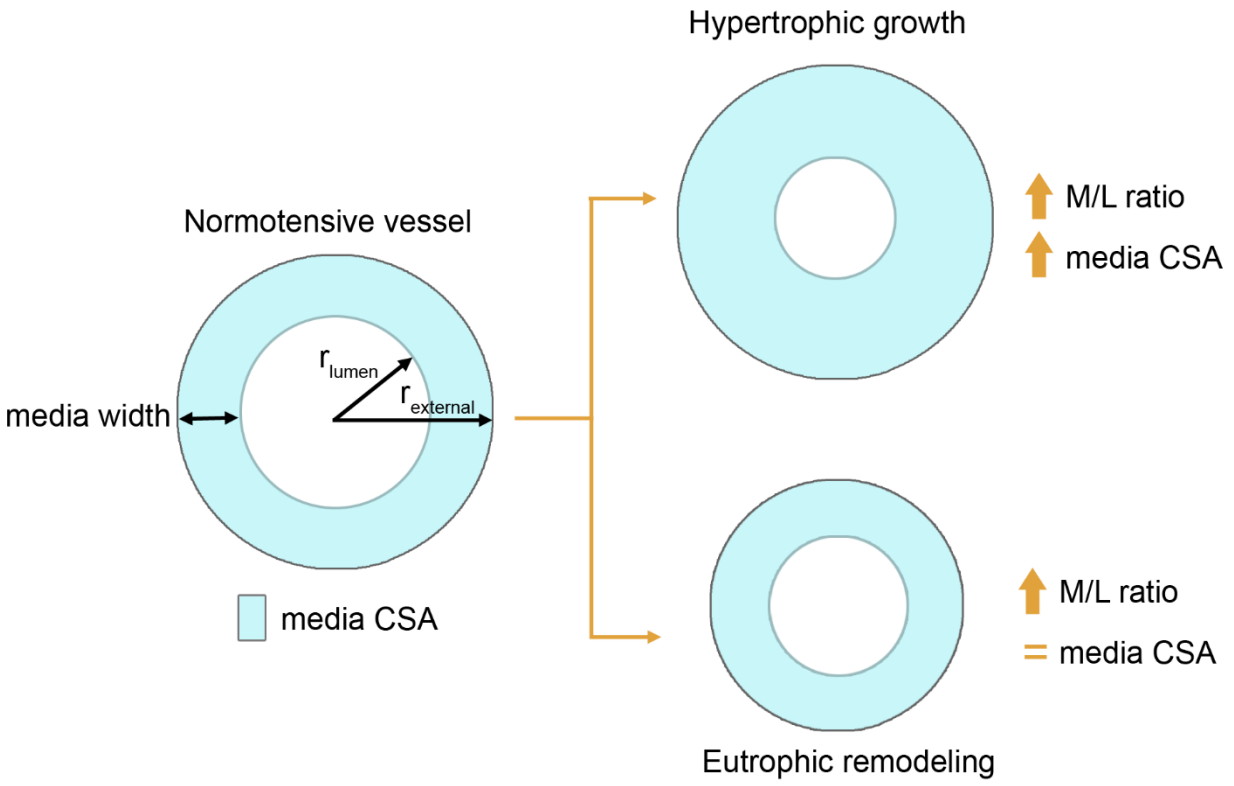

Figure 3. Major forms of arterial remodeling. Arterial remodeling may be categorized in terms of structural changes of the vascular wall. Hypertrophic growth and eutrophic remodeling are both characterized by an increase in M/L ratio and increased or unchanged media CSA, respectively. During hypotrophic remodeling media CSA is decreased (not shown). Remodeling may be further classified according to changes in lumen, where a decrease in lumen size refers to *inward* remodeling. An increase in lumen size denotes *outward* remodeling (not shown).

Remodeling can be *inward* or *outward* depending on whether the lumen diameter is decreased or increased. Inward remodeling denotes a reduction in lumen size, while outward remodeling denotes an increase. Remodeling is categorized as hypertrophic, if there is net growth, and eutrophic, if there is no net growth.[39] Vessels that undergo hypotrophic remodeling exhibit a decrease in the amount of wall material and have a smaller lumen; a reduced media cross-sectional area (CSA).

Hypertrophic growth develops in patients[54] and animal models[46, 55] with secondary hypertension. Growth is characterized by a higher volume of wall material per unit area of vessel such that the media/lumen (M/L) ratio and media CSA are increased.[56] This can be ascribed in part to VSMC hypertrophy and hyperplasia,[10, 31] which leads to thickening of the vessel wall that encroaches on the lumen. Deposition of ECM collagen by VSMC also contributes to a thicker media[57] and fibronectin contributes to vessel wall thickening by enhancing cell proliferation.[58] In essential hypertension, resistance vessels undergo inward eutrophic remodeling.[50, 59] Eutrophic remodeling is characterized by a reduced lumen diameter (increase in M/L ratio) and unaltered media CSA.[56] Thus eutrophic vessels have no net change in vessel wall area. Maintenance of the media CSA in eutrophic remodeling is believed to be attributed to inward growth and rearrangement of VSMC around a smaller lumen and simultaneous cellular apoptosis localized to the outer periphery of the vessel.[47, 48] Increased apoptosis in small arteries has been observed in SHR, at 8 and 12 weeks of age.[47] ECM deposition has also been shown to contribute to eutrophic remodeling.[31, 48] In small arteries from SHR and patients with essential hypertension, collagen,[30, 31] fibronectin[60] and proteoglycan[61] accumulation are significantly increased.

The key regulators of vascular remodeling are VSMC and the ECM. VSMC exhibit a high degree of phenoytypic plasticity[62] and phenotype is determined by biochemical (platelet-derived growth factor, PDGF and transforming growth factor-β, TGF-β), extracellular (collagen, elastin, and matrix metalloproteinases, MMP) and biophysical (blood flow and BP) factors.[63, 64] VSMC display a quiescent contractile phenotype under physiological conditions to facilitate contraction and relaxation important for regulating vascular tone and function. During biological stress or injury VSMC can lose their contractile properties (eg. down-regulation of contractile proteins)[64] and differentiate into an active synthetic phenotype. For instance, shear stress induces the secretion of growth factors, PDGF and TGF-β,[65] which can stimulate phenotypic switching of VSMC. Pro-inflammatory mediators, including TNF-α and interleukin-6, have also been implicated in VSMC activation.[66] Cytokines may also promote VSMC apoptosis during remodeling via death receptors including TNFα receptor.[67] Synthetic VSMC are able to migrate, proliferate, produce ECM proteins and inflammatory cytokines, and promote calcium deposition.[63] Thus, phenotypic switching is an important mechanism underlying vascular remodeling. In SHR, VSMC exhibit a synthetic phenotype; the expression of smooth muscle contractile proteins, α-smooth muscle actin and smooth muscle 22α, were reduced in aorta and cultured VSMC, and this coincided with enhanced proliferation and migration.[68] Migration is a well recognized process in VSMC proliferation and hyperplasia, which are known to contribute to vascular wall thickening. Synthetic VSMC are major producers of ECM proteins including collagen, laminin, fibronectin, and MMP, which promote migration,[69, 70] and can in turn activate VSMC or alter the ECM, thereby influencing remodeling and vascular elasticity. For example, MMP play an important role in matrix composition by modulating ECM degradation[71] to facilitate the reorganization of cells during remodeling. And fibronectin has been shown to promote the synthetic VSMC phenotype

via ERK/MAPK signaling.[72] Adhesion of VSMC to fibronectin anchor it to the matrix and this is regulated by integrins. Integrin-binding promotes migration and is associated with ECM/integrin/focal adhesion sites that also influence vessel elasticity.[73] This underscores the dynamic interaction between VSMC and the ECM and identifies the in-out and out-in cross-talk as an important mechanism for regulating vascular structure, VSMC activity, and stiffness. It should be noted that VSMC senescence can also influence changes in vascular function and remodeling. Scenescent VSMC are cells that can no longer divide, but may also have a secretory phenotype to produce inflammatory mediators, growth factors, and proteases that would likewise drive remodeling and changes in stiffness.[74]

In addition to VSMC hypertrophy/hyperplasia and ECM deposition, endothelial dysfunction contributes to structural changes. Endothelial dysfunction was first recognized in patients with essential hypertension[75] and is now recognized as important component of hypertension irrespective of etiology.[76] Because EC regulate VSMC proliferation,[77, 78] an intact endothelim is required to regulate vascular remodeling. Thus, a disrupted endothelium would invariably lead to abnormal remodeling processes. The endothelium can control vascular remodeling directly through NO, which is important for regulating vascular function. Endothelial dysfunction is associated with impaired vasomotor response (eg. reduced dilation)[75] and while one of the most essential functions of NO is inducing vasodilation, it is also an anti-growth molecule. The absence of endothelial nitric oxide synthase (eNOS) leads to thickening of the vessel wall,[79] which suggests vascular remodeling is in part due to reduced NO availability or signaling. In addition, the endothelium may influence vascular remodeling via inflammatory processes orchestrated by EC to promote VSMC growth and proliferation,[51, 80] rather than having direct actions on VSMC.

b) Changes in the mechanical behaviour of vessels contributes to a smaller lumen

Arterial compliance is an important mechanical property of the vascular wall and is defined as the *absolute* change in volume (ΔV) for any given change in pressure (ΔV/ΔP). It describes the ability of vessels to buffer changes in pressure and the capacitance of a vessel (the volume of blood a vessel can hold at a given pressure). Arterial compliance is determined by both passive vascular structure (original volume) and the distensibility of the vessel (stiffness of the components that make up the arterial wall). Compliance is directly related to distensibility, where compliance is the product of distensibility and volume, C = (D)(V). Distensibility describes the elastic properties of the vessel wall and is the *relative* or fractional change in volume (ΔV/V) for a given change in pressure ([ΔV/V]/ΔP). Thus, compliance and distensibility reflect the elasticity of vessels. They can be measured as changes in lumen CSA rather than volume because arterial length remains relatively constant.[81] Compliance can also be estimated from the stress-strain curve of a vessel. The stress-strain relationship determines the elastic modulus – the mathematical description of stiffness.[82]

Vascular stiffening is a risk factor for future cardiovascular disease,[83] mortality in hypertensive patients,[84] stroke,[85] and dementia.[86] Elevated BP increases the rate of vascular stiffening and the degree of stiffening increases with age.[87] Stiffness is a passive mechanical property of the vessel wall and describes the relationship between changes in volume and pressure. It is the mathematical inverse of compliance and is determined in most part by two ECM proteins – elastin and collagen – that make up the elastic and non-distensible components of the vascular wall. Elastin is the major constituent of elastic fibers that make up the elastic lamina. It is the most abundant ECM protein, comprising more than 50% of the dry weight in large arteries.[88] It provides reversible

elasticity, while collagen provides structural strength[89] and prevents failure at high pressure. The undulating elastic lamina straightens with increasing pressure. At physiological pressures, elastin bears most of the mechanical load; the elastic lamina is mostly straight[90, 91] compared to less than 10% of the collagen fibres.[91, 92] However, at higher pressures the load is carried by more collagen fibres and the stiffness of collagen limits vessel distension.[91]

The relative amounts of elastin and collagen are maintained through processes of protein synthesis and degradation.[93, 94] Although elastin is a highly stable protein, the amount of elastin is essentially finite in the adult. Elastic fibers undergo only a short period of synthesis during development, after which elastinogenesis ceases or falls to undetectable levels.[95] Thus, damaged or fragmented elastic fibres are generally not replaced and instead collagen deposition is favored. Elastin fragmentation was associated with increased collagen production,[96] which was associated with decreased distensibility, increased stiffness, and greater wall stress in SHR and normotensive animals.[97] Increased collagen deposition has been observed in resistance arteries from hypertensive patients[30] and in experimental hypertension.[31]

An increase in collagen relative to elastin shifts vascular mechanics to a stiffer range; as more collagen becomes load-bearing, the less distensible the vessel becomes. Augmented vessel stiffness would lead to a smaller lumen if compliance is reduced since distension would be restricted. In addition, vessel stiffness may *structurally* contribute to a smaller diameter. Elastin deficiency was shown to reduce arterial lumen diameter and induce proliferation and reorganization of VSMC.[98, 99] Indeed, deposition of ECM proteins may contribute to a reduction

in lumen by anchoring VSMC in a chronically constricted vessel such that a smaller lumen persists.[100]

More recently the view that vessel stiffness is due to ECM proteins has been expanded to include VSMC as important components in arterial stiffening with regards to contractility and VSMC-ECM interactions.[101, 102] The endothelium also plays a role in stiffening. NO regulates arterial compliance and elasticity[103] and removal of the vascular endothelium has been shown to augment arterial compliance in normotensive rats and SHR.[104]

c) Vascular dysfunction

Resistance vessels are in a partial state of contraction and can alter their diameter (constrict or dilate) in the face of changing pressure. This myogenic behaviour is due to the inherent ability of VSMC to contract or relax in response to transmural pressure independent of neural, metabolic, and hormonal factors.[105, 106] Tonic contraction is important for blood flow autoregulation and maintaining vascular resistance. Under physiological conditions, CBF is maintained at approximately 50 ml per 100 g of brain tissue per minute.[107] Since changes in BP alter the resistance against which blood flows, assuming Poiseuille's law applies, the vessel diameter must change for CBF to be maintained. This is accomplished by myogenic behaviour which allows cerebral arteries to constrict in response to elevations in pressure and dilate at lower pressures.[108] Thus, a decrease in vessel size would reduce CBF, while an increase in diameter would increase flow. Autoregulation functions across a range of cerebral perfusion pressures between ~60 to 160 mm Hg.[107, 109] At pressures between 120 and 160 mm Hg large cerebral arteries are responsible for

most of the autoregulation.[110] Outside these limits autoregulation is lost. For example, during hypertension myogenic constriction is insufficient to withstand excessive pressures above 160 mm Hg in cerebral arterioles and 200 mm Hg in cerebral arteries, leading to forced dilation.[107, 110] The loss of myogenic control and forced dilation would decrease vascular resistance and lead to uncontrolled increases in CBF.

In general, elevations in intraluminal pressure increase myogenic constriction.[111, 112] In hypertension, calcium-dependent and independent pathways that control contraction and relaxation of VSMC become dysregulated leading to an enhanced contractile state.[112] In SHR vessels, myogenic constriction increases;[113-115] in mesenteric arteries this occurs during the development of hypertension and during established hypertension, but only at high pressures.[116, 117] In the brain, cerebral arteries from hypertensive rats[118] and penetrating arterioles from SHRSP[119] also have enhanced tonic constriction. However, it should be noted that while these serve as evidence to support enhanced vascular tone in hypertension, in some cases a decrease in myogenic response in SHR mesenteric arteries[117] and cerebral arteries[120] have been observed. Reduced endothelium-dependent relaxation can also contribute to increased myogenic constriction. Endothelium-derived NO opposes myogenic constriction and is an important regulator of vascular tone.[41, 121] However, in hypertension this control is lost due to endothelial dysfunction. NO deficiency[122] and increased production of endothelium-derived constrictors are associated with hypertension and lead to enhanced pressure-induced arteriolar constriction.[123, 124] The role of endothelium-derived constricting factors is supported by the fact that in SHR enhanced myogenic constriction was attenuated by removing the endothelium.[123]

Abnormal dynamic response to vasomotor challenge has also been observed. Endothelium-dependent relaxation to an agonist was reduced in SHR arterioles and this was attributed to impaired NO synthesis or action.[125] Vascular stiffening might contribute to this. It has been suggested that stiffening could alter endothelial function; eNOS was activated in EC grown in distensible tubes exposed to pulsatile flow, but not when grown in stiff tubes.[126] This suggests that reduced compliance may lead to impaired NOS activity, which would further promote vascular stiffening.[89] [127] Response to a constrictatory stimulus such as noradrenaline has also been shown to be enhanced in SHR and this was associated with endothelial dysfunction and increased COX-derived constricting prostanoids.[128]

Reduced dynamic responses superimposed upon increased tonic constriction are important functional changes in arteries that would invariably result in a smaller internal diameter. There is evidence to suggest that a hypercontractile state may contribute to vascular remodeling. For instance, chronic vasoconstriction in arterioles leads to progressive inward remodeling resulting in a smaller lumen,[129] and remodeling can be prevented by inhibiting constriction.[129] As mentioned previously, this may be explained by a remodeled matrix where VSMC would be tethered around a constricted lumen.[100] A smaller vessel radius due to changes in geometry and enhanced myogenic tone suggest dysfunctional autoregulation consistent with reductions in resting CBF because flow is proportional to the size of the vessel. In response to elevations in BP, eutrophic remodeling and hypertrophic growth serve to decrease wall tension by reducing the vessel radius, according to the Law of LaPlace. However, a smaller radius would proportionately decrease CBF and as such myogenic response would compensate by increasing the vessel diameter. However, enhanced myogenic tone and/or reduced relaxation/enhanced constriction to

vasomotor challenge would limit the ability of the vessel to autoregulate and normal CBF would not be maintained.

1.1.3 Important resistance arteries in the brain

Blood is directed to the brain via two pairs of major supply arteries; left and right vertebral and internal carotid arteries. Each carotid artery is responsible for providing approximately 40% of the total perfusion requirement of the brain.[1] At the base of the brain, the major supply arteries (carotid and vertebrobasilar) terminate in a unique vascular structure called the Circle of Willis. This vascular manifold creates a network of arteries in the brain that allow for collateral perfusion of the cerebral hemispheres. Three pairs of large arteries branch off the Circle of Willis – the anterior and posterior cerebral arteries, and the MCA – which allows for efficient re-direction of blood. Therefore, blood could be diverted around an occlusion in a segment of the Circle of Willis or one of the major arteries for delivery to brain tissue that would otherwise become ischemic. The MCA is the main blood vessel that supplies the frontal, parietal, and temporal lobes. Unlike large arteries in the periphery, large cerebral arteries and pial arteries have the largest impact on parenchymal blood flow by generating two-thirds of the vascular resistance in the brain,[130, 131] making them important regulators of blood flow in the brain. Parenchymal arterioles and capillaries account for the remaining vascular resistance.[131] The large arteries exit the Circle of Willis and branch into progressively smaller arteries and arterioles along the brain surface. These pial arteries branch into even smaller blood vessels that infiltrate the brain parenchyma and give rise to penetrating arterioles that fill the Virchow-Robin space. These vessels connect the pial vasculature with the capillary beds that perfuse the interior of the brain. There are several features

that make penetrating arterioles unique segments of the cerebrovasculature. First, penetrating arterioles play a more significant role in regulating BP because along with capillaries, they determine ~40% of the total vascular resistance in the brain.[130, 132-135] Second, unlike surface arteries and pial arterioles, penetrating arterioles are not highly branched which allows them to control blood flow to very discrete regions of the cortex and act as a bottleneck to blood flow between the pial vasculature and the capillary bed. Most importantly, penetrating arterioles are enveloped by astrocyte endfeet[136] and they interact with other parenchymal elements including neurons, glial cells, and pericytes to control CBF and the delivery of oxygen and glucose.[137] Direct innervation causes neurotransmitter-mediated vascular responses,[138] and astrocytes can sense neuronal activity to release vasoactive factors that mediate vascular responses.[139-143] The direct action on vascular response is attributed to astrocyte-derived mediators including K^+, D-serine, carbon monoxide, and arachidonic acid metabolites (prostaglandin E_2, epoxyeicosatrienoic acid, and 20-hydroxyeicosatetraenoic acid).[143, 144]

However, penetrating arterioles might be more vulnerable to mechanical stresses caused by hypertension because they branch directly from the large cerebral arteries and Circle of Willis.[145, 146] As a result, the white matter which they supply may experience greater pressure and pulsatility.[146] Indeed, the white matter is the most susceptible brain region to hypoxia due to the watershed effect.[147, 148] Watershed areas of the brain receive blood from two main arterial networks. The junctions between anterior, middle, and posterior cerebral arteries are considered such regions. These watershed zones are highly vulnerable to ischemia/hypoxia because they receive blood from the most distal branches of the arteries (eg. penetrating arterioles) and are therefore likely to become hypoperfused.

1.1.4 The clinical importance of cerebral arteries in cardiovascular disease

While cross-sectional studies examining the relationship between hypertension and cognitive function show heterogenous results,[149] longitudinal studies generally indicate that increases in BP are associated with cognitive impairment.[149] Vascular stiffening also leads to increased pulse pressure, and pulse wave velocity and is associated with cognitive impairment.[150, 151] Indeed, arterial stiffening is a stronger predictor of cognitive decline than BP.[152]

When cognitive performance was compared, hypertensive patients performed more poorly than normotensive individuals in all domains of cognitive function tested, including memory, executive function, and processing speed.[153] Regional CBF is increasingly reduced over time in hypertension and affects different areas of the brain including the cortices and hippocampus.[154] During memory tasks hypertensive individuals have reduced CBF responses compared to healthy subjects.[155] Cognitive decline is also observed with heart failure; the estimated prevalence is between 30 – 80%.[156] In patients with heart failure, grey and white matter damage is related to autonomic, emotional and cognitive deficits,[157] that may be associated with reduced CBF.[158] Hypoperfusion was observed in heart failure patients in cortical and hippocampal brain regions,[158] which are areas also affected in Alzheimer disease.[159] In a rat model, chronic cerebral hypoperfusion led to a decline in learning and memory, which was related to increased amyloid β and amyloid precursor protein deposition in the hippocampus.[160] In humans, this association is less clear; hypoxia-induced protein expression of amyloid β was shown to increase in post mortem brain[161] but amyloid β or tau accumulation did not correlate with reduced CBF when assessed by positron emission tomography.[162]

Antihypertensive treatment is beneficial against cognitive impairment or decline[163-165] and can reduce the risk for Alzheimer in patients with normal cognition and mild cognitive impairment.[166] In turn, treated hypertension is associated with lower Alzheimer disease neuropathology including neuritic plaques and neurofibrillary tangles.[167] Long-term antihypertensive therapy improves CBF and reduces cerebrovascular resistance.[168]

Together these studies suggest hypertension and heart failure-induced changes in CBF play an important role in facilitating cognitive decline and dementia.

1.1.5 Alternative treatment strategies for the treatment of hypertension – stilbenoids

Hypertensive vascular changes are preventable with early treatment using conventional anti-hypertensive drug therapy and can be stopped or reversed with delayed treatment.[169] Medications that lower vascular resistance include beta-blockers,[170] thiazide-type diuretics, calcium-channel blockers, alpha-blockers,[171] angiotensin-converting enzyme inhibitors and angiotensin receptor blockers.[172] However, almost a third of hypertensive patients are resistant to the maximum tolerated dose of combination anti-hypertensive drug therapy.[173, 174] As such, natural health products have been gaining popularity in recent years as alternatives to conventional pharmacotherapies. This includes the use of stilbenoids, which are naturally occurring phenolic compounds, such as resveratrol. Stilbenoids exert various biological activities such as reducing inflammation and oxidative stress, inhibiting platelet activity, lipogenesis, and melanogenesis, protecting against ischemia-reperfusion injury, reducing cellular hypertrophy, glycemic control, neuroprotection, and anticancer effects.[175]

Resveratrol (trans-3,5,4'-trihydroxystilbene) is is widely sold over-the-counter as a natural health supplement. It is found in various plant species including grapes and related products such as red wine.[176] Moderate wine consumption is associated with reduced cardiovascular disease and has been linked to low cardiovascular mortality in France despite a diet high in saturated fats.[177, 178] This so-called French Paradox is purportedly due to the health benefits of resveratrol given the antioxidant effects it has on the cardiovascular system.[179] In recent decades, resveratrol has emerged to possess a wide-array of biological effects against atherosclerosis,[180] hypertension,[181] cancer,[182] obesity,[183] diabetes,[183] stroke,[184] and Alzheimer's disease.[185]

Resveratrol is well-tolerated at high doses (2 g twice daily) with mild gastrointestinal effects in humans[186] but its clinical application remains limited despite its purported therapeutic benefits. Resveratrol is a stilbenoid consisting of two phenol rings linked by an ethylene bond and exists as two geometric isomers – *cis* and *trans* (Figure 4). Most studies have focused on *trans*-resveratrol, which is reported to be the predominant naturally occurring form given it is more sterically stable.[187] Indeed, *cis*-resveratrol is generally low or absent in grapes[188] but might be produced from the *trans*-isomer because varying amounts are present in wine.[189] Although these isomers share some biological effects, *trans*-resveratrol is considered to have greater biological activity.[190] However, due to the photosensitivity of resveratrol, exposure to daylight and UV radiation readily induces isomerization of 60-90% of *trans*-resveratrol to the less bioactive *cis*-isomer.[191, 192] Further, resveratrol is weakly acidic having poor aqueous solubility (0.05 mg/ml).[193] This presents a challenge in drug formulation since poorly soluble drugs require higher doses to reach therapeutic concentrations when taken orally. While the oral absorption of resveratrol is high

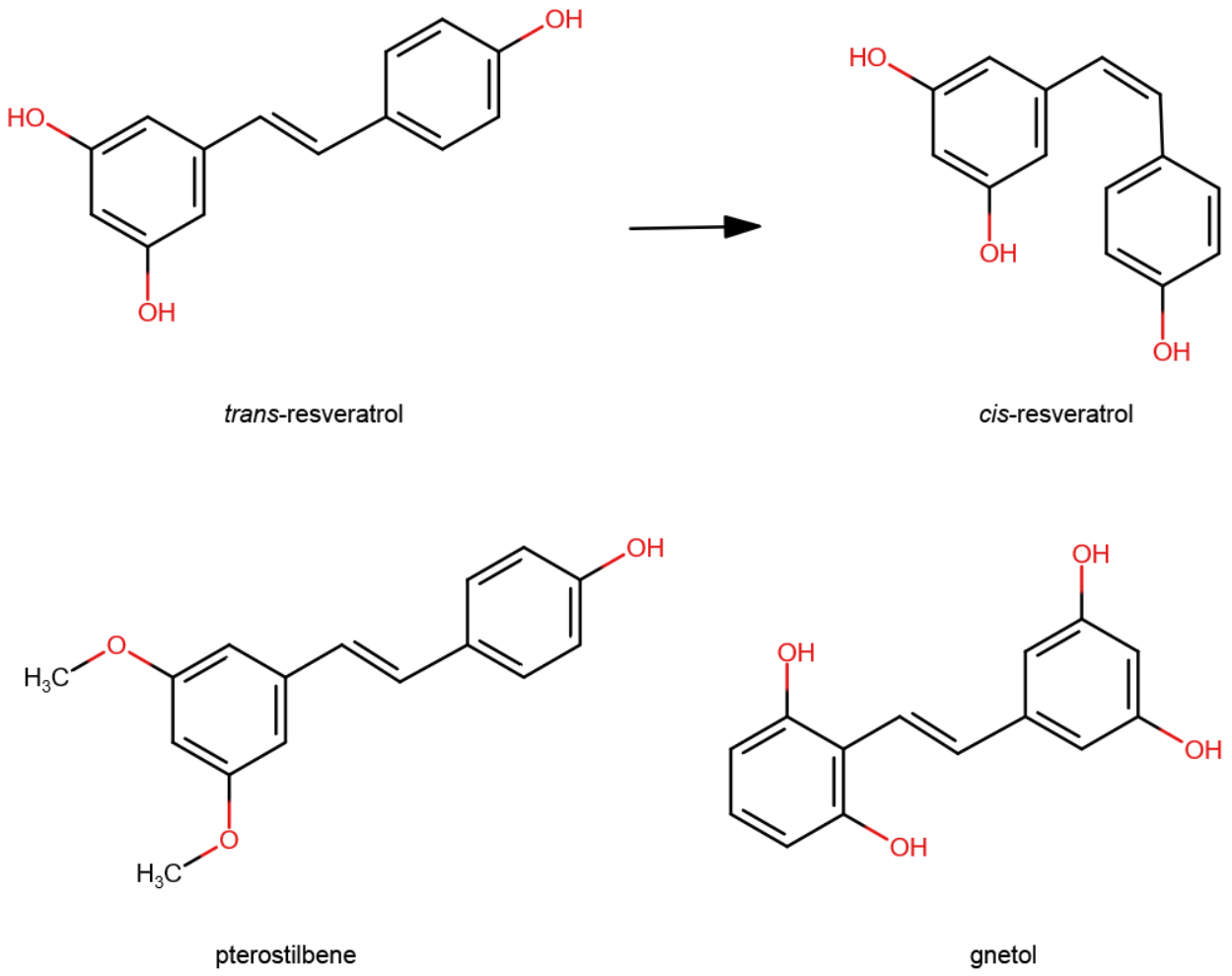

Figure 4. Chemical structures of stilbenoids.

(70%), bioavailability is low (from negligible to 20%)[194-196] because resveratrol is rapidly metabolized (sulfate and glucuronic acid conjugation of the phenol groups and hydrogenation of the double bond)[195] and mostly protein bound (98%).[193] In addition, resveratrol follows first-order degradation and is unstable in human plasma.[193] Indeed, only a low amount of resveratrol is

detectable in the plasma after a high dose (5 g) is administered.[197] It should be noted that this far exceeds the recommended daily allowance of 1 g resveratrol and given that one litre of red wine contains only 2 mg, an annual consumption of 31.7 L (based on reported per capita consumption) would be equivalent to 5000x lower than the recommended dose.[198]

There are a variety of methods that have been proposed to increase the clinical efficacy of resveratrol. The oral bioavailability of resveratrol can be improved using delivery systems like encapsulation into lipid nanocarriers or liposomes, emulsions, micelles, solid dispersions, nanocrystals, and polymeric nanoparticles.[199] These methods enhance solubility, increase stability, prevent degradation, and provide controlled release. Other efforts have focused on co-supplementation with phytochemicals (eg. piperine),[200] utilizing pro-drugs (eg. 3,5,4'-tri-*O*-acetylresveratrol),[201] resveratrol metabolites,[202] glycosylated red grape cell-resveratrol,[203] and alternate routes for administration.[204]

Analogues of resveratrol have also been identified as suitable alternatives to resveratrol treatment. One such naturally occurring compound is pterostilbene (*trans*-3,5-dimethoxy-4'-hydroxystilbene) which is found in blueberries and grapes.[205] It possesses similar biological activity to resveratrol but has a greater pharmacokinetic profile and enhanced pharmacological effects.[206] Pterostilbene is chemically and structurally similar to resveratrol except that it contains two methoxyl groups (-OCH_3) instead of two hydroxyl groups (-OH) (Figure 4). The latter are sites for conjugation (ie. glucuronidation and sulfation) in resveratrol, whereas the methoxyl groups in pterostilbene prevent these reactions. In line with this pterostilbene was determined to undergo less glucuronidation than resveratrol in rat plasma,[196] suggesting pterostilbene has greater

metabolic stability. This may in part explain the prolonged half-life of pterostilbene (105 minutes)[207]which is seven-times greater than the half-life of resveratrol (14 mins).[207] In turn, bioavailability of pterostilbene (80%) is substantially greater with one study approximating it to be 3-4 fold greater than resveratrol.[196] Studies show that pterostilbene is safe for consumption in doses up to 250 mg/day.[208] At this dose pterostilbene was reported to lower both systolic and diastolic BP in patients with high cholesterol; however, participants were allowed to be on other medications.[209]

Another less-known resveratrol derivative is gnetol (*trans*-2,6,3',5'-tetrahydroxystilbene) which is found in several plant species of the genus *Gnetum.* In rats, gnetol is highly distributed but rapidly glucuronidated and has low bioavailability (6%).[210] *In vitro* and *in vivo*, it possesses pharmacological effects similar to resveratrol and pterostilbene.[196, 210, 211] Consumption of seed extracts derived from the melinjo tree (*G. gnemon*) during gestation attenuated hypertension development in the offspring of fructose-fed rats.[212] Interestingly, gnetol inhibits butyrylcholinesterase and acetylcholinesterase,[213] suggesting a potential role for the treatment of Alzheimer disease.

1.2. Research Aims & Objectives

Although the brain is known to be an important target of hypertension, there is a paucity of information related to how the brain vasculature becomes abnormal in the face of high BP. First, while the MCA is one of the most studied vessels in the brain in experimental models of hypertension, including SHR and SHRSP, it has yet to be studied in hypertensive animals also predisposed to developing heart failure, an important cardiovascular disease downstream to the development of hypertension. In addition, the effects of stilbenoid treatment have not been investigated in the brain. Secondly, the most commonly studied vessels in the brain in different experimental models of hypertension are mostly superficial (ie. found on the brain surface). These include large cerebral arteries – basilar and pial arteries, the MCA – and pial arterioles. [214-222] Yet, the penetrating arterioles, which are some of the most important cerebral vessels for regulating brain perfusion have not been widely examined.

This thesis characterizes the hypertensive vascular changes of MCA and penetrating arterioles with respect to structure, mechanical behaviour, and function. This work constitutes 2 major aims:

Aim 1 – To determine the effects of hypertension with risk of heart failure on the vascular properties of MCA in the SHHF rat and to evaluate the effects of stilbenoids.

Objectives:

1. Characterize the structural changes of MCA in SHHF.
2. Characterize the mechanical behaviour of MCA in SHHF.
3. Determine the effects of resveratrol, pterostilbene, and gnetol on BP lowering.

4. Determine the effects of resveratrol, pterostilbene, and gnetol on MCA vascular changes.

Aim 2 – To determine the effects of hypertension alone or with risk of heart failure on the vascular properties of penetrating arterioles.

Objectives:

1. Characterize the structural changes of penetrating arterioles in SHHF and SHR.
2. Characterize the mechanical behaviour of penetrating arterioles in SHHF and SHR.
3. Characterize the functional behaviour of penetrating arterioles in SHHF and SHR.

2 Materials & methods

2.1 Animals

Male Sprague Dawley (SD) rats, phenotypically lean SHHF rats, Wistar-Kyoto (WKY) rats, and SHR were obtained from Charles River (Senneville, Quebec, Canada). The SHHF rat is a genetic model of human hypertension that is characterized initially by spontaneous hypertension at 4 months but further develop symptoms of heart failure, including compensated left ventricular hypertrophy and cardiac remodeling.[223] Progression to mid- and late-stage heart failure in the SHHF rat will occur at 16-18 months.[223] Animals were housed under a 12-h light/dark cycle at 22°C and 60% humidity and fed *ad libitum*. Animal studies were conducted according to guidelines set by the Animal Care Committee of the University of Manitoba and the Canadian Council of Animal Care.

2.1.2 BP measurements

For studies requiring treatment with stilbenoids, 7-week-old SD and SHHF rats were acclimatized for 2 weeks before they were trained for BP measurement using tail cuff plethysmography (CODA non-invasive BP system; Kent Scientific, Torrington, CT). Systolic BP was measured biweekly. For the remainder of studies, systolic BP was measured once in SD, SHHF, WKY and SHR at 17 – 18 weeks of age (4-5 months) using tail cuff plethysmography (Mouse and Rat Tail Cuff BP (MRBP) System; IITC Life Science, Woodland Hills, CA). Rats were placed into MRBP restrainers for two or three days for a period of 20 min/day prior to BP measurements to familiarize rats with the BP testing environment. BP measurements were recorded at least 3 times every 3 –

5 minutes. All acceptable readings were obtained within an hour, after which rats were released from their restrainer to prevent undue stress. Acceptable traces were characterized by an even pattern of rising tail pulses from the point where systolic BP begins to the highest pulse (mean BP).

2.1.2 Stilbenoid treatments

SD and SHHF were treated for 8 weeks by oral gavage once daily with vehicle or low doses of resveratrol, pterostilbene, and gnetol (Sigma Aldrich-Canada, Oakville, ON, Canada; Cayman Chemical, Ann Arbor, MI, USA; and Sabinsa Corporation, East Windsor, NJ, USA). A dose of 2.5 mg/kg/d was selected based on our previous study that showed vascular improvement using low dose resveratrol in SHR.[224]

2.2 Isolation and cannulation of cerebral vessels

Rats were euthanized when they reached 17 – 19 weeks of age by overdose with isoflurane. Heparin (1 ul/g body weight) was injected into the saphenous vein to prevent coagulation of blood in the vasculature. After decapitation a midsagittal cut was made in the cranium and the temporal bones were cut laterally. The dura was removed, and the brain was collected in ice-cold Krebs solution (118 mmol/L NaCl, 4.65 mmol/L KCl, 1.18 mmol/L $MgSO_4$, 1.18 mmol/L $KHPO_3$, 2.5 mmol/L $CaCl_2$, 25 mmol/L $NaHCO_3$, 5.5 mmol/L glucose, 0.026 mmol/L EDTA).

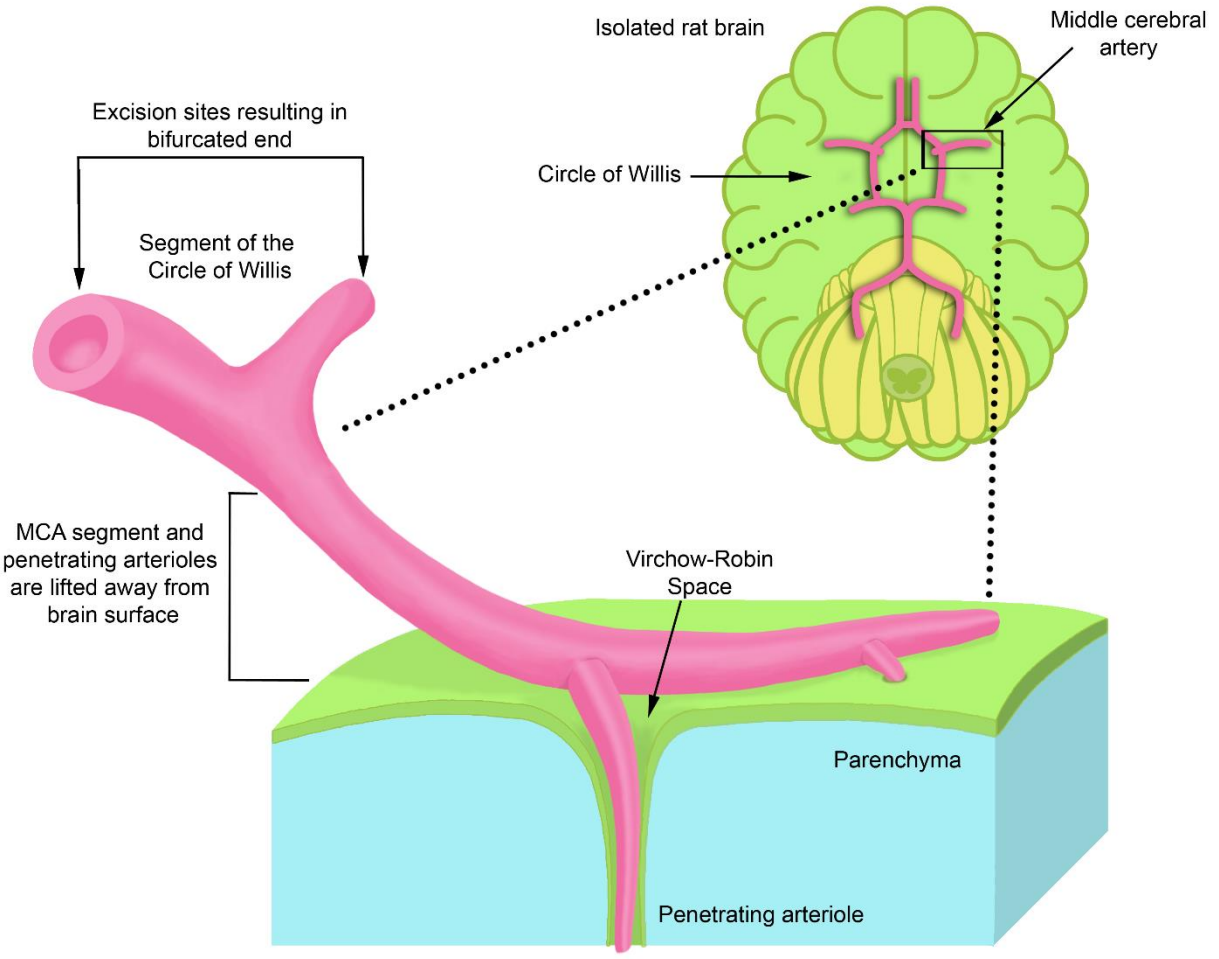

Figure 5. Isolation of the MCA and penetrating arterioles. The MCA was located and cut from the Circle of Willis creating a bifurcated end. The MCA was peeled away from the brain surface and branching penetrating arterioles separated from the brain parenchyma via the Virchow-Robin space and cut below the brain surface. Once a long enough segment could be excised the MCA was cut opposite the bifurcated end to release the vessel.

The MCA was isolated by first cutting the anterior cerebral artery and posterior communicating artery creating a bifurcated end (Figure 5). As the MCA was lifted away from the brain surface, penetrating arterioles that branched from the MCA separated from the brain parenchyma through the Virchow- Robin space. Penetrating arterioles were cut at a point below the brain surface to release the MCA-penetrating arteriole unit. A final cut was made along the length of the MCA to separate it from rest of the vasculature. For MCA studies, penetrating arterioles were cauterized so the vessel could be pressurized. For penetrating arterioles studies, a segment of a penetrating arteriole (500 – 1000 μm) devoid of lateral branches was further excised from the MCA. To maintain consistency and ensure unbiased sampling, only first order penetrating arterioles (those that branch directly off a segment of the MCA) were used. For ease of cannulation, penetrating arterioles were excised with part of the MCA still intact so a bifurcated end would result. This allowed for minimal direct manipulation of penetrating arterioles when cannulating. In some cases, the penetrating arterioles were curved or twisted and had to be excised away from the MCA completely.

Arteries were mounted in a pressure myograph chamber (Living Systems Instrumentation, Burlington, VT) containing Krebs buffer and were studied as a "closed-system" preparation (ie. one end was cannulated and the other was occluded/tied off) with no flow through the system. One end of the vessel was cannulated onto a micro-cannula and was slowly perfused intraluminally with Krebs solution to remove red blood cells. The other end of the vessel was closed-ended (tied onto a micro-cannula without cannulation). Both ends were secured with nylon ties such that the walls were parallel without stretch. For the MCA studies, the entire length of the MCA was cannulated.

2.3 Pressure myography preparation

MCA and penetrating arterioles were allowed to equilibrate for 45 – 60 minutes in aerated (20% O_2 and 5% CO_2) Krebs buffer (pH 7.4; 37°C) at constant intraluminal pressures of 30 and 60 mm Hg, respectively. The diameter after equilibration was defined as the baseline diameter. Viability of MCA were tested using 125 mM KCl and were considered viable if they constricted more than 50% of their baseline diameter. Viablity of penetrating arterioles were tested using $1x10^{10}$ M [Arg^8] vasopressin. Constriction of at least 15% was considered viable. After vessels were tested for viability, they were allowed to equilibrate again in Krebs solution for 30 – 60 mins prior to the start of experiments. The intraluminal perfusate remained unchanged throughout experiments.

2.4 Morphological measurements

Vessels were deactivated by bath perfusion using Ca^{2+}-free Krebs solution (118 mmol/L NaCl, 4.65 mmol/L KCl, 1.18 mmol/L $MgSO_4$, 1.18 mmol/L $KHPO_3$, 25 mmol/L $NaHCO_3$, 5.5 mmol/L glucose, 0.026 mmol/L EDTA) containing a calcium chelator (1 mM EGTA) for 30 - 60 minutes at constant intraluminal pressure. Deactivation removes calcium required for vascular tone and function so that passive arterial/arteriolar properties could be measured. Lumen and media dimensions were measured at three points along the length of the vessels at constant intraluminal pressure.

2.5 Wall composition of penetrating arterioles

After morphometric analysis, to determine the composition of vessel media, deactivated penetrating arterioles (60 mm Hg) were bath-perfused with Ca^{2+}-free Krebs buffer containing 1.5% glutaraldehyde for one hour at room temperature. Following fixation, vessels were washed three times in Ca^{2+}-free Krebs buffer and transferred to 70% ethanol at 4°C for short term storage before being processed. Vessels were post-fixed with 1% osmium tetroxide for 30 minutes at room temperature. Post-fixed arterioles were dehydrated with increasing ethanol concentrations and 100% methanol, and subsequently embedded in Embed 812 resin. Thin sections (70-90 nm) were cut on a Reichert ultrathin microtome. Electron micrograph grids were stained with 2% uranyl acetate for 45 minutes and lead citrate for 10 minutes. Electron micrographs were taken with a Philips CM10 electron microscope at 13,500x and 25,000x. Micrographs were imaged in four quadrants and three images were taken randomly in each quadrant per vessel. The areas occupied by collagen fibres, elastin, matrix and VSMC were measured by tracing regions of interest using ImageJ for collagen/elastin ratio, VSMC area/total medial area and ECM area/total medial area calculations.

2.6 Mechanobiology of cerebral vessels

Deactivated vessels were primed by slowly raising the intraluminal pressure from 3 to 140 mm Hg three times. If a kink developed in the vessel, the cannulae were adjusted so the vessel walls became parallel. The intraluminal pressure was then incrementally increased in 10-steps from 3 to 140 mm Hg. Intraluminal pressure and vessel diameters at three regions of interest along the length the vessels were recorded using IonOptix IonWizard software with VesAcq acquisition

module for vessel diameter, along with the IonOptix VesCam and Data System Interface (IonOptix LLC, Westwood, MA).

2.7 Analysis of mechanical data

The various structural and mechanical parameters were calculated using formulae that are summarized in Appendix A. The M/L ratio was calculated as the ratio of the media width (MW) to lumen diameter (Di). The media CSA, which is the measurement of the amount of vascular media was obtained from the MW and the circumference of the vessel or by subtracting the internal CSA from the external CSA:

$$\boldsymbol{CSA} = \boldsymbol{\pi}\frac{\left(\boldsymbol{D_e}^{\boldsymbol{2}} - \boldsymbol{D_i}^{\boldsymbol{2}}\right)}{\boldsymbol{4}}$$

$\boldsymbol{D_e}$ and $\boldsymbol{D_i}$ are external and lumen diameters, respectively. Arterial diameter (external diameter and lumen), MW, M/L ratio, and media CSA were corrected for body weight differences between SD and SHHF controls. This was done by multiplying the structural parameters with the square-root of the ratio of the SHHF and SD body weights: $(SHHF/SD)^{0.05}$.[31] Therefore, the structural parameters obtained in SD rats were multiplied by a coefficient = 0.82 (average body weights: SHHF – 374.7g, SD – 562.5g) to normalize vascular parameters that might differ significantly due to animal size rather than hypertensive changes. No correction was made between WKY and SHR because body weights were similar.

Media strain, which reflects pressure-induced changes in diameter, was calculated as:

$$\boldsymbol{\varepsilon} = \frac{(\boldsymbol{D} - \boldsymbol{D_o})}{\boldsymbol{D_o}}$$

D is the lumen diameter for a given intraluminal pressure and D_o is the baseline diameter at 3 mm Hg. Media stress was determined by:

$$\sigma = \frac{PD}{2\omega}$$

P is the intraluminal pressure, D is the internal diameter and ω is the media (wall) thickness. Pressure is converted as 1 mm Hg = 1.334 x 10^3 dyn/cm^2. The elastic modulus EM was determined by fitting the stress-strain data to the exponential equation ($y = ae^{bx}$) using least squares analysis:

$$EM = \sigma_O e^{\beta\varepsilon}$$

σ_o is stress at the baseline diameter and β is a constant related to the rate of increase in the stress-strain curve. The slope of the EM versus stress curve reflects the intrinsic stiffness of the wall components.

Remodeling index is the percentage difference in the lumen diameters of hypertensive and normotensive vessels that is due to remodeling:

$$\left[\frac{((D_i)_n - (D_i)_{remodel})}{((D_i)_n - (D_i)_h)}\right] \times 100$$

$(D_i)_n$ and $(D_i)_h$ are mean lumen diameters of normotensive and hypertensive vessels, respectively.

$$(D_i)_{remodel} = \left[\left((D_e)_h^{\,2} - 4 \times {CSA_n}/{\pi}\right)\right]^{0.5}$$

$(D_e)_h$ is the external diameter of hypertensive vessels. Growth index is the percentage of the difference in the lumen diameters of hypertensive and normotensive vessels that is due to hypertrophy:

$$\left[\frac{(\boldsymbol{CSA_h - CSA_n})}{\boldsymbol{CSA_n}}\right] \times \mathbf{100}$$

CSA_n* and *CSA_h are mean media CSAs of normotensive and hypertensive vessels, respectively.

2.8 Functional properties of penetrating arterioles

Arterioles were equilibrated at 60 mm Hg and the diameter measured (D_{eq}). Vessels were then preconstricted with $1x10^{9}$ M [Arg^{8}] vasopressin and were allowed to reach maximal contraction (D_o) before relaxing with agonist. Vascular function was tested with glutamate/D-serine (10^{-7} – 10^{-3}M), acetylcholine (10^{-9}M – 10^{-3}M), and sodium nitroprusside (10^{-9}M – 10^{-4}M) in Krebs with 10^{-9}M [Arg^{8}] vasopressin. Agonists were applied by bath perfusion in increasing concentrations and vessel diameters (D_x) were recorded using IonOptix/VesAcq. Functional responses were calculated in terms of percent diameter change (Figure 6) using the following formulae:

$$\%\,\boldsymbol{response} = \left(\frac{\boldsymbol{D_x - D_o}}{\boldsymbol{D_{eq} - D_o}}\right) \times 100\%$$

- Do is the diameter when preconstricted
- Dx is the diameter when agonist is applied
- Deq is the baseline diameter at 60 mm Hg

A positive value represents a relaxant response. Conversely, a negative value indicates constriction.

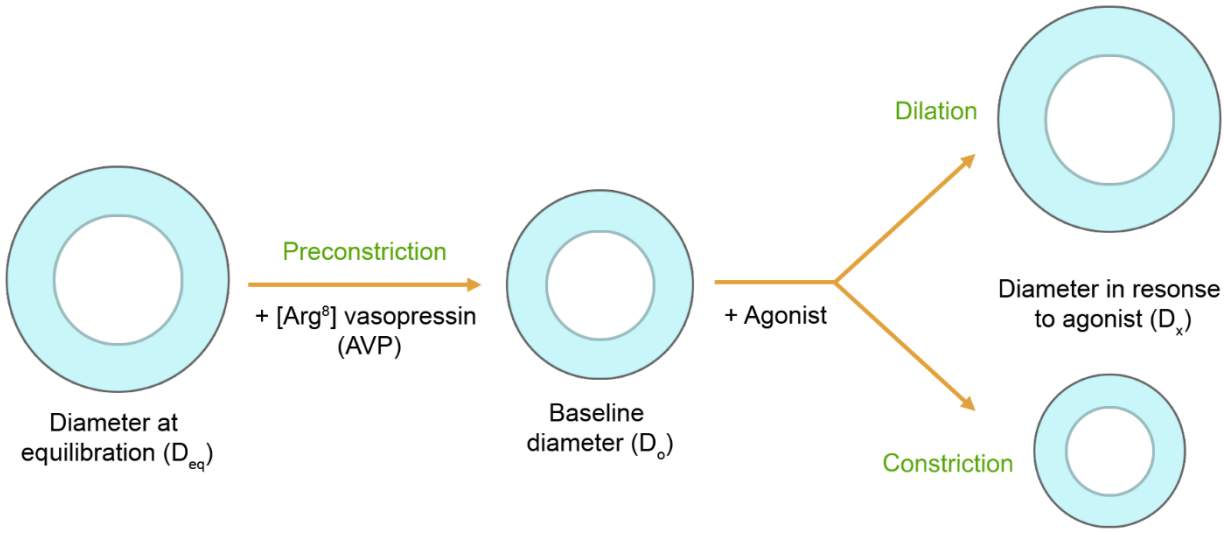

Figure 6. Schematic of functional methodology. Vessels were equilibrated (D_{eq}) at 60 mm Hg and then preconstricted with [Arg^8] vasopressin to increase the dynamic range for vascular response. The diameter when preconstricted was D_o. Afterward, increasing concentrations of glutamate/D-serine, acetylcholine, and sodium nitroprusside were applied to the vessel. The new diameter is D_x.

2.9 Statistical analysis

Results are expressed as mean ± SEM. Statistical differences were evaluated using the following: For the MCA study, one-way analysis of variance (ANOVA) with multiple comparisons (eg. Bonferroni) was used for body weight and geometrical parameters. BP was evaluated by two-way ANOVA. Mechanical properties were analyzed first by non-linear regression (compliance) or

linear regression (stiffness). Non-linear regression was performed using an exponential growth equation and the k-value was used for subsequent analysis using one-way ANOVA with multiple comparisons similar to slope obtained using linear regression analysis. For the penetrating arteriole study t-tests were used to compare weight, BP, geometry, and wall composition. Non-linear (compliance) or linear regression (stiffness) with subsequent t-tests were used for mechanical properties. Functional responses were compared using non-linear regression using best-fit. Value of $p<0.05$ was considered to be significant.

3 Results

3.1 Hypertensive vascular modifications in MCA from SHHF rats

Vascular properties of MCA were characterized and the effect of stilbenoids on hypertension-induced changes were determined. This was conducted as part of a larger study in which the effects of hypertension and predisposition for heart failure were evaluated in the MCA, peripheral arteries (mesenteric resistance arteries) and the heart, in parallel. Only vascular changes observed in the brain are discussed. First, vascular structure and mechanics were characterized in normotensive and SHHF rat arteries. The effects of stilbenoid treatment on BP lowering and vascular changes induced by high BP were then investigated.

3.1.1 Body weight and BP

Mean body weights and BP parameters for SD and SHHF rats were determined and are summarized in Table 1. At 17 weeks of age, SD rats exhibited greater body weights compared to SHHF rats ($p<0.01$ vs. SD; Figure 7A and Table 1). Body weights were not affected by 8-week treatment with resveratrol, pterostilbene, and gnetol (2.5 mg/kg/d). The significant difference in body size was considered in later experiments, where structural parameters were normalized to body size as described in the Methods. SHHF rats exhibited elevated systolic BP (Figure 7B), which was significantly increased at 17 weeks of age ($p<0.01$ vs. SD; Table 1). In SHHF rats, elevated diastolic BP ($p<0.01$ vs. SD) and mean arterial pressure ($p<0.01$ vs. SD) were also observed; however, pulse pressures were similar to SD rats. Stilbenoids did not have any effect on systolic BP or other BP parameters.

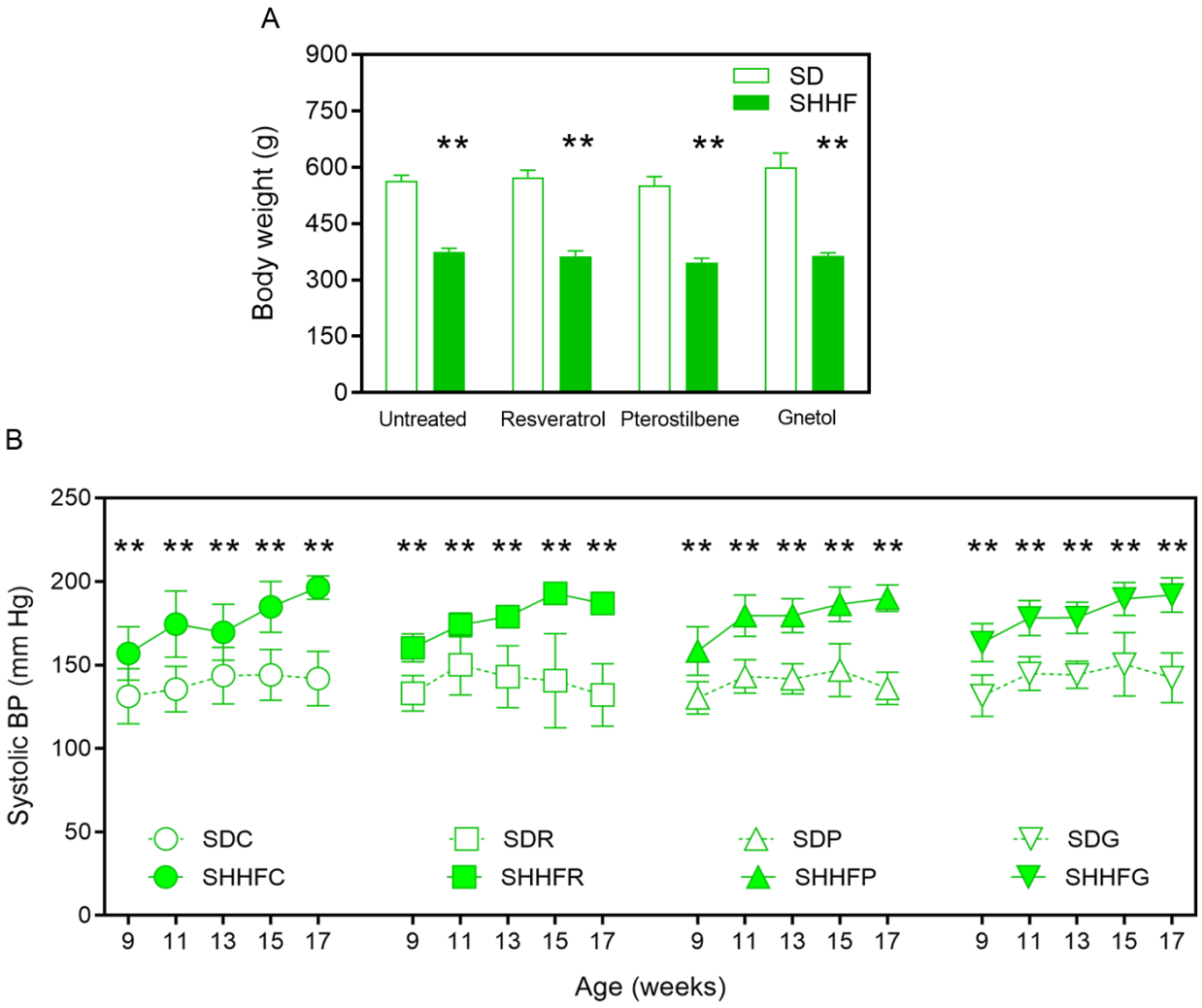

Figure 7. Body weights and 8-week time course of systolic BP of SD and SHHF rats. (A) SHHF rat had significantly smaller body weights than SD rat, which was unaffected by 8-week treatment with resveratrol, pterostilbene, and gnetol (2.5 mg/kg/d). (B) Systolic BP was significantly elevated in SHHF rats. Stilbenoid treatment had no effect on systolic BP. SDC/SHHFC – untreated controls, SDR/SHHFR – resveratrol treated; SDP/SHHFP – pterostilbene treated; and SDG/SHHFG – gnetol treated. Data shown as mean ± SEM. $^{**}p<0.01$ vs. untreated SD. n = 6-8.

Table 1. Summary of body weights and BP parameters in 17-week-old SD and SHHF rats

	SD				SHHF			
	C	**R**	**P**	**G**	**C**	**R**	**P**	**G**
Body weight, g	564±15	574±19	552±24	600±38	375±10**	363±14**	351±12**	364±9**
Systolic BP, mm Hg	142±6	132±7	136±3	142±5	194±3**	187±5**	190±3**	192±4**
Diastolic BP, mm Hg	95±5	86±7	92±5	98±8	145±4**	134±7**	129±7**	143±5**
Mean arterial pressure, mm Hg	108±6	102±7	104±5	105±4	162±4**	151±6**	152±6*	159±5**
Pulse pressure, mm Hg	40±8	46±4	42±2	44±8	40±9	48±8	48±8	48±7

C – control, R – resveratrol, P – pterostilbene, G – gnetol. Data shown as mean ± SEM. $^{*}p<0.05$, $^{**}p<0.01$ vs. SD.

3.1.2 Structural modifications of MCA and the effects of stilbenoids

Arterial structure was assessed in terms of geometry. Reported values were measured under passive conditions (Ca^{2+}-free Krebs) at 30 mm Hg in MCA. In untreated SHHF rat cerebral arteries, changes in external and internal diameters were insignificant. However, M/L ratio was increased ($p<0.05$ vs. SD; Figure 8A) as a function of increasing media thickness ($p<0.01$ vs. SD; Table 2), which suggests diametric parameters had a combined effect on M/L ratio and media widths, even though changes in external ($p=0.9$ vs. SD; Table 2) and lumen diameters ($p=0.3$ vs. SD; Table 2) were individually negligible. Changes in Media CSA were also determined to be insignificant ($p=0.3$ vs. SD; Figure 8B). Arteries from untreated SHHF rats exhibited 58% remodeling and 44% growth (Table 2). Treatment with resveratrol, pterostilbene, and gnetol over the course of 8-weeks normalized media widths and M/L ratio in SHHF rats. (Table 2 and Figure

8A). Pterostilbene and gnetol had some influence on remodeling (49% and 39%, respectively; Table 2) but stilbenoids exerted their effects mostly on growth (resveratrol, 4%; pterostilbene, 7%; gnetol, -10%).

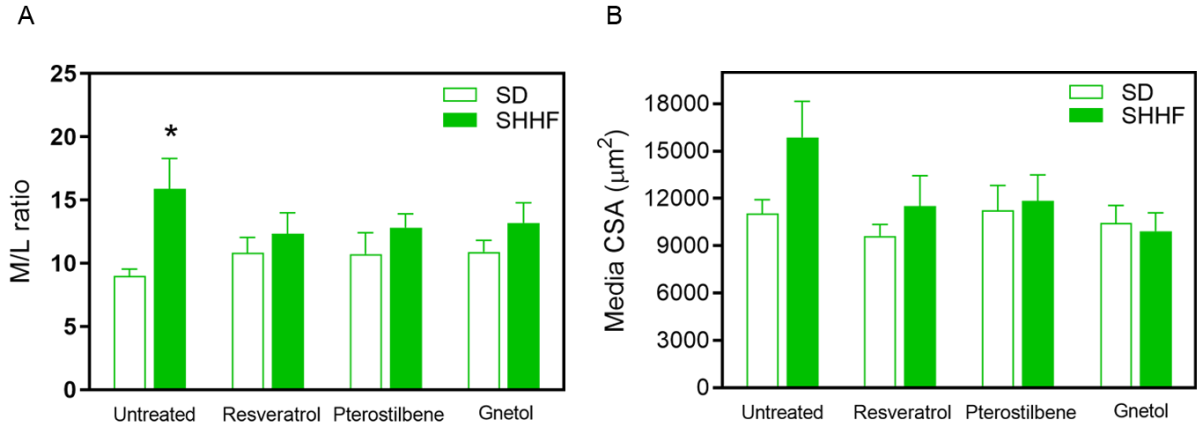

Figure 8. M/L ratio and media CSA of MCA from SD and SHHF rats. (A) M/L ratio of arteries from untreated SHHF rats was significantly increased. Following 8-weeks of treatment stilbenoids normalized M/L ratio in SHHF rats. (B) Media CSA was increase in untreated SHHF rat MCA but this was insignificant ($p=0.3$) and there was no effect with stilbenoid treatment. Data shown as mean ± SEM. *$p<0.05$ vs. untreated SD rats. n = 6-8.

Table 2. Summary of geometrical parameters and indices for remodeling and growth of MCA in 17-week-old SD vs. SHHF rats and the effect of stilbenoids

	SD				SHHF			
	C	**R**	**P**	**G**	**C**	**R**	**P**	**G**
External diameter, µm	202±6	177±12	189±10	181±10	220±10	204±18	200±10	185±12
Lumen diameter, µm	171±5	146±12	153±14	150±9	168±10	165±16	159±8	147±12
Media width, µm	15±1	15±1	15±2	15±1	26±3**	20±2	21±2	19±2
Remodeling index, %	-	-	-	-	58	55	49	39
Growth index, %	-	-	-	-	44	4	7	-10

C – control, R – resveratrol, P – pterostilbene, G – gnetol. Data shown as mean ± SEM. **p<0.01 vs. SD.

3.1.3 Mechanical behaviour of MCA and the effects of stilbenoids

Geometric remodeling due to thickening of the arterial wall (Table 2) reduced circumferential stress in MCA from untreated SHHF rat. This was given by the isobaric stress curve, which was shifted downwards (Figure 9A) resulting in a slope change characteristic of lowered media stress (p<0.01 SHHF vs. SD rat; Figure 9B). Media stress was improved with stilbenoid treatment in SHHF rat MCA ($p<0.$01 vs. untreated SHHF; Figure 9B); however, treatment failed to normalize stress completely ($p<0.$01 treated SHHF vs. untreated SD; Figure 9B). Interestingly, gnetol treatment had an effect on isobaric stress in normotensive rats (p<0.01 vs. untreated SD).

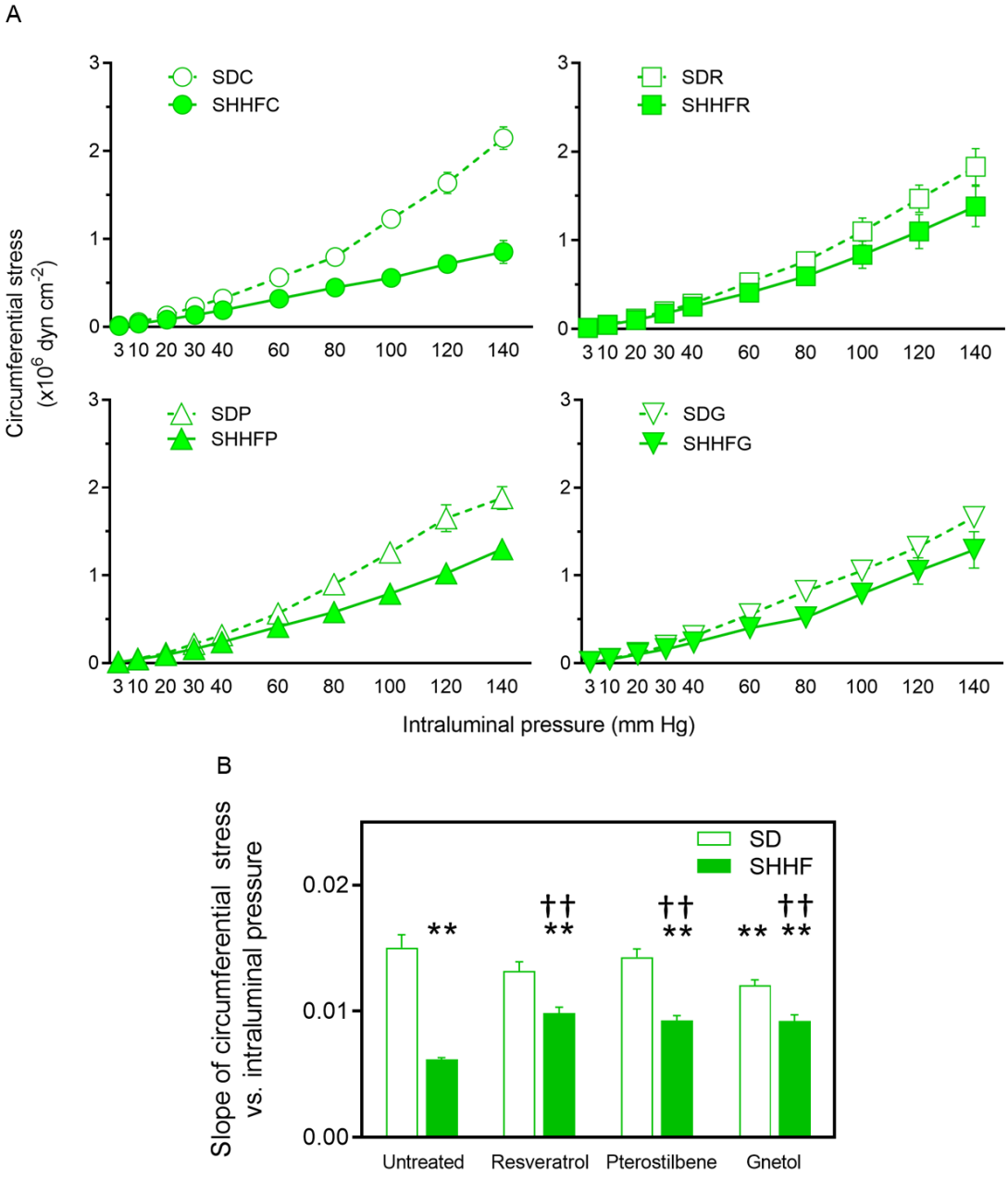

Figure 9. Isobaric stress relationships for MCA from SD and SHHF rats and the effect of stilbenoids. (A) The circumferential stress-pressure curve of untreated and treated SHHF rat arteries were shifted downwards compared to untreated SD arteries. (B) The slope of circumferential stress vs. pressure was reduced in untreated SHHF rat arteries. Treatment with

resveratrol, pterostilbene, and gnetol (2.5 mg/kg/d) for 8-weeks attenuated slope changes compared to untreated SHHF but did not restore isobaric stress to normal. Gnetol treatment reduced isobaric stress in normotensive rats. Data shown as mean ± SEM. $^{**}p<0.01$ vs. untreated SD; $\dagger\dagger p<0.01$ vs. untreated SHHF. n = 6-8.

When media stress was plotted against strain, there was a leftward shift in the stress-strain curve in arteries from untreated SHHF rat (Figure 10A, top left). When differences were quantified, the k-value was increased ($p<0.01$ vs. untreated SD; Figure 10B), suggesting that vascular compliance was reduced in SHHF rat MCA. However, stilbenoid treatment failed to improve compliance; there was a leftward shift in the stress-strain curves and the k-values remained significantly higher in SHHF rat arteries ($p<0.05$ and $p<0.01$ vs. untreated SD; Figure 10B).

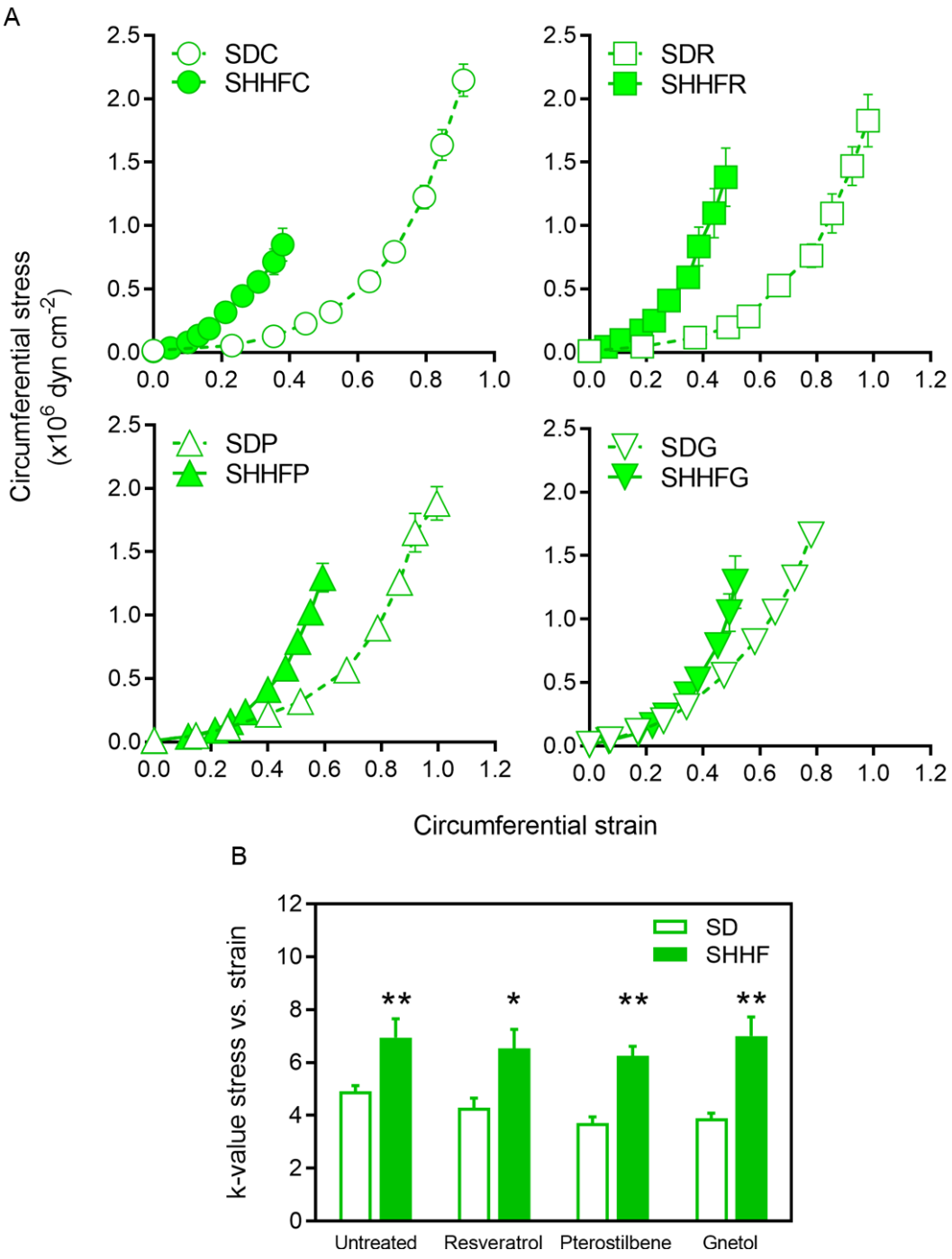

Figure 10. Wall stress-strain relationships for MCA from SD and SHHF rats and the effect of stilbenoids on vascular compliance. (A) The stress-strain curve of untreated SHHF rat arteries

was shifted leftwards. (B) The k-value was increased in untreated SHHF rat. Treatment for 8-weeks with resveratrol, pterostilbene, and gnetol (2.5 mg/kg/d) had no effect on the stress-strain relationship in SHHF rat. *p<0.05 and **p<0.01 vs. untreated SD. Data shown as mean ± SEM. n = 6-8.

The fractional deformation (strain) due to an applied force (stress) describes the elastic modulus of a material. It is the ratio of stress to strain, where the slope of the stress-strain relationship is defined as the incremental elastic modulus. This is a mechanical parameter used to describe the stiffness of a vessel and is determined by both arterial geometry (M/L ratio) and the intrinsic stiffness of the components making up the vascular wall (ie. load-bearing materials such as collagen and elastin). These properties change when a force (ie. stress) is applied to an artery; therefore, the elastic modulus will change depending on pressure. Incrementally increasing intraluminal pressure seemed to shift the isobaric elastic modulus curve leftward in untreated and treated SHHF rat arteries (Figure 11A). However, when quantified as a function of slope of elastic modulus vs. pressure, there were no significant differences between untreated SD and SHHF rat (p=0.6; Figure 11B), nor was there an effect of stilbenoid treatment on slope.

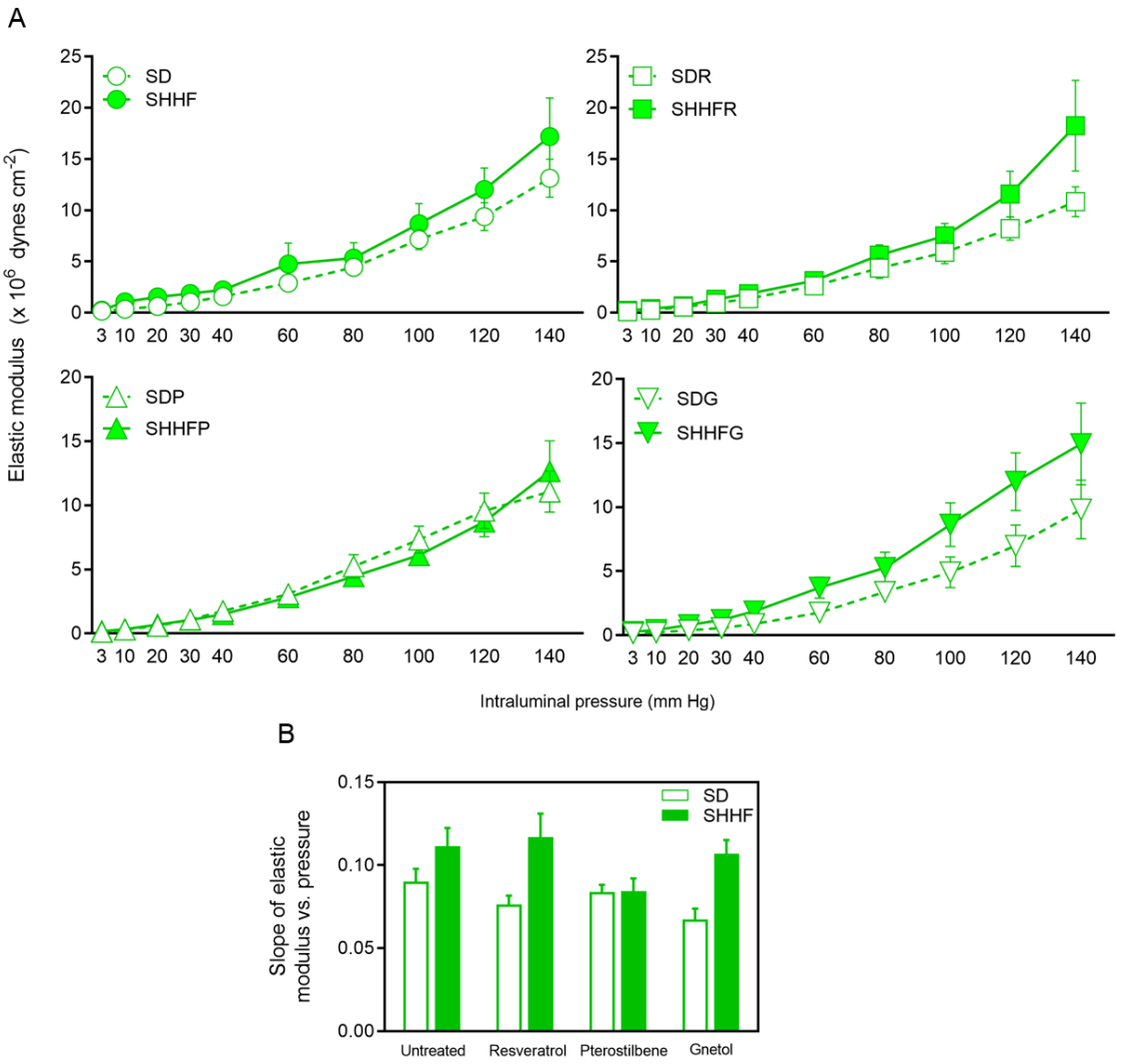

Figure 11. Isobaric elastic modulus of MCA from SD and SHHF rats and the effect of stilbenoids: arterial stiffness due to arterial geometry and wall component stiffness. (A) Elastic modulus vs. pressure was similar in arteries from SD and SHHF rats; untreated and treated with resveratrol, pterostilbene, and gnetol (2.5 mg/kg/d) for 8-weeks. (B) This was quantified by changes in the slope of elastic modulus vs. pressure. Data shown as mean ± SEM. **p<0.01 vs. untreated SD; ††p<0.01 vs. untreated SHHF. n = 6-8.

When elastic modulus was plotted against circumferential stress there was a leftward shift in MCA from untreated SHHF rats (Figure 12A, top left). Comparison of the slope of the elastic modulus vs. stress curve, revealed a greater slope in SHHF rat arteries ($p<0.01$ vs. SD; Figure 12B). This slope defines the stiffness of arteries determined only by wall components, where arterial geometry is mathematically eliminated as a determinant of stiffness. The slope of the elastic modulus vs. stress curve from treated SHHF rat arteries were all reduced towards normal with stilbenoids; however, only pterostilbene and gnetol completely normalized slope (†$p<0.05$ and ††$p<0.01$ vs. SHHF; Figure 12B).

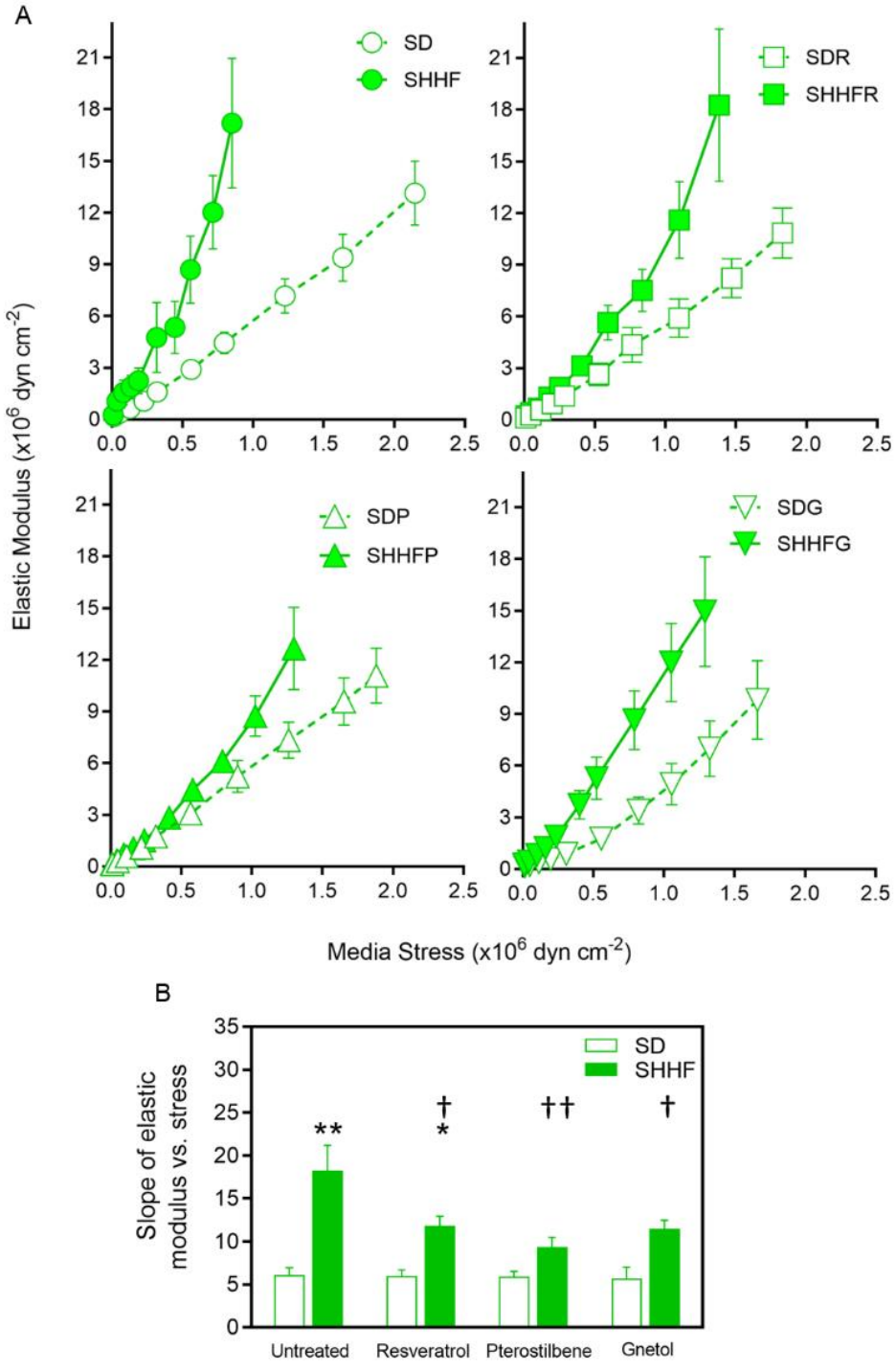

Figure 12. Elastic modulus vs. stress curve of MCA from SD and SHHF rats and the effect of stilbenoids on wall component stiffness. (A) The elastic modulus vs. stress curve was shifted

leftwards and (B) slope of elastic modulus vs. stress was significantly increased in in untreated SHHF rat MCA. Slope of the elastic modulus vs. stress curve was significantly reduced by stilbenoids and was normalized with pterostilbene and gnetol, but not resveratrol. Data shown as mean ± SEM. *p<0.05 and **p<0.01 vs. untreated SD; †p<0.05 and ††p<0.01 vs. untreated SHHF. n = 6-8.

3.2 Hypertensive vascular modifications in penetrating arterioles from SHHF rat and SHR

This portion of the thesis characterized vascular properties pertaining to structure, mechanics, and function of penetrating arterioles in SHHF rats and SHR, models for hypertension with risk for developing heart failure and hypertension alone, respectively. First, vascular structure and mechanics were characterized in hypertensive models vs. respective normotensive controls (SD or WKY rats). The microstructural basis for the mechanical properties of penetrating arterioles were determined by quantifying constituents that made up the arteriolar wall. The functional properties were then measured using acetylcholine, glutamate and D-serine, and sodium nitroprusside.

3.2.1 Body weight and BP

At 17 weeks of age, SHHF rats exhibited smaller mean body weights than SD rats ($p<0.01$; Figure 13A and Table 3). Mean body weights of SHR did not differ from WKY rats ($p=0.3$). Systolic BP was significantly increased in SHHF ($p<0.01$ vs. SD) and SHR rats ($p<0.01$ vs. WKY rat; Figure 13B and Table 3). Other BP parameters including diastolic BP and mean arterial pressure were also elevated in SHHF ($p<0.01$ and $p<0.01$ vs. SD, respectively) and SHR rats ($p<0.01$ and $p<0.01$ vs. WKY. respectively) (Table 3). However, pulse pressures of SHHF and SHR rats were similar to respective normotensive controls.

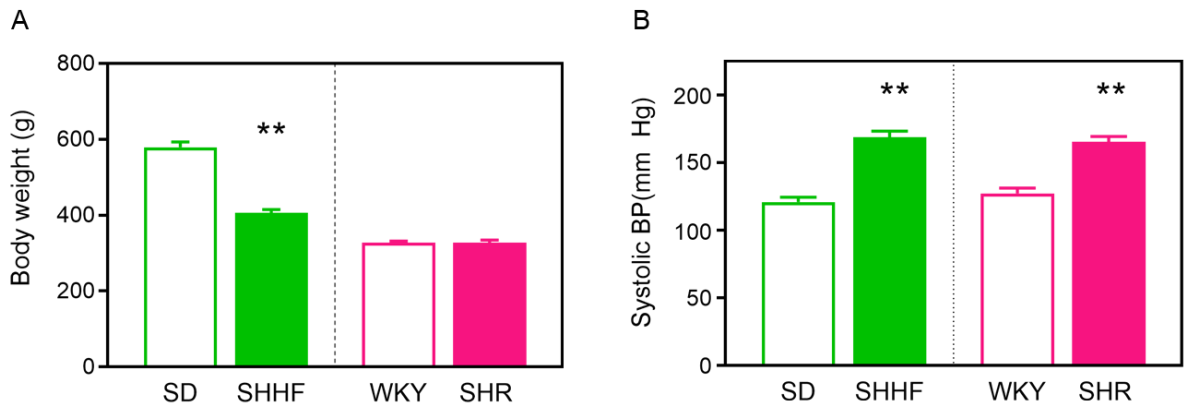

Figure 13. Mean body weights (g) and systolic BP in SHHF vs. SD rats and SHR vs. WKY rats. (A) SHHF rats had significantly reduced mean body weights (g) compared to SD rats. There was no difference in mean body weight between SHR and WKY rats (p=0.3). (B) Systolic BP was significantly elevated in SHHF rats and SHR. Data shown as mean ± SEM. **p<0.01 vs. normotensive control. n = 7-9.

Table 3. Summary of body weights and BP parameters in 17-week-old SD, SHHF, WKY, and SHR rats

	SD	SHHF	WKY	SHR
Body weight, g	579 ± 14	406 ± 9**	329 ± 6	327 ± 5
Systolic BP, mm Hg	121 ± 4	169 ± 5**	127. ± 4	161 ± 3**
Diastolic BP, mm Hg	71± 6	108± 7**	65± 6	100± 2**
Mean arterial pressure, mm Hg	88± 5	128± 6**	86± 5	122± 3**
Pulse pressure, mm Hg	50± 4	61± 4	62± 4	65± 2

Data represents mean ± SEM. **p<0.01 vs. normotensive control (SD vs. SHHF; WKY vs. SHR).

3.2.2 Structural modifications of penetrating arterioles

Arteriolar structure was examined in terms of geometry and parameters are summarized in Table 4. Since SD rats were significantly larger in body weight compared to SHHF rats, geometric parameters for SD were normalized as previously described to avoid confounding the comparisons of arteriolar structure. Geometry was not corrected for body weight in WKY rats since body weights were similar to SHR rats. In penetrating arterioles from SHHF rats, changes in external diameter were negligible (p=0.2 vs. SD; Table 4) but there was a tendency towards decreasing lumen diameter (p=0.08 vs. SD; Table 4). M/L ratio was significantly increased in SHHF rat vessels (p<0.01 vs. SD; Figure 14A) despite constant media width (p=0.4), suggesting a decreasing trend in lumen diameter was sufficient to induce significant geometric changes. Since media CSA remained unchanged, eutrophic remodeling predominates in penetrating arterioles of SHHF rats.

Table 4. Summary of geometrical parameters and indices for growth and remodeling of penetrating arterioles

	SD	SHHF	WKY	SHR
External diameter, µm	71.4 ± 6	58.4 ± 6	71.0 ± 5	64.6 ± 6
Lumen diameter, µm	56.3 ± 5	41.3 ± 5	56.0 ± 4	45.9 ± 5
Media width, µm	15.2 ± 1	17.1 ± 2	15.0 ± 1	17.7 ± 1
Growth index, %		-9		5
Remodeling index, %		121		96

Representative arterial parameters and indices are shown for intraluminal pressure of 60 mmHg. Data represents mean ± SEM.

In SHR arterioles, M/L ratio was increased (p<0.01 vs. WKY), but not media CSA (Figure 14B). Wall thickness remained unchanged (Table 4), therefore increased M/L ratio was due to the combined effects of external (p=0.5 vs. SD; Table 4) and lumen diameter (p=0.3 vs. SD; Table 4) changes, despite individual insignificance. Vessels from SHR also underwent eutrophic remodeling since M/L ratio was increased (p<0.01 vs. WKY), but not media CSA (Figure 14B). SHHF rat arterioles exhibited 121 % remodeling and -9% growth, whereas those vessels from SHR exhibited remodeling and growth indices of 96 % and 5 %, respectively (Table 4).

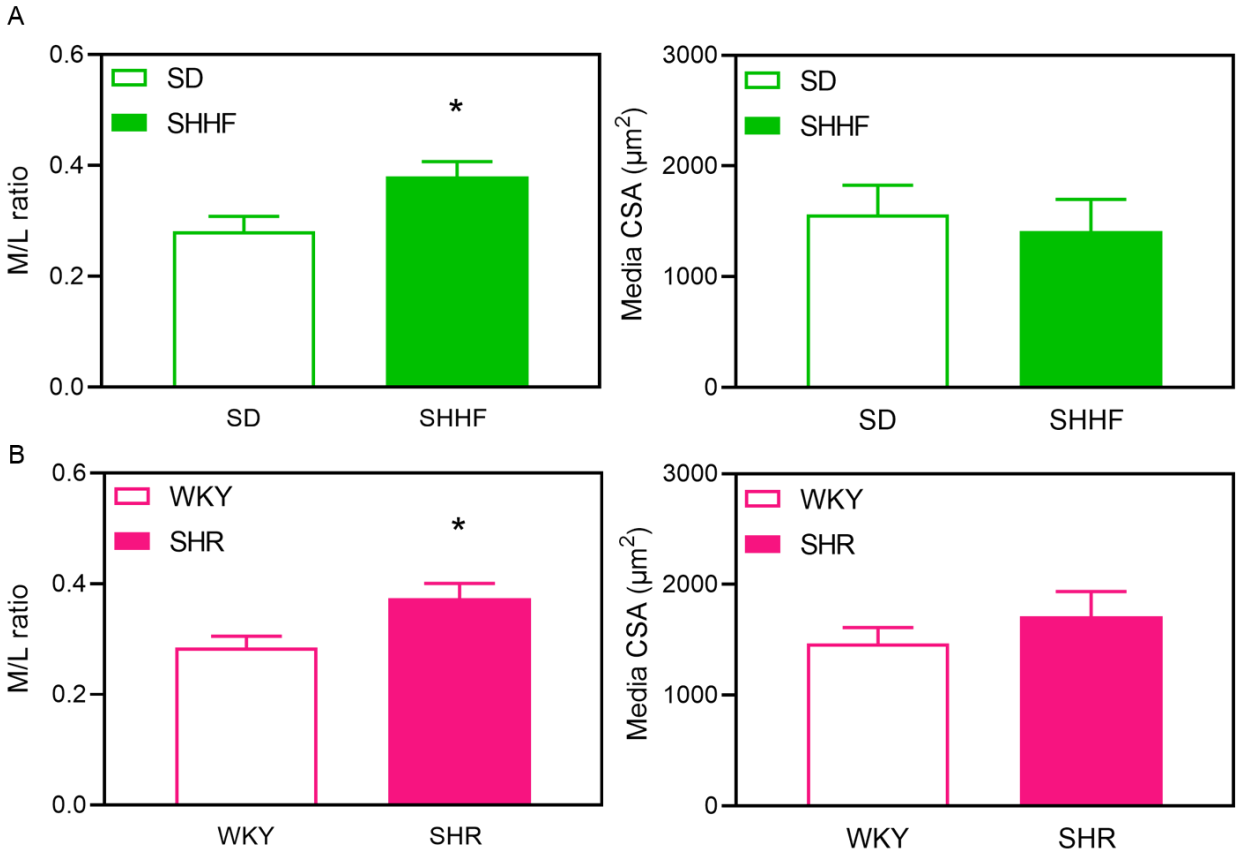

Figure 14. M/L ratio and media CSA of penetrating arterioles from SHHF vs. SD rats and SHR vs. WKY rats. (A) M/L ratio was increased in SHHF rat penetrating arterioles without corresponding changes in media CSA (p=0.5). (B) A similar increase in M/L ratio and unchanged media CSA (p=0.5) were observed in SHR vessels. Data shown as mean ± SEM. **p<0.01 vs. normotensive control (SD vs. SHHF; WKY vs. SHR). n = 7-9.

3.2.3 Mechanical behaviour of penetrating arterioles

Representative pressure myography traces used to measure vessel dimensions for calculating mechanical parameters are provided in Appendix B: Figure 22. Wall stress was reduced in SHHF rat and SHR penetrating arterioles. This was represented by a rightward shift in the stress – pressure curve (Figure 15A and B, left) and reduced slope of stress vs. pressure curve ($p<0.01$ SHHF vs. SD rats; Figure 15A, right and $p<0.01$ SHR vs. WKY rats; Figure 15B, right). This reduced media stress was a consequence of geometric remodeling (ie. increased M/L ratio) of the arteriolar wall.

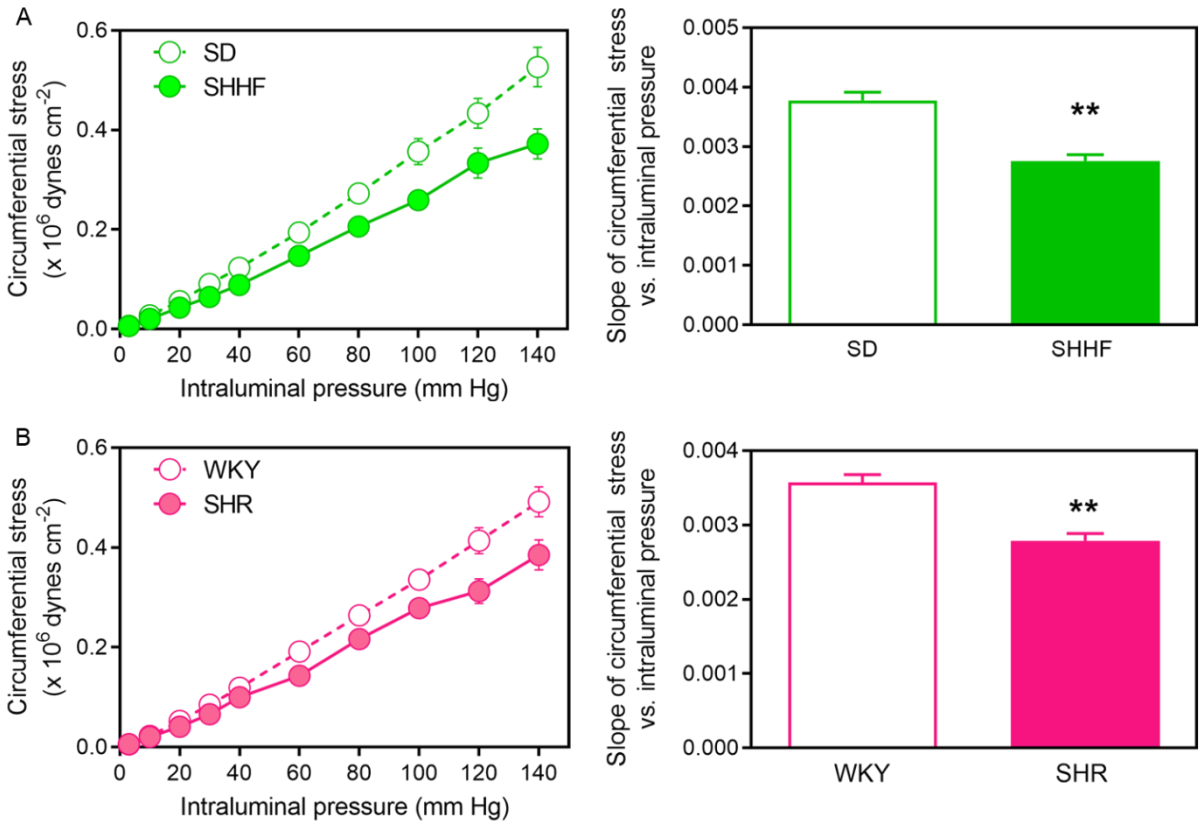

Figure 15. Isobaric stress of penetrating arterioles in SHHF vs. SD rats and SHR vs. WKY rats. Stress – pressure curve (left) in penetrating arterioles from SHHF rats (A) and SHR (B) are shifted right compared to SD and WKY rats, respectively. The slopes of stress vs. pressure (right) were significantly reduced. Data shown as mean ± SEM. $^{**}p<0.01$ vs. normotensive control (SD vs. SHHF; WKY vs. SHR). n = 7-9.

Penetrating arterioles from SHHF rats exhibited reduced vascular compliance when circumferential strain was plotted against media stress: the stress-strain curve shifted leftwards (Figure 16A, left) and the k-value was significantly increased ($p<0.01$ vs. SD; Figure 16A, right). For SHR, the k-values were significantly reduced ($p<0.01$ vs. WKY; Figure 16B, right), suggesting penetrating arterioles were more compliant.

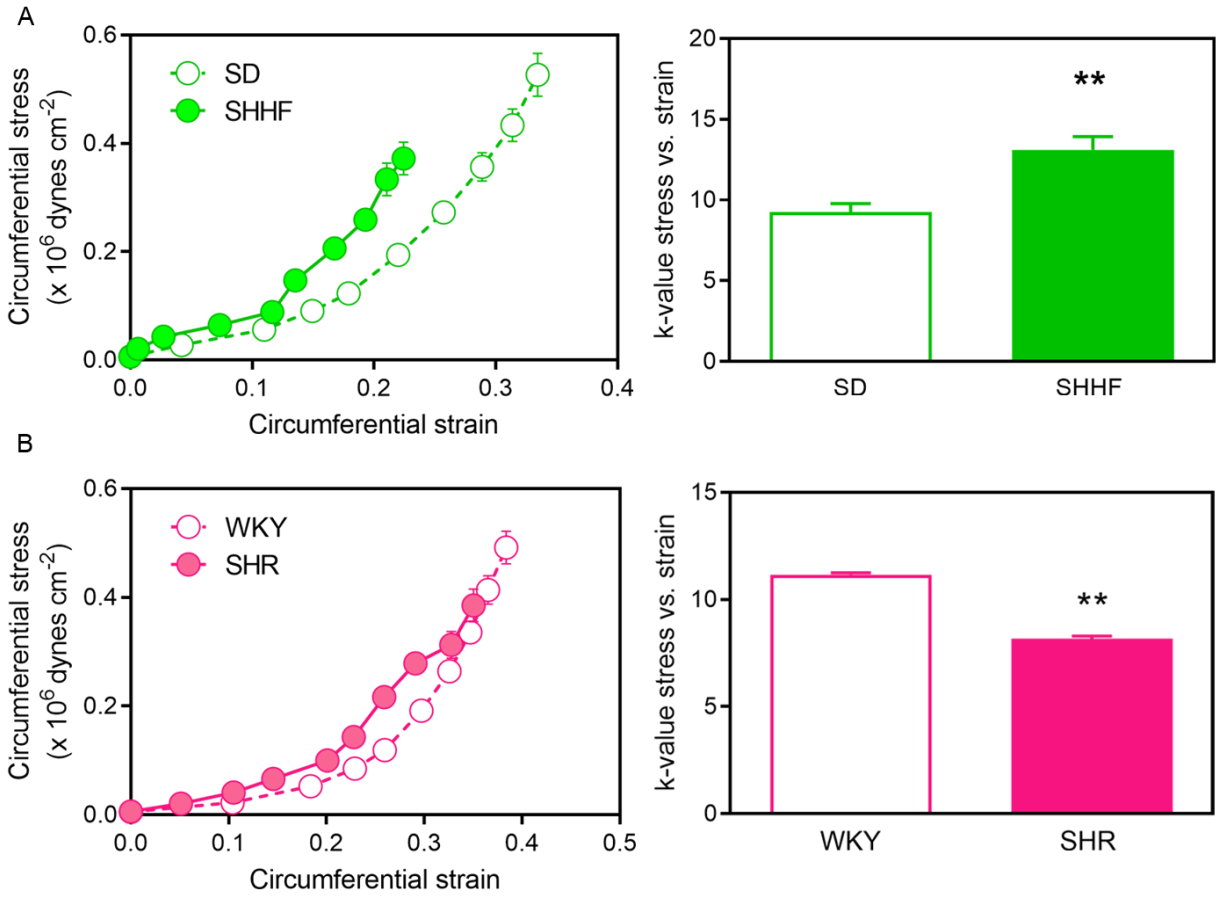

Figure 16. Compliance of penetrating arterioles in SHHF vs. SD rats and SHR vs. WKY rats. (A) The stress – strain curve was shifted leftward and the k-value was increased in arterioles from SHHF rats. (B) In SHR arterioles, the k-value was significantly reduced. Data shown as mean ± SEM. $^{**}p<0.01$ vs. normotensive control (SD vs. SHHF; WKY vs. SHR). n = 7-9.

The observation that penetrating arterioles were less compliant in SHHF rats was consistent with changes in vascular stiffness. Both the geometry and the structural elements of the arteriolar wall contribute to stiffening in penetrating arterioles in SHHF rats. This was demonstrated by a leftward shift in the elastic modulus when plotted against pressure (Figure 17A, left) and stress (Figure 18A, left), which corresponded with greater slopes ($p<0.05$ vs. SD; Figure 17A right and $p<0.01$ vs. SD; Figure 18A, right).

In contrast, the isobaric elastic modulus curve shifted rightward in SHR vessels (Figure 17B, left) and the slope was significantly reduced ($p<0.05$ vs. WKY; Figure 17B, right), suggesting these vessels are less stiff. When elastic modulus was plotted against stress, wall component stiffness was similar between SHR and WKY rats (Figure 18B). Thus, increased compliance is controlled by geometry, where increased M/L ratio but not components of the vascular wall contributes to a reduction in stiffness of SHR penetrating arterioles.

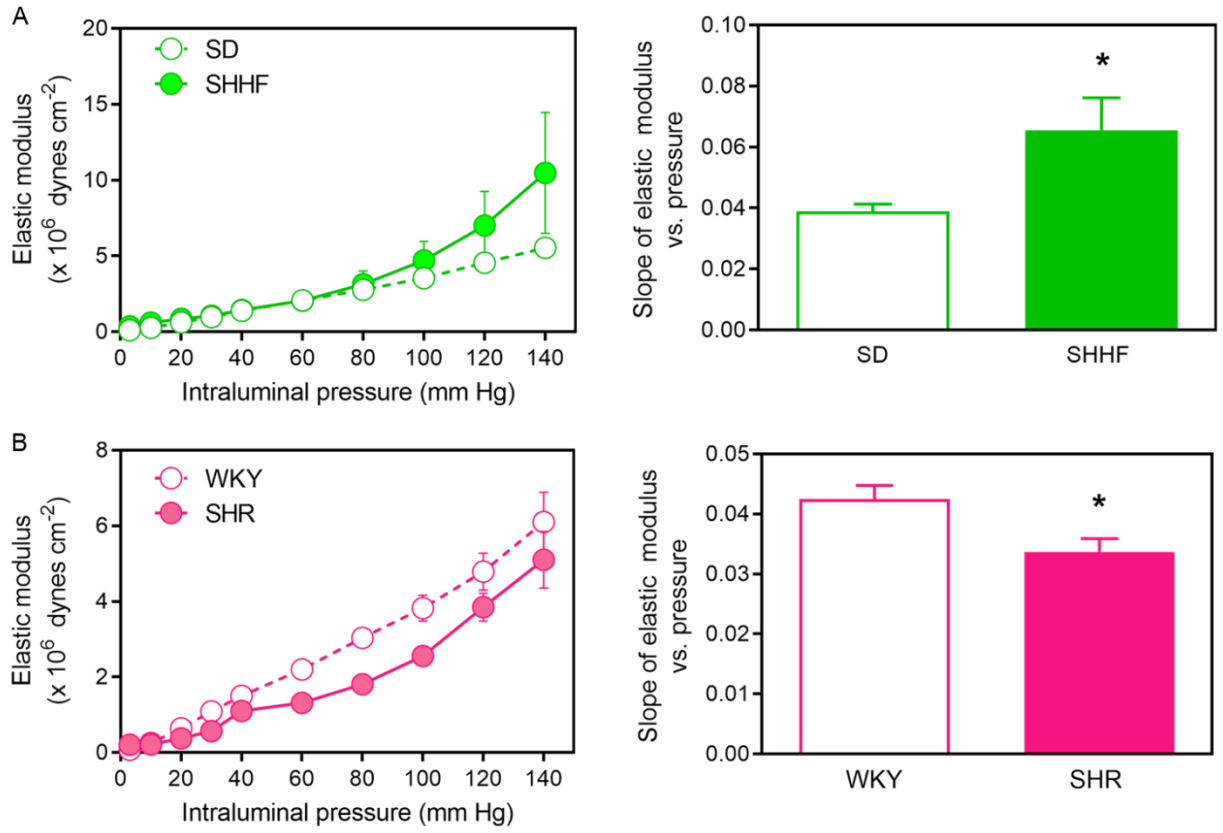

Figure 17. Isobaric elastic modulus of penetrating arterioles from SHHF vs. SD rats and SHR vs. WKY rat: arterial stiffness due to arterial geometry and wall component stiffness. (A) The elastic modulus – pressure curve was shifted leftward and the slope was significantly increased in SHHF rat arterioles. (B) In SHR, the elastic modulus – pressure curve shifted rightward and the slope was significantly reduced. Data shown as mean ± SEM. *p<0.05 vs. normotensive control (SD vs. SHHF; WKY vs. SHR). n = 7-9.

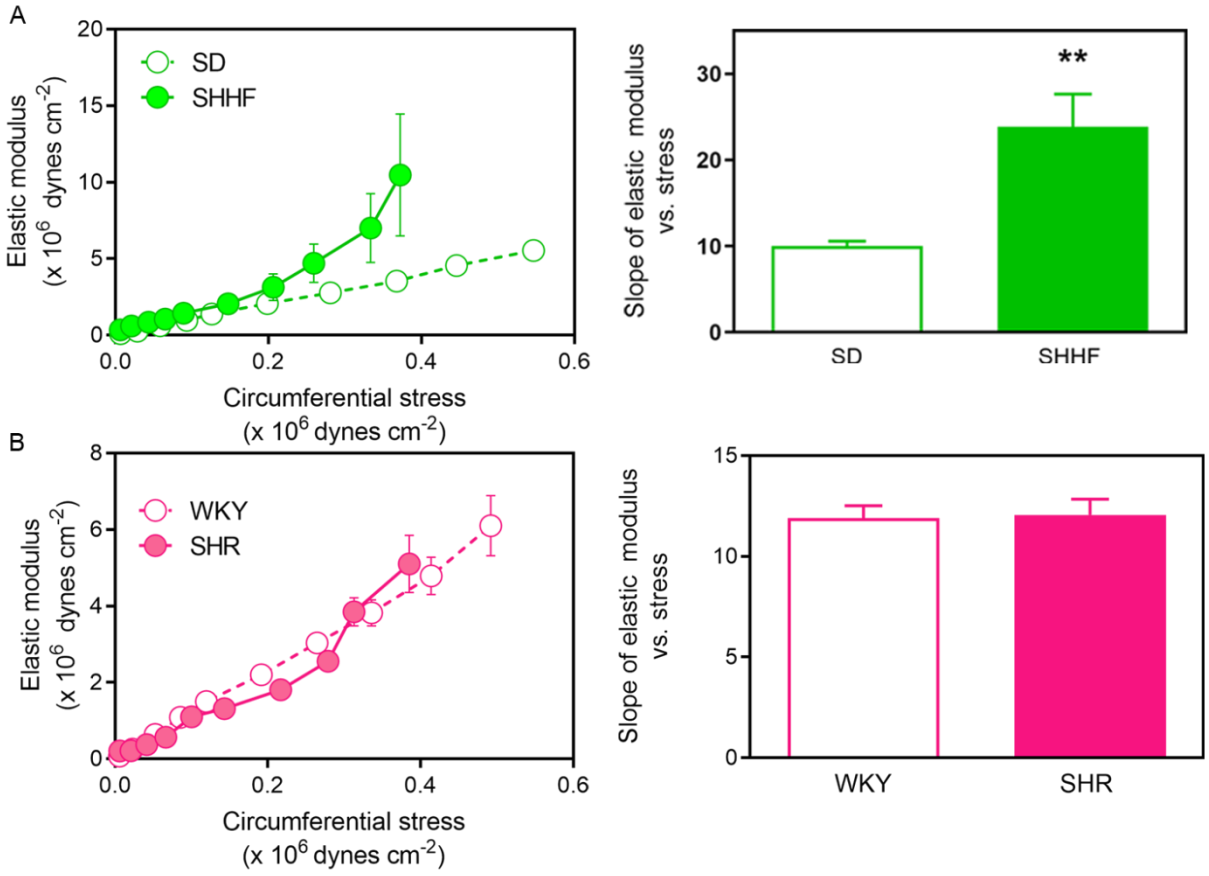

Figure 18. Wall component stiffness of penetrating arterioles in SHHF vs. SD rats and SHR vs. WKY rats. (A) The elastic modulus – stress curve shifted left and the slope was increased in SHHF rat arterioles. (B) In SHR vessels, the elastic modulus – stress curve and slope remained unchanged in SHR relative to WKY rat. Data shown as mean ± SEM. $^{**}p<0.01$ vs. SD. n = 7-9.

3.2.4 Wall composition

Transmission electron micrographs of penetrating arterioles from SHHF and SD rats are shown in Figure 19. In general, vessels had mature amorphous elastic fibres composed of electron-dense and compact elastin in healthy penetrating arterioles (Figure 19A). Ultimately these fibres occupied most of the elastic lamina and were oriented longitudinally. Collagen fibrils had a microtubular appearance packed mostly horizontally into straight segmented bundles, which were typically deposited in the adventitial ECM (Figure 19A). In vessels from SHHF rat, elastin accumulation and amorphous elastic fibres were scarce, and the elastic lamina was lost (Figure 19B) or showed varying degrees of fragmentation (Figure B.1 and B.2). The collagenic matrix was rich with collagen fibrils seen as microtubular bundles in parallel (Figure B insert) or as transverse cross-sections (Figure B insert). Taken collectively, this suggests that the elastic matrix was less abundant and highly disorganized in SHHF rat penetrating arterioles, whereas the collagenic matrix was associated with deposition of collagen fibres. The areas occupied by elastin and collagen were measured and the collagen/elastin ratio of arterioles from SHHF rats were significantly increased ($p<0.05$ vs. SD; Figure 19C). This was consistent with increased arterial stiffness and wall component stiffness (Figures 17 and 18). There were no changes in VSMC (Figure 19D) or ECM content (Figure 19E), which identifies an abundant collagenic matrix as the major determinant of increased arteriolar stiffness in SHHF rats.

Penetrating arterioles from WKY rats had a matrix typified by mature elastic fibres mostly associated with the elastic lamina and collagen fibrils predominating in the adventitia (Figure 20A). As seen in SD rat, elastic fibres were amorphous and composed of elastin that was electron-dense and collagen fibres were microtubular and organized in horizontal bundles. We observed

similar collagenic and elastic matrices in vessels from SHR (Figure 20B). This was confirmed by a collagen/elastin ratio that was maintained in SHR arterioles (p=0.6 vs. WKY; Figure 20C). Also, areas occupied by VSMC and ECM remained unchanged (p>1 vs. WKY; Figure 20D and E, respectively). These data are consistent with the changes in elastic properties of SHR penetrating arterioles, which we identified as having unchanged wall component stiffness.

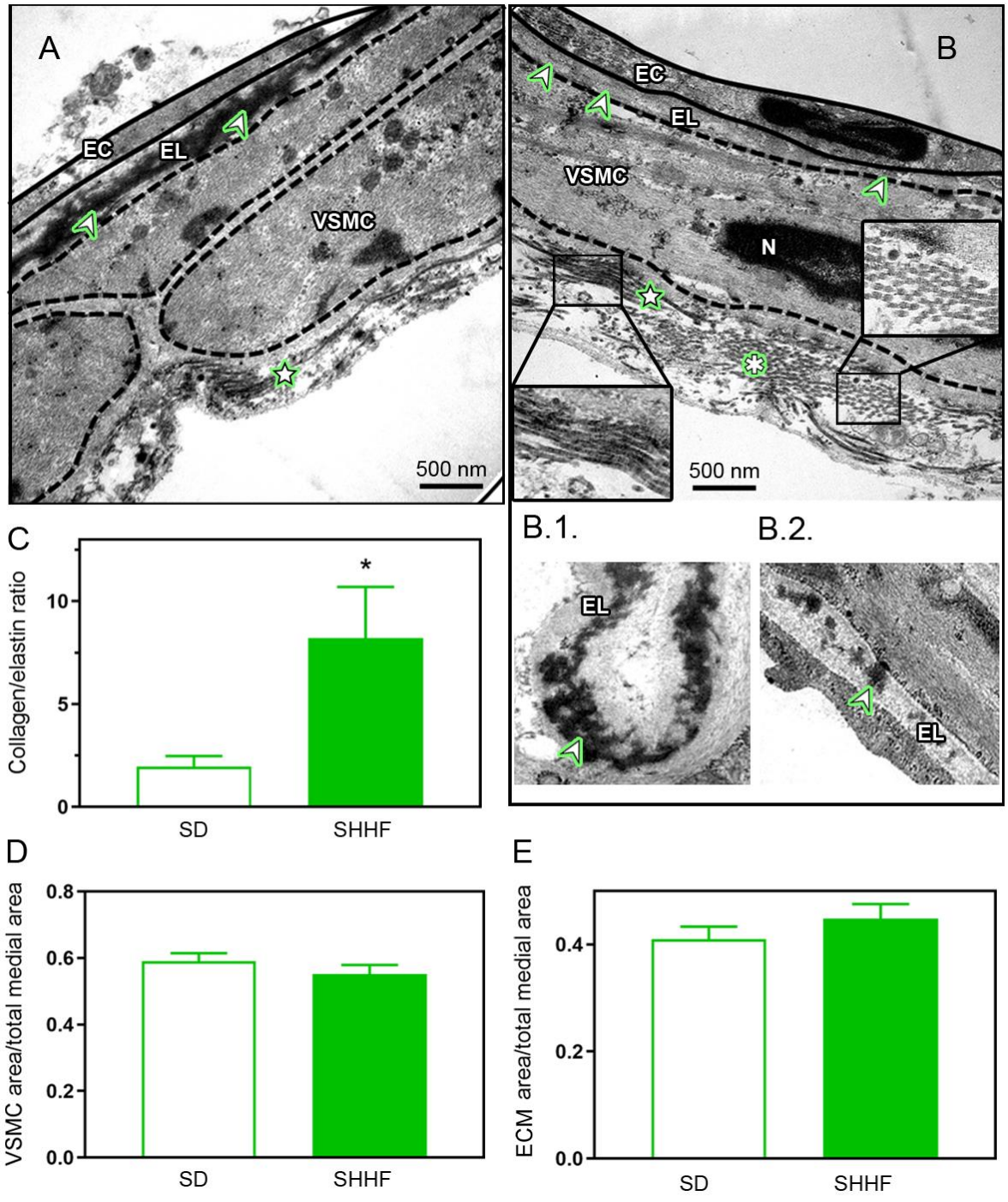

Figure 19. Quantification of wall components that contribute to stiffness in penetrating arterioles from SD and SHHF rats. Transmission electron microscopy (25,000x magnification) of penetrating vessels shows three distinct layers: the adventitia with ECM elements, VSMC of

the medial layer, and the intima with the elastic lamina and associated endothelium. In SD rat arterioles, electron-dense elastin formed mature elastic fibres of the elastic lamina (A, arrowhead) and collagen fibres were mostly identified in the adventitial ECM (A, star). In SHHF rat arterioles, only remnants of elastic fibres remained (B, arrowhead) or there were varying degrees of fragmentation of the elastic lamina (B.1 and B.2, arrowhead), while the collagenic matrix was abundant with collagen fibrils (B, star and asterisk). The collagen/elastin ratio was significantly greater in SHHF rat penetrating arterioles (C). There were no changes related to VSMC (D) or matrix (E) size. EL, elastic lamina; ECM, extracellular matrix; VSMC, vascular smooth muscle cells; EC, endothelial cell; N, nucleus. Arrowhead, mature elastic fibres of EL; star, longitudinal collagen; asterisk, transverse collagen. Data shown as mean ± SEM. *$p<0.05$ vs. SD. n = 7-11.

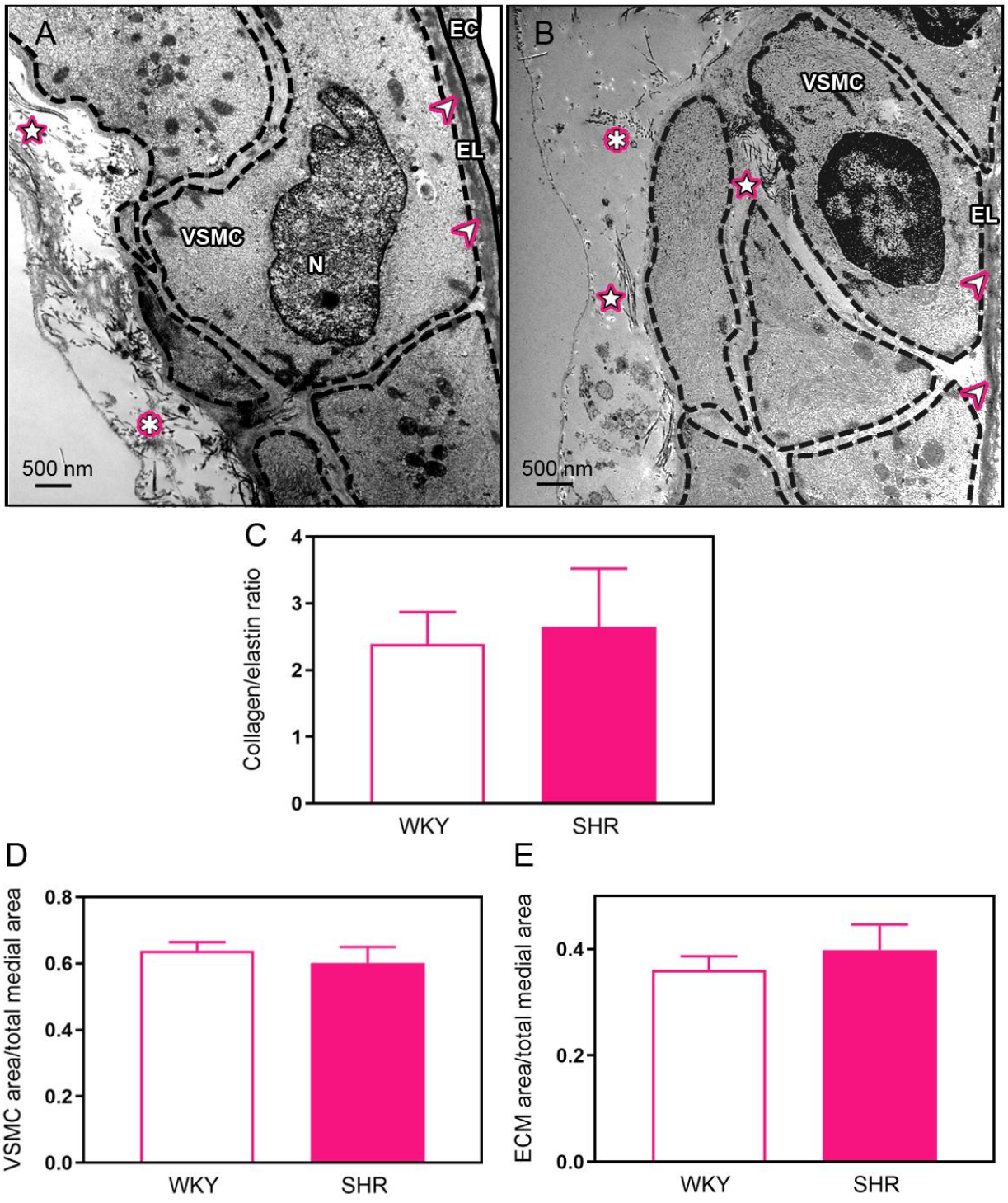

Figure 20. Quantification of wall components that contribute to stiffness in penetrating arterioles from WKY rats and SHR. Transmission electron microscopy (13,500x

magnification) of penetrating vessels in WKY rats (A, arrowhead) and SHR (B arrowhead) showed deposition of elastin in the elastic lamina, while collagen fibres were mostly found in the adventitial layer (A and B, star and asterisk). There was no difference in collagen/elastin ratio (C) or size of areas occupied by VSMC (D) or matrix (E) between WKY rat and SHR (C). EL, elastic lamina; ECM, extracellular matrix; VSMC, vascular smooth muscle cells; EC, endothelial cell; N, nucleus. Arrowhead, mature elastic fibres of EL; star, longitudinal collagen; asterisk, transverse collagen. Data shown as mean ± SEM. n = 8-9.

3.2.5. Functional responses in penetrating arterioles – global vasomotor responses

To study global functional responses in SHHF rats and SHR, penetrating arterioles were pressurized at 60 mm Hg and preconstricted with 10^{-9}M [Arg^{8}] vasopressin to increase the dynamic range for vasomotor responses. Only vessels that preconstricted >15% of their baseline diameter were used to study functional responses. Vasodilation to increasing doses of glutamate with D-serine was significantly reduced in arterioles from SHHF rats (p<0.01 vs. SD; Figure 21A) and these responses decayed with higher concentrations of glutamate. There were no differences in vasodilatory responses to acetylcholine between SD and SHHF rat arterioles; initially low concentrations (less than 10^{-7}M) induced vasoconstriction followed by vasodilation (Figure 21C). Increasing concentrations of sodium nitroprusside induced vasoconstriction in arterioles from SHHF rats, while concentrations 10^{-7}M or greater resulted in increasing relaxation in SD rat vessels (Figure 21E). Vasodilatory responses to glutamate with D-serine, were comparable between WKY rats and SHR (Figure 21B). Vasomotor responses in WKY followed a trend similar to that observed in SD and SHHF rats (initial vasoconstriction followed by vasodilation); however, it induced relaxation in SHR vessels (p<0.05 vs. WKY; Figure 21D). Vasomotor response to sodium nitroprusside was significantly impaired in SHR (p<0.05 vs. WKY; Figure 21F).

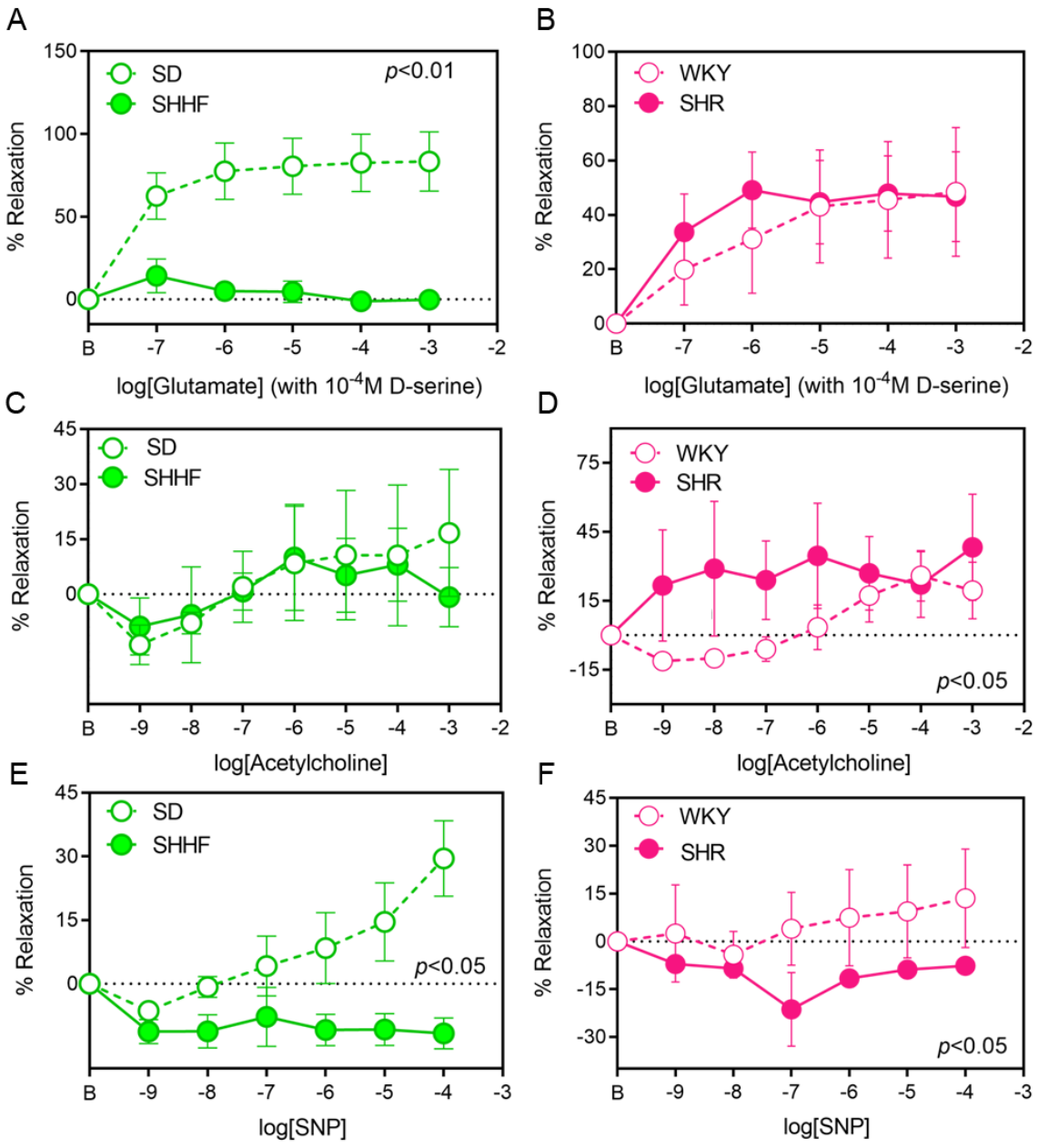

Figure 21. Vasomotor responses of penetrating arterioles from SHHF rats and SHR. (A) Relaxation of penetrating arterioles to glutamate/D-serine was reduced in SHHF vs. SD rats (non-linear regression). (C) Acetylcholine induced similar patterns of relaxation in SD and SHHF rats but (E) NO-donor sodium nitroprusside elicited constrictor responses in SHHF. (B) Vessels from

SHR had normal responses to glutamate/D-serine, whereas (D) acetylcholine-induced relaxation was increased and (F) responses to sodium nitroprusside lead to constriction. Data shown as mean ± SEM. n = 5-9.

4 Discussion

4.1 Hypertensive vascular modifications in MCA from SHHF rats and the effect of stilbenoid treatment

4.1.1. Vascular changes in untreated SHHF rats

There is limited information about the hypertensive vascular changes of cerebral arteries when predisposed to developing heart failure. The most commonly used experimental models of hypertension to study the brain vasculature are SHR and SHRSP, whereas the use of SHHF rats is less widespread. The SHHF rat models human heart disease in that it superimposes risk of heart failure upon hypertension,[223, 225] which distinguishes it from other hypertensive models. Thus, the SHHF rat is an ideal model to study the effects of hypertension with the added risk for heart failure on the MCA – one of the best studied cerebral vessels. There are several reasons why these vessels are often the focus of experimental studies. First, the MCA is easily accessible; being a large superficial artery, it can be isolated from the base of the brain and then cannulated. Second, these vessels are often the site of occlusions that lead to stroke, hence the use of SHRSP. Third, they are important regulators of brain blood flow because they carry a substantial amount of the total vascular resistance in the brain.

This study was the first, to our knowledge, to characterize the structural properties and mechanical behavior of brain resistance arteries in SHHF rats *ex vivo*. The effect of elevated BP on SHHF rat cerebral arteries was geometric remodeling characterized by an increase in M/L ratio, which was a consequence of thickening of the vessel wall. A negligible increase in media CSA indicates structural changes should be attributed to eutrophic remodeling. However, growth and remodeling

indices were 43.6% and 58.0%, respectively, suggesting the structural changes cannot be explained by eutrophic remodeling alone but rather a combination of remodeling and hypertrophic growth likely occurs in these vessels. Earlier reports have described eutrophic remodeling in SHRSP[222] and young SHR (during early hypertension)[219] cerebral arteries (MCA and pial), which exhibited smaller lumens.[214] Similarly, MCA from adult SHR had greater M/L ratios but no evidence of arterial wall growth.[219] Thus, it is apparent that eutrophic remodeling of cerebral arteries is a common adaptation to increasing BP in different hypertensive strains. However, hypertrophic growth also contributes to vascular remodeling in SHHF rat cerebral vessels, which distinguishes it from models of hypertension alone or those that are stroke-prone.

In effect, geometric remodeling reduced the stress experienced by the arterial wall due to the circumferential distribution of strain across a thicker media. Thus, thickening of the wall allows the vessel to withstand chronic elevations in BP by decreasing the mechanical load. Given that the primary function of the MCA is to direct blood flow toward the microcirculation, remodeling of these arteries might protect the distal cerebral vessels from the effects of hypertension and the cardiac abnormalities preceding failure. By 3-5 months of age, SHHF rats develop cardiac hypertrophy of the left ventricle.[226] We confirmed this in a parallel study by demonstrating that 17 week old SHHF rats have left ventricular hypertrophy and diastolic dysfunction.[227]

Compliance of cerebral arteries was reduced in SHHF rats; however, structural remodeling did not contribute to changes in elastic properties. Although wall component stiffness increased, thickening of the wall counteracted this effect such that arterial stiffness due to geometry and wall component stiffness remained the same. Therefore, reduced compliance was dictated by greater

wall component stiffness, but not geometry. This suggests that stiffer structural elements compensate for thickening of the arterial wall, so that normal brain perfusion is maintained in the face of elevated BP. Similarly, peripheral resistance arteries stiffen,[31, 32] and SHR mesenteric resistance arteries have a greater ratio of collagen to elastin.[31] MCA from SHR also show similar reductions in compliance and distensibility.[219]

Interestingly, there are bed-specific differences in arterial wall abnormalities in SHHF rats. Recently we reported that while both mesenteric and cerebral beds exhibit increased M/L ratio, mesenteric arteries only undergo eutrophic remodeling consistent with unchanged media CSA and 97% remodeling index.[228] There were also regional differences related to compliance and stiffness between mesenteric and cerebral vessels. Eutrophic remodeling produced a trend in decreasing compliance that approached statistical significance (p=0.07) in mesenteric arteries. Further, these vessels had no changes in wall component stiffness. Therefore, in the mesenteric bed elevations in BP lead to changes predominantly in geometric structure but not mechanical properties; whereas, in MCA hypertensive changes occur at the level of structure and mechanics.

4.1.2. The effect of stilbenoid treatment on vascular changes in SHHF rats

The effects of stilbenoid treatment on hypertensive vascular changes of cerebral arteries in SHHF rats are unknown. Previously, resveratrol was shown to attenuate remodeling and changes in mechanical behaviour in mesenteric arteries in SHR.[224] We hypothesized that resveratrol would have similar effects in MCA from SHHF rats and that its analogues may possess similar, if not improved, actions. In 17-week-old SHHF rats, stilbenoid treatment attenuated hypertrophic

growth; resveratrol and pterostilbene reduced growth substantially (by 39.9% and 36.6%, respectively), whereas gnetol completely prevented growth (-10%). In contrast, stilbenoid treatment had little-to-modest effect on eutrophic remodeling, which was reduced by 9.4% with pterostilbene and 19% with gnetol treatment, but only 3.5% with resveratrol. Since increased wall thickness and M/L ratio were attenuated in stilbenoid-treated SHHF rats, these changes can be mostly attributed to the anti-growth effect of stilbenoids. Because stilbenoids failed to lower elevated BP in SHHF rats, this suggests that vascular wall structure was improved as a result of the direct effects of stilbenoids on the arterial wall and not secondary to BP lowering. Clinical reports have shown that changes in the M/L ratio predict cardiovascular events independent of BP lowering.[40, 229] Thus, stilbenoid treatment may offer benefits for the structural integrity of cerebral arteries associated with better cardiovascular outcome, despite no effect on BP. This would recommend stilbenoids as a useful complement to conventional antihypertensive medications. However, the effect of resveratrol on BP should not be discounted altogether; a systematic review and meta-analysis of clinical trials suggests higher doses of resveratrol (>300 mg/day) can lower BP.[230] In one clinical trial, 50 mg/day of resveratrol was sufficient to reduce BP when added to standard antihypertensive treatment.[231] Thus, a higher dose of stilbenoids should be attempted in SHHF rats.

While, increased M/L ratio in untreated SHHF rats was sufficient to reduce the circumferential wall stress in cerebral arteries in the face of elevated BP, stilbenoid treatment reverses geometric remodeling and nearly normalizes wall stress, although it never reaches the levels of untreated SD rats. Stilbenoid treatment reduced wall component stiffness without augmenting compliance in

SHHF rat arteries. This suggests that a reduction in M/L ratio countered the reduction in wall component stiffness, such that compliance remained the same.

If structure and compliance are used as measures of treatment outcome, it is evident that pterostilbene did not manifest an advantage over other stilbenoids. For instance, pterostilbene showed similar effects on geometric remodeling and compliance to resveratrol and gnetol, despite having the greatest bioavailability and prolonged half-life.[196, 210, 211] And yet, even with a >10-fold difference in bioavailability, pterostilbene and gnetol similarly normalized wall component stiffness. However, this effect was absent with resveratrol, which is more bioavailable than gnetol. This suggests that affinity to receptor targets and potency should be investigated further. Preliminary studies already reveal potential differences in stilbenoid interactions with targets. Resveratrol is a non-selective inhibitor of enzymes cyclooxygenase (COX)-1 and COX-2,[232] which catalyze the biosynthesis of prostanoids. Angiotensin II (Ang II) plays a role in vascular remodeling, VSMC growth, and collagen deposition.[233] Exposure to ang II induced vascular changes dependent on the COX-1 pathway and COX-1 inhibition prevented alterations in structure, stiffness, and ECM components of resistance arteries.[234] The inhibitory activity of resveratrol towards COX-1 (IC_{50} = 2.6 μM; [232] 0.8 μM[235]) and COX-2 (IC_{50} = 2.2 μM;[232] 1 μM[235]) were shown to be comparable to pterostilbene (IC_{50} = 4.8 μM;[232] 0.7 μM[235] and 1.3 μM;[232] 0.8 μM[235], respectively). However, another study suggested resveratrol was a weak COX-2 inhibitor (IC_{50} = 1 μM and selectivity index COX-1/COX-2 = 0.5 μM) and that hydroxylated but not methoxylated analogues such as pterostilbene (IC_{50} = 1.3 μM[232]) were more potent against COX-2.[236] In general, reported IC_{50} values for pterostilbene are smaller than resveratrol suggesting greater potency of this methoxylated analogue. The role of COX-2 in hypertension is unclear. In

arteries, COX-2 derived products reduced vascular remodeling in response to haemodynamic changes.[237, 238] Yet, endothelin-1 was shown to induce the expression of remodeling genes via pathways involving COX-2/prostacyclin.[239] Further, COX-2 derived mediators may contribute to cardiac remodeling; treatment with a COX-2 inhibitor after myocardial infarction in mice improved cardiac function, and reversed hypertrophy and interstitial collagen.[240]

Another molecular target of stilbenoids are peroxisome proliferator-activated receptors (PPAR), which are steroid hormone receptors involved in inflammation[241] and oxidative stress.[242] Pterostilbene activated PPARα in a concentration-dependent manner; at high concentrations it induced greater PPARα activation than ciprofibrate, a known PPAR agonist.[243] However, resveratrol failed to activate PPARα leading the authors to suggest pterostilbene is a more potent activator of PPARα than resveratrol, at least in rat hepatic cells.[243] In the brain however, resveratrol was a selective activator of PPARα (and PPARγ) in mouse cortical cultures and bovine brain microvessel EC.[244] Yet another study suggested it may act as a PPAR antagonist due to its ability to displace reference ligands from PPARα and PPARγ (IC_{50} 27 – 32 μM).[245] The binding affinity of resveratrol to PPARα in that study was Ki = 2.7 μM,[245] while gnetol was predicted to have greater binding affinity (-8.4 kcal/mol) to PPARα *in silico* compared to a standard agonist (-6.5 kcal/mol).[246] However, it is difficult to make direct comparisons related to affinity and potency based on the current literature, which warrants additional studies. Importantly, PPARα-deficient mice had more pronounced pressure overload-induced cardiac hypertrophy and dysfunction, which was associated with increased expression of inflammatory markers and ECM remodeling.[247]

Many of the effects of resveratrol have been shown to be mediated by adenosine monophosphate-activated protein kinase (AMPK).[248] Resveratrol activates AMPK, which phosphorylates eNOS[249] to enhance endothelial NO generation important for modulating VSMC function and growth. AMPK activation by resveratrol reduces left ventricular hypertrophy in SHR and inhibits hypertrophic signaling.[181, 250, 251] *In vitro*, gnetol and pterostilbene prevented endothelin-1 mediated hypertrophy of cardiomyocytes via AMPK activation, but neither stilbenoid, including resveratrol, reduced left ventricular hypertrophy or activated the AMPK pathway in SHHF rats.[227] Although, these stilbenoids were beneficial for diastolic dysfunction.[227] AMPK activation was increased in mesenteric arteries from SHR[252] and SHHF rats.[228] In contrast, AMPK activation remained unchanged in SHHF rat cerebral arteries even with stilbenoid treatment (not shown),[228] despite an antihypertrophic effect on vessels. This suggests that AMPK signaling does not mediate the effects of resveratrol or its analogues on SHHF rat MCA. However, AMPK is not the only molecular target of resveratrol. It can increase endothelial NO through various pathways[253] including stimulating extracellular signal-regulated kinase (ERK) to likewise increase eNOS activity. Activation of ERK was increased in SHR mesenteric arteries[254] and resveratrol attenuated remodeling by blocking enhanced ERK signaling,[224] whereas ERK activation was normal in SHHF rat mesenteric arteries and MCA (not shown).[228] We suggest stilbenoids act on cerebral arteries via mechanisms independent of AMPK or ERK activation, including those involving anti-inflammatory and antioxidant processes. [211, 255, 256]

Some of the effects of resveratrol are mediated through sirtuin-1 (SIRT1), a class III histone deacetylase. Overexpression of SIRT1 in VSMC attenuated Ang II-induced hypertension, improved vascular remodeling, and inhibited reactive oxygen species (ROS) production, vascular

inflammation, and collagen accumulation in mouse aorta.[257, 258] Resveratrol induced SIRT1-mediated deacetylation of eNOS on lysine residues and enhanced endothelial NO production.[259] Both VSMC SIRT1 overexpression and resveratrol prevented high fat high sucrose-induced arterial stiffness.[260] This effect of SIRT1 was associated with anti-inflammatory and antioxidant effects such as preventing nuclear factor-kappa B (NFκB) activation and vascular cell adhesion molecule 1 (VCAM1) inhibition.[260] Further, resveratrol attenuated high fat high sucrose- and high glucose-induced ROS production in rat aorta and EC, respectively, by attenuating elevated expression of NADPH oxidase, a ROS generator, and reversing SIRT1 downregulation.[261] Importantly, oxidative stress plays an important role in hypertension as it stimulates different redox-sensitive processes, including cellular proliferation/hypertrophy, ECM degradation/deposition, and inflammation.[262] Indeed antioxidant treatment using vitamins corrected vascular remodeling and endothelial function in mesenteric arteries from SHRSP.[263]

The role of inflammation in hypertension has been well documented and is a component of the disease process that is modulated by anti-inflammatory and immunomodulatory effects of resveratrol. Indeed, resveratrol has been reported to be beneficial towards vascular remodeling and reduced elasticity that underly hypertension by modulating inflammatory pathways. For instance, resveratrol attenuated VSMC proliferation induced by pro-inflammatory cytokine, tumor necrosis factor alpha (TNFα).[264] The anti-growth effect was attributed to cell-cycle arrest, which was associated with a decrease in cyclins and cyclin-dependent kinases.[264] Resveratrol also inhibited TNFα-induced expression of MMP, which play a critical role in vascular stiffening, via NFκB inhibition.[264] During inflammation, recruitment and infiltration of inflammatory cells is facilitated by cell adhesion molecules and chemokines. Resveratrol inhibits such molecules and

can interfere with the recruitment of inflammatory cellular mediators. Resveratrol reduced intercellular adhesion molecule 1 (ICAM1) and VCAM1 in TNFα- and lipopolysaccharide-stimulated EC, and prevented monocyte and granulocyte adhesion to EC.[265] Further, resveratrol reduced the binding activity and expression of chemokine receptors on monocytes,[266] which are involved in immune cell-EC interactions that contribute to vascular inflammation. Similar anti-inflammatory and immunomodulatory effects have been observed with pterostilbene. This stilbenoid was shown to inhibit the expression of VCAM1 and ICAM1 in TNFα-stimulated VSMC by suppressing NFκB and MAPK signaling.[267]

The modes of action of resveratrol, pterostilbene, and gnetol on cerebral vessels have yet to be fully elucidated. However, these previous studies support already described anti-inflammatory and antioxidant processes as potential mechanisms by which these stilbenoids might exert their effects on vascular structure and compliance. To confirm this would require additional studies. However, it is also important to consider that these stilbenoids stimulate different pathways to exert their effects even though they are structurally analogous. In a model of brain aging and dementia (senescence accelerated mice P8),[268] the expression of mitochondrial manganese superoxide dismutase (MnSOD), which is important for breaking down free radicals, was reduced and was rescued by pterostilbene but not resveratrol.[269] However, pretreatment of cardiomyocytes with resveratrol showed it increased MnSOD activity without altering protein expression[270] and likely involves the FOXO pathway.[271] In contrast, upregulation of MnSOD by pterostilbene was unaccompanied by SIRT1 expression changes, [269] suggesting modulation of antioxidant enzymes by stilbenoids occurs, at least in part, through divergent mechanisms.

There is a scarcity of information related to the mechanism(s) by which gnetol acts. Interestingly, we showed that gnetol reduced wall stress in healthy cerebral arteries. We propose an enhanced antioxidant potential of gnetol as a possible explanation. With a greater number of hydroxyl substituents compared to resveratrol and pterostilbene, gnetol may be a more potent antioxidant due to a greater capacity for scavenging radicals. A comparison of six stilbenes, including resveratrol, showed that a greater number of hydroxyl groups was associated with enhanced antioxidant activity.[272] The location of hydroxyl groups is also important; resveratrol analogues with 3,4-dihydroxyl groups or those possessing *ortho*- or *para*-dihydroxyl were the most potent antioxidants.[272-275] Other polyphenols such as flavonoids with more phenolic hydroxyl groups also have greater antioxidant activities.[276] More studies are required to compare the antioxidant activities of the stilbenoids in this study. However, stronger antioxidant effects may be sufficient to reduce normal levels of oxidative stress in healthy vessels, thereby resulting in structural changes that would reduce wall stress. Interestingly, vascular remodeling was absent in healthy vessels treated with gnetol; however, one can observe a negligible decrease in media CSA (Figure 8B). This might explain the reduction in stress given that this was not observed with resveratrol or pterostilbene treatment. It is unclear whether a reduction in wall stress in healthy vessels is maladaptive, but the absence of remodeling suggests this is unlikely in these arteries.

4.2 Hypertensive vascular modifications in penetrating arterioles from SHHF rats and SHR

Most of the extant knowledge of the brain microvasculature is derived from studies on superficial resistance arteries, yet penetrating arterioles are one of the most important regulators of vascular resistance and blood flow in the brain. Given this, the brain is an important target organ for hypertension, which is a leading risk factor for stroke,[277, 278] cognitive decline, and dementia.[12, 278] In addition, heart failure potentiates the risk for cognitive decline[16] and promotes the progression to dementia or Alzheimer disease.[17] This study describes for the first time the structural properties, mechanical behaviour, and functional responses in penetrating arterioles from SHHF rats and SHR *ex vivo*.

4.2.1. Structure

Structural changes in penetrating arterioles from SHR and SHHF rats were assessed in terms of geometry. Vessels from both hypertensive strains showed similar structural changes. There was an increase in M/L ratio, despite only a decreasing trend in external and lumen diameters (not significant) and unchanged wall thickness. Constant media CSA suggests these arterioles underwent eutrophic remodeling. This was confirmed by remodeling indices of 124% in SHHF rats and 96% in SHR. Remodeling is probably inward, due to the tendency towards a smaller lumen. Inward eutrophic remodeling is the predominant structural change in resistance arteries during essential hypertension.[19, 279] Previously, pial arterioles from SHRSP were shown to possess smaller diameters.[53] However, in contrast to the findings of this study, hypertrophic growth was described in pial vessels from SHRSP and SHR.[215, 221] Thus, there are regional differences in

remodeling of vessels (eg. hypertrophy of surface arterioles vs. eutrophic remodeling of penetrating arterioles in SHR; combination remodeling of MCA – see previous section vs. eutrophic remodeling of penetrating arterioles in SHHF rat). Differential remodeling may also be due to the size of the vessels (MCA <250 μm vs. penetrating arterioles <100 μm, in this study). A gradient of vascular remodeling was discussed previously by Allen *et. al*., suggesting that hypertrophic response decreases with decreasing vessel size.[280]

Limited studies have investigated the structure of penetrating arterioles in hypertensive models. One study observed hypertrophic growth of these arterioles in SHRSP, where remodeling was most pronounced in vessels <35 μm in diameter.[220] Recently, penetrating arterioles from SHRSP were described as having smaller external and lumen diameters.[119] Remodeling was described as inward hypertrophic growth due to increased media thickness and increased M/L ratio; however, they failed to report the media CSA.[119] Thus, SHR with higher incidence of cerebrovascular disease (ie. stroke) have distinct differences in remodeling of penetrating vessels vs. SHHF rats or SHR. Similar geometric remodeling in SHHF rat and SHR suggests the added risk for heart failure does not induce structural changes in penetrating arterioles different from those in hypertension alone. This is interesting given that left ventricular hypertrophy develops earlier in the heart failure-prone strain (3-5 months vs. 5 months SHR),[226, 281] where earlier onset of cardiac abnormalities might be expected to influence the progression of remodeling.

4.2.2. Mechanical behaviour

Eutrophic remodeling leads to a reduction in wall stress in SHHF rats and SHR penetrating arterioles. Hypertrophic growth that gives rise to a smaller lumen has also been shown to reduce media stress[37, 215] and is thought to protect downstream arterioles, capillaries, and venules from increases in BP.[56, 150, 221, 282] To understand this, recall that blood flow and media stress are largely influenced by the lumen radius, according to the laws of Laplace and Poiseuille. Failure to remodel has been shown to cause blood-brain barrier breakdown, cerebral edema, and cerebrovascular pathology.[150, 282] This suggests that target organs are more vulnerable to pressure-induced damage if remodeling of supplying vessels does not result in a smaller lumen and/or thicker wall in response to increasing BP. Thus, we might expect a greater M/L ratio in SHHF rat and SHR penetrating arterioles to also be protective. It is important to note however, that while remodeling may be adaptive initially, long-term it is invariably detrimental because it increases vascular resistance, which can lead to cerebral hypoperfusion and the development of ischemic lesions[56, 132, 150, 283] and increases the incidence of life-threatening cardiovascular events.[40, 229] For this reason, vascular remodeling in the brain has been identified as a potential risk factor for cerebrovascular disease.[56, 132]

Penetrating arterioles from SHR and SHHF rats exhibit differences in compliance; it was reduced in SHHF rats, but increased in SHR. Thus, the same structural modifications due to eutrophic remodeling influences mechanical properties of penetrating arterioles differently in these hypertensive strains. Decreased compliance would reduce buffering capacity by limiting arteriolar wall distension with increasing intraluminal pressure. Thus, while penetrating arterioles may

structurally adapt in the face of increasing BP to reduce the amount of wall stress, these same modifications likely contribute to the pathogenesis and maintenance of hypertension in the brain by reducing vascular compliance. Further, isobaric stiffness, which is related to geometry and stiffness of structural elements, and wall component stiffness were increased. Therefore, reduced compliance can be ascribed not only to increased M/L ratio, but to stiffer elements that make up the vessel wall. Vascular thickening can result from VSMC hypertrophy and hyperplasia,[10, 31] endothelial dysfunction,[79] and deposition of matrix elements.[57] Quantification of collagenic and elastic matrices in cross-sections of penetrating arterioles from SHHF rats revealed a greater fraction of collagen to elastin. There was no evidence for enlargement of the matrix or growth of VSMC, suggesting enhanced stiffness was likely due to matrix restructuring resulting from collagen/elastin imbalance but not enlargement of the ECM or cellular hypertrophy.

Since the elastic lamina was scarce or highly disorganized, elastin degradation likely contributes to matrix dysregulation. ECM remodeling is modulated by MMP and tissue inhibitors of metalloproteinases (TIMP), and pathological changes can result in an imbalance leading to abnormal expression of MMP and their inhibitors that contribute to increased elastin degradation and collagen deposition.[71] Various MMP are known elastases (MMP2, MMP7, MMP9, and MMP12) and collagenases (MMP1 MMP2, MMP3, and MMP9), which digest elastin and collagen, respectively.[48, 71] Changes in haemodynamics, vascular inflammation, and ROS can regulate the activities of MMP.[284, 285] In hypertensive patients, serum MMP9 was elevated, whereas TIMP1 was reduced,[286] suggesting increased elastin degradation by MMP9 due to reduced inhibition by TIMP1. Increased MMP9 expression correlated with increased systolic BP in essential hypertension and increased MMP2 and MMP10 predominated in end-organ damage once

hypertension was established.[287] However, increased TIMP1 has also been associated with elevated MMP9 expression.[288] These changes were significantly correlated with arterial stiffness in hypertensive patients,[288] likely owing to TIMP1 inhibition of collagen degradation by MMP9. Elevated serum MMP3 expression was also strongly associated with arterial stiffness.[289] Increased MMP9 and TIMP1 levels correlated with greater left ventricular mass and diastolic dysfunction in hypertension.[290] In SHHF rats, left ventricular collagen was increased at 13 months of age and changes in MMP and TIMP were observed during compensatory hypertrophy and heart failure; MMP2, MMP9, and MMP3 expression were increased, whereas TIMP4 was decreased.[291] A collective glance at these studies emphasize the dynamic turnover of matrix components regulated by MMP that contribute to abnormal collagen/elastin expression that underpin arterial stiffening. In general, abnormal MMP and TIMP expression is expected to bias the ECM architecture towards more fragmentation of elastin than collagen, leading to excessive collagen deposition. Because collagen is a non-distensible material, the stiffening of penetrating arterioles from SHHF rats can be attributed to the accumulation of collagenic material. This may be perpetuated by enhanced collagen synthesis by various cells of the arteriolar wall. Ang II stimulates VSMC collagen production in SHR, which is mediated by AT_1 receptors via MAP/ERK signaling.[57] Endothelium-derived NO modulates collagen metabolism in VSMC[292] and EC may also produce collagenic products. Aged EC undergo morphological changes when stimulated with TNFα resulting in a VSMC-like phenotype and increased collagen expression.[293] Collagen production has also been demonstrated in fibroblasts in response to Ang II-induced endothelin-1 expression.[294, 295]

SHR penetrating arterioles were less stiff and more compliant in spite of constant wall component stiffness. This was represented by a rightward shift of the elastic modulus vs. pressure curve. This

was confirmed by quantifying the collagenic and elastic matrices, which were similar in terms of abundance and organization in WKY rats and SHR. Thus, geometric changes but not wall component stiffness contributes to improved compliance. Because wall stiffness (collagen/elastin ratio) was unchanged, this suggests that the elastic range of these vessels increased; elastin continue to function at higher pressures rather than shifting the mechanical load to collagen. The redistribution of mechanical load within the ECM may be attributed to matrix interactions with adhesion proteins like transmembrane integrin receptors. Integrins regulate MMP expression by promoting synthesis at the transcriptional level and converting inactive pro-MMP to active proteases.[296] Mesenteric resistance arteries from SHR exhibited elevated expression of $\alpha_v\beta_3$ and $\alpha_5\beta_1$ integrins and collagen.[31] Integrins like $\alpha_5\beta_1$ interact with ECM adhesion protein, fibronectin[297] to form complexes that serve as anchorage sites to matrix and cytoskeletal elements. Fibronectin, $\alpha_5\beta_1$, and the number of focal VSMC-elastic lamina adhesion complexes were increased in SHR arteries.[298, 299] Thus, a greater number of fibronectin-$\alpha_5\beta_1$ sites might contribute to increased VSMC-elastic lamina connections, thereby transferring the mechanical load to elastic components.[73] This might provide a mechanism to explain the absence of changes in elastin/collagen content or mechanical behaviour in SHR arteries[298] or unchanged wall component stiffness despite improved compliance in SHR penetrating arterioles reported here. Therefore, this may represent a mechanical adaptation to increasing BP. In SHRSP, pial arterioles were also observed to be less stiff and more compliant; however, this change in mechanics was attributed to an increase in elastin content.[214, 215, 220, 221]

Because integrins are connected directly to the ECM, changes in the anchoring of cells to matrix materials would reorganize the vascular architecture.[100] In turn, extracellular signals may be

transduced to cytoskeletal elements to promote VSMC restructuring.[100] Despite increased M/L ratio in SHR arterioles, there were no quantitative changes related to VSMC or the matrix. The number of fibronectin-integrin complexes that might suggest topographical restructuring of VSMC should be a future line of research.

Taken together, an upward shift in elasticity suggests penetrating arterioles undergo mechanical adaptations during elevations in BP but not when there is greater risk for heart failure. Thus, SHHF rats may be more prone to cerebrovascular damage than SHR.

4.2.3. Vascular function

Endothelium-dependent and independent vasomotor responses were investigated in penetrating arterioles from SHHF rats and SHR to determine functional abnormalities. Glutamate/D-serine, acetylcholine, and sodium nitroprusside elicited concentration-dependent relaxation of penetrating arterioles from normotensive animals. In SHHF rats, endothelium-dependent relaxation to glutamate/D-serine was completely abolished in penetrating arterioles and high concentrations induced constriction. Glutamate-induced vascular relaxation in the brain is mediated by N-methyl-D-aspartate receptors (NMDAR) which leads to the production of NO,[300] which diffuses to underlying VSMC. NO stimulates soluble guanylyl cyclase (sGC) and produces a rise in cyclic GMP (cGMP) levels,[301, 302] thereby causing dilation. NMDAR are present in cerebral arteries; coactivation by glutamate/D-serine dilated MCA from mice in an endothelial and eNOS-dependent manner.[303] They are also present in VSMC.[304] Previously, agonist-mediated endothelium-dependent vasodilation was reduced in SHR arterioles and this was attributed to impaired NO

synthesis or action.[125] However, impaired NO synthesis by the endothelium is not the most probable explanation for the abnormal vasomotor responses in SHR and SHHF rats in this study, since the NO donor, sodium nitroprusside, failed to relax vessels causing constriction instead. Rather this suggests a decreased responsiveness of VSMC to NO. This may be due to reduced sGC expression or activity. Changes in the redox state of sGC can render it insensitive to NO. [305] Indeed, oxidative stress in mesenteric arteries from SHR was associated with reduced sGC expression and activity, and impaired cGMP-dependent relaxation.[306] In young SHR aorta, expression of α_1 and β_1 subunits of sGC, cGMP and its receptor were reduced by 6 weeks of age, [307] suggesting the sGC/cGMP pathway becomes impaired early during disease progression and may contribute to the pathogenesis of hypertension. Thus, in SHHF rats, attenuated glutamate-induced relaxation of penetrating arterioles is likely due to VSMC dysfunction, whereas in SHR adaptive responses maintain normal relaxation to glutamate, at least in the brain.

Metabotropic glutamate receptors (mGluR) have been identified in parenchymal vessels and are present in both EC and VSMC.[308] mGluR activation dilates cerebral vessels i*n vivo* and relies on products of the arachidonic acid cascade, including epoxyeicosatrienoic acids (EET) and COX-2 metabolites.[309] A similar mechanism via mGluR activation may exist for glutamate-induced relaxation in penetrating arterioles observed in SHR. However, it was shown previously that isolated MCA did not change their diameter to mGluR agonist (S)-3,5-dihydroxyphenylglycine, yet relaxed to direct application of EET.[309] Stimulation of another glutamate receptor, alpha-amino-3-hydroxy-5-methylisoxazole-4-propionate receptors (AMPAR) also induces dilation of cerebral arterioles *in vivo*.[310] Although, AMPAR was shown to be present in primary cultures of cerebral microvascular EC,[311] AMPAR-mediated relaxation of cerebral arterioles does not require

eNOS, COX-2, and cytochrome P-450 epoxygenase but depends on adenosine receptor activation.[310] Thus there are possible pathways that may mediate glutamate-induced vasodilation in SHR but more studies are required to confirm this.

In SHHF rat arterioles, constriction to high concentrations of glutamate and sodium nitroprusside suggests reduced VSMC responsiveness to NO coincides with the release of endothelium-derived constricting factors, such as endothelin-1, Ang II, COX products, and hydroxyeicosatetraenoic acids.[312] We propose that the mechanism by which SNP induces constriction is via the activation of G_q-protein coupled receptors (GPCR) on VSMC by endothelium-derived constricting factors. This would lead to the transduction of the phospholipase C pathway forming inositol triphosphate (IP_3) and diacylglycerol (DAG). IP_3 activates sarcoplasmic reticulum IP_3-activated Ca^{2+} channels to stimulate the release of Ca^{2+} to initiate VSMC contraction. IP_3 receptor-mediated Ca^{2+} influx may contribute to agonist-induced contraction of VSMC and myogenic behaviour.[313] Alternatively, DAG activates protein kinase C (PKC) which may also play a role in VSMC contraction.[314] In addition, extracellular Ca^{2+} influx via voltage-dependent L-type Ca^{2+} channels may contribute to an increase in intracellular Ca^{2+}.[315] Normal or potentiated endothelium-dependent relaxation to acetylcholine in SHHF rat and SHR arterioles, respectively, also suggests vascular adaptations that involve endothelium-derived relaxing or hyperpolarizing factors, that are products of the arachidonic acid cascade[312] and may involve gap junction communication between EC and VSMC.[316] However, it should be noted that acetylcholine has been shown to act directly on venous SMC; therefore, acetylcholine might also induce dilation via an endothelium-independent manner.[317]

It must be noted that response to acetylcholine varied with concentration in healthy vessels, with vasoconstriction occurring at low concentrations and vasodilation occurring with high dose acetylcholine. The constriction response is not without precedent having been reported previously in the literature. Notably, topically applied acetylcholine (10^{-7} and 10^{-5} M) to pial arterioles in newborn piglets elicited vasoconstriction. This response was blocked by indomethacin but L-nitroarginine (an NO synthase inhibitor) had no effect on constriction in the presence or absence of indomethacin. However, the effects of acetylcholine can vary depending on age, species, vascular bed and concentration used.[318, 319 319] In juvenile pigs, acetylcholine relaxed pial arterioles which was inhibited by L-nitroarginine with or without indomethacin and was associated with increased cyclic GMP.[319] In coronary arteries of baboons, acetylcholine elicits a biphasic response at high doses (constriction followed by dilation), while it induces only relaxation at low concentrations.[318] In iliac arteries of baboon and coronary arteries of dogs, acetylcholine resulted in only vasodilation at all doses, whereas a biphasic response was observed in coronary arteries from calves at high doses.[318] Vasoconstriction may result from the direct activation of VSMC muscarinic receptors and is likely mediated by prostanoids. In newborn pig, acetylcholine-induced arteriolar constriction was associated with increased prostanoid levels and was blocked by muscarinic (M1) antagonists.[320] In baboon coronary arteries, vasoconstriction and vasodilation responses were blocked by atropine, a nonselective muscarinic receptor antagonist.[318]

The results of this study have not been consistent with findings in other vascular beds and are therefore novel. Whereas acetylcholine-induced relaxation was maintained (SHHF rats) or enhanced (SHR) in penetrating arterioles, these responses were impaired in mesenteric arteries from SHR[321, 322] and SHRSP.[323, 324] In mesenteric arteries from SHRSP, the release of NO and

endothelium-derived hyperpolarizing factor were reduced.[323] However, it has also been suggested that impaired endothelium-dependent relaxation to acetylcholine in mesenteric resistance arteries from SHRSP does not involve a reduced endothelium-derived relaxing factor or responsiveness to it, but rather some substance that interferes with the release and/or action of that factor.[324]

Because SHR exhibit learning and memory impairments,[325, 326] our findings identify the potential vascular contributions to cognitive decline and dementia related to hypertension and heart failure. Cognitive impairment occurs with aging in various rat strains (eg. SD, WKY, Long-Evans, Fisher-344, and Emd:Wi-AF/Han) and can be detected as early as 14 weeks depending on the behavioural test employed[327] but this is aggravated by hypertension. At 12 months of age, these animals take longer and make more errors in radial maze tests than normotensive SD rats.[328] SHR, SD, and WKY rats all exhibit age-related decreases in spatial learning and memory but SHR were more impaired than the other strains at the same age (12 months), while SD performed the best.[329] Spatial learning and memory deficits in aged rats corresponded with abnormal hippocampal activity[330] and decreased mGluR5 expression in the dendrites of the CA1 region.[331] Age-related cognitive decline was also associated with decreases in brain volume[332] and neuronal atrophy.[333] Similar brain-related changes are also observed in SHR; by 4-7 months of age these animals begin exhibiting brain atrophy,[334] including neuronal loss in the hippocampus, and astrocytic reaction.[335]

4.3 Summary

The key findings of this study are summarized in Appendix C: Table 6. We demonstrate that predisposition for heart failure superimposed upon hypertension induces regional differences in

remodeling within the cerebrovascular bed; combined hypertrophic and eutrophic remodeling of MCA vs. purely eutrophic remodeling of penetrating arterioles. MCA from SHRSP undergo eutrophic remodeling[222] before pial arteries,[282] suggesting the effects of hypertension present first in large cerebral arteries and that remodeling of these vessels may protect distal vessels. However, the present study showed that despite lowered wall stress in MCA, remodeling was insufficient to protect downstream vessels in SHHF rats, which underwent eutrophic remodeling. Remodeling of MCA was attenuated with stilbenoids due to their anti-growth properties, despite no effect on BP. Eutrophic remodeling was similarly observed in penetrating arterioles of SHR, which suggests the added risk for heart failure does not influence the remodeling phenotype.

There were no regional differences in compliance in SHHF rats; however, the determinants of compliance differed. Reduced compliance was controlled by geometric changes and increased collagen deposition in penetrating arterioles, whereas compliance of MCA was determined by only increased wall component stiffness. The latter was improved by stilbenoids in SHHF rat cerebral arteries but was insufficient to normalize compliance. The mechanics of penetrating arterioles were different in SHR; the elastic range was increased such that vessels were less stiff and more compliant. We suggest that predisposition for developing heart failure induces changes in mechanical behavior that might predict a greater risk for cerebral hypoperfusion, which may contribute to the development of cognitive decline and dementia. Mechanical changes of SHR penetrating arterioles are probably an adaptive response to normalize CBF.

In the present study, endothelium-mediated relaxant responses were attenuated in SHHF rat penetrating arterioles to glutamate, but not to acetylcholine. In contrast, SHR penetrating arterioles

maintained normal glutamate-induced relaxations but exhibited a potentiated relaxant response to acetylcholine. Relaxations to NO donor sodium nitroprusside in both strains resulted in constriction, suggesting reduced vasodilatory responsiveness of VSMC to NO, which may coincide with the release of constricting factors. Functional adaptations were evident in SHR (glutamate/D-serine) and SHHF rats (acetylcholine), which may involve activation of alternate receptors or release of endothelium-derived relaxing factors or an NO/endothelium-independent mechanism. However, in the case of SHR, adaptations lead to enhanced relaxation responses.

The dissimilar vascular properties in SHHF rats and SHR reported here may be due to strain-specific differences in humoral activity, inflammation, and oxidative status, despite a similar genetic background. This may be extrapolated, in part, from studies investigating sex differences in BP and response to pharmacotherapy. For instance, mean arterial pressure was shown to be higher in male SHR compared to females.[336] Ang II type 1 receptor antagonists such as losartan and irbesartan can be effective treatments in SHR[337, 338] and SHHF rats.[339] However, endothelial dysfunction improved better with losartan in female SHR than males,[338] while female SHHF rats were resistant to the antihypertensive effects of irbesartan observed in males, even with successful receptor antagonism.[340] Sex-specific response to pharmacotherapy in SHR were related to increased ang II AT_2 receptors but not eNOS,[338] whereas differences in humoral activity (ie. plasma renin activity and urinary endothelin excretion) may explain differences in SHHF rats.[340] Levels of EET were greater in female vs. male SHR but blocking epoxide hydroxylase had no effect on mean arterial pressures, suggesting EET does not play a role in sex differences related to BP in SHR.[336] Studies directly comparing SHHF rats and SHR also provide clues that may explain differences. For example, these strains have been shown to respond differently to doxorubicin (DOX) treatment, where SHHF rats surprisingly exhibited less cardiotoxic effects to DOX than

SHR.[341] This was attributed to differences in arachidonic acid metabolism; DOX increased EET in both strains but only leukotriene D4 was elevated in SHR.[341] SHHF rats also exhibited more pulmonary oxidative stress (reduced ascorbate and heme oxygenase-1), inflammation (increased macrophage activation, neutrophils, and TNFα), and impaired iron homeostasis (increased ferritin and reduced iron-binding capacity) than SHR.[342] Left ventricular mass was increased over time in both strains, but changes in BP correlated with alterations in ventricular Ca^{2+}-dependent NOS activity, eNOS expression, and plasma NO levels only in SHHF rats.[343] Compared to male SHR, SHHF rats exhibited elevated levels of aldosterone, atrial natriuretic peptide, and greater plasma renin activity; the latter was also increased in female SHHF rats but was temporally delayed compared to males.[344] Thus, vascular processes sensitive to oxidative, inflammatory, and humoral influences may provide a mechanism explaining strain-specific differences related to mechanical behaviour and function in cerebral vessels from SHHF rats vs. SHR.

Improved mechanical behavior and functional adaptations in SHR arterioles suggest outcomes related to hypertension, such as the risk of cerebral hypoperfusion, might be reduced in SHR. An increased M/L ratio without a corresponding increase in media CSA implies a smaller vessel diameter in both SHHF rats and SHR, which in turn suggests a decrease in resting cerebral perfusion. However, greater compliance and reduced stiffness exhibited by vessels in SHR would increase the capacity to accommodate changes in blood flow despite a smaller diameter. Whereas, reduced compliance and increased stiffness in SHHF rats would further promote a reduction in CBF. Further, relaxation response when challenged with acetylcholine was increased in SHR. Taken together, this suggests maximal flow capacity might be maintained in SHR through mechanisms involving acetylcholine. Although relaxation to acetylcholine was normal in SHHF

rats, dynamic responses to another dilatory stimulus, glutamate/D-serine, was entirely abnormal. Therefore, likely both resting CBF and the maximal flow capacity are reduced in SHHF rats, which may accelerate the development of cognitive decline in these animals. However, SHR can develop cognitive impairment and cerebral damage relatively early in their lifetime. Therefore, it is unclear how improved vascular mechanics and enhanced function benefit SHR, but it may represent a delay in the onset of hypertension-induced cognitive decline compared to SHHF rats. While cognitive function and microanatomical changes in the brain of SHR have been well characterized there is still a need to further elucidate potential differences in SHHF rats.

5 Conclusion

The findings of the present study provide new insight into the vascular abnormalities of superficial cerebral arteries and penetrating arterioles in SHHF rats and SHR. There were regional differences in geometric remodeling and determinants of compliance in the cerebrovasculature of SHHF rats. Stilbenoids attenuated vascular abnormalities, but there was no difference in the effectiveness of treatment between resveratrol, pterostilbene, and gnetol. Despite similar remodeling in SHHF rat and SHR arterioles, vascular adaptations improved stiffness/compliance and enhanced function in hypertension, but not when there was a propensity for heart failure. Thus, resting CBF and maximal flow capacity might be maintained in SHR but reduced in SHHF rats, which may accelerate the development of cognitive impairment in these animals. This implicates differential vascular abnormalities that might influence the development and progression of cognitive decline in hypertension alone vs. with the risk for heart failure.

6 Future directions

6.1 Conducted vasomotor responses

Vasomotor responses initiated from local sites can spread over multiple vascular branches, coordinating local vascular resistance with vascular responses across the arterial network to effectively regulate changes in CBF.[345] Due to the paucity of information related to the conduction of vasomotor responses in penetrating arterioles, we attempted preliminary studies related to conducted vascular function.

6.1.1 Methodology development

To study conducted vasomotor responses, conventional pressure myography was combined with microejection methods. This is distinct from bath application of an agonist in that the agonist is applied locally (Appendix D: Figure 23). Thus, local responses initiated at the site of administration and responses that travel to a secondary site along the length of the vessel can be measured. Penetrating arterioles from SD and SHHF rat were isolated and cannulated as described in section 2 of this thesis. Glass microcannulae (<3 µm diameter tip) were backfilled with agonist, mounted to a micromanipulator, and connected to a picospritzer (10-15 psi). Different pulse durations (length of time agonist is administered; 450 msec, 1s, 5s, and 10s), pressures (30, 45, and 60 mm Hg), and concentrations of acetylcholine (1M, 0.5M, 0.25M, 0.1 µM, 1µM, and 10 µM) were attempted. During initial stages of method development, water was tested as a vehicle control in MCA and a cannula position of ~50 µm from the vessel wall was chosen by utilizing a blue dye to determine the distance with minimal agonist spread. Testing vasomotor responses

involved the following steps: 1) measurement of local response to agonist at zone 2 and 2) measurement of conducted response at zone 1 (~500 µm downstream of zone 2) while applying agonist at zone 2 (Appendix D: Figure 23).

6.1.2 Preliminary findings

Acetylcholine produced the best response at 1M concentration when administered at 5s duration at 60 mm Hg. The majority of healthy vessels tested exhibited a biphasic response to acetylcholine (ie. constriction proceeded by relaxation; Appendix E: Figure 24A) similar to global responses to increasing concentrations of acetylcholine (Figure 21C and E). However, the degree of constriction seems to be greater than dilation (Appendix E: Figure 24B and C, respectively). Penetrating arterioles from SHHF rats also exhibited a biphasic response to acetylcholine. In one vessel tested, the predominant conducted response was relaxation. When different parameters including (Appendix E: Figure 24B) percent constriction, (2C) percent dilation, (2D) rate of response, and (2E) rate of recovery were compared there was a trend in decreasing rates of response and recovery, as well as, a tendency towards enhanced constriction and reduced relaxation to acetylcholine. We suggest further studies to increase the value of *n* to improve statistical power and to test these responses in SHR. In addition, since the present study revealed global response to glutamate/D-serine was reduced in SHHF rat arterioles, conducted responses to glutamate should also be investigated in penetrating vessels from SHHF rats and in SHR.

6.2 Effects of mechanical strain on cultured VSMC from penetrating arterioles

Blood vessels express most predominantly connexin (Cx) 37, Cx40, Cx43, and Cx45.[346] which make up gap junctions considered to be important for conducted vasomotor responses. Studies suggest that mice with Cx40-deficiency or with mutant Cx40 exhibit elevated arterial pressures and the amplitude and duration of conducted vasodilation (but not conducted vasoconstriction) are attenuated in arterioles.[347, 348] In SHR, Cx37 expression, is significantly reduced in the endothelium of mesenteric arteries.[349] Since preliminary conducted functional studies represent potential abnormalities related to conducted vasomotor responses, the effects of mechanical strain were tested.

6.2.1 Methodology development

For these initial studies we employed a FlexCell® tension system (FlexCell International, Burlington, NC, USA), which is a computer-controlled bioreactor that uses vacuum pressure to apply cyclical strain to cells cultured on flexible bottom plates. Upon application of the vacuum the flexible bottom deforms, and the overlying cells are stretched. This was used to simulate the mechanical forces exerted under physiological and hypertensive states. First, VSMC were isolated from SD and SHHF rat arterioles (<70 μm) by modifying protocols described previously in mouse.[350, 351] VSMC were cultured on elastin-coated flexible bottom plates and were verified by immunocytochemistry using α-SMC actin (Sigma Aldrich, St. Louis, MO, USA) as a cellular marker for VSMC and RECA-1 (Abcam, Cambridge, UK) for EC. Cyclical mechanical strain was applied to VSMC to achieve ~20% maximal distension on the culture surface,[352] to replicate the mechanical forces due to hypertension. For physiological stretch, ~5% distension was applied.[36,

[353] Both protocols were performed over the course of 12 hours at a cyclical frequency of 0.25 hz. Afterward, VSMC protein lysates were prepared in RIPA buffer and Cx37 (Abcam, Cambridge, UK), Cx40 (Millipore, Burlington, MA, USA), and Cx43 (Millipore, Burlington, MA, USA) expression were detected by conventional western blotting, where β-actin was used as a loading control.

6.2.2 Preliminary findings

Cultured VSMC isolated from rat arterioles were confirmed by immunofluorescence of α-SMC (representative image shown in Appendix D: Figure 24A) and absence of RECA-1 staining. Preliminary quantification of Cx37 and Cx40 were inconclusive (not shown). Cx43 was upregulated in SD rat VSMC subjected to hypertensive stretch (Appendix F: Figure 25B). Levels of Cx43 were lower in VSMC isolated from SHHF rats during physiological stretch and were likewise increased during hypertensive stretch; however, Cx43 levels remained lower than in SD rats. We recommend pursuing a more comprehensive analysis of Cx expression in association with conducted functional studies in SHHF rat and SHR arterioles, especially with regards to Cx43. Although, our preliminary findings were inconclusive for other Cx mentioned herein, it would be premature to exclude them from future investigations.

6.3 Vascular properties of penetrating arterioles in brain slices

The penetrating arterioles used in the present study are divorced from their microenvironment and lack the sympathetic and parasympathetic innervations, as well as, cellular interactions *in situ.*

Therefore, we attempted integrating conventional pressure myography with 2-photon imaging to develop a modified *ex vivo* technique[354] to study penetrating arterioles in brain slices.

6.3.1 Methodology development

Cortical brain slices (~250 µm thick) were prepared from intact brain by vibratome in cold, oxygenated artificial cerebrospinal fluid (aCSF; pH 7.4). Pressure myography of penetrating arterioles were attempted in slices using glass microcannulae (<3 µm diameter tip) mounted to a micromanipulator and connected to a pressure transducer. Vessels were continuously bath perfused with aCSF at 37°C.

6.3.2 Experimental observations

The cannulation of vessels in brain slices has been successfully implemented by the Filosa group.[354] However, several obstacles arose while attempting to adapt the technique. Manual cannulation of brain slices is technically challenging, and successful cannulations were rare. Difficulty cannulating can be ascribed in part to intact meninges, which acted as a physical barrier to a vessel "opening." To work around this, two different methods were employed. First, the cannula was used to "pierce" through the meninges; however, due to the "stickiness" and flexibility of the brain slices attempts were usually unsuccessful. Second, the meninges were removed, either by stripping the brain of this layer prior to slicing or by cutting the outer edge of the brain slice. This often resulted in the loss of vessels. When a vessel was successfully cannulated (Appendix G: Figure 26) other obstacles were noted. First, it was difficult to confirm the cannula was indeed in the vessel and not below or above the plane of the arteriole. Second, not all cannulations resulted

in successful pressurization of the vessel. Indeed, even when pressurization was reached incrementally increasing intraluminal pressure failed to change the vessel diameter; sometimes this was unexplainable and other times it was due to a blocked cannula. Due to the very small diameter of the cannula tip, blocked cannulas were very common.

Despite these challenges, the use of this innovative technique would be most ideal for studying penetrating arterioles under conditions that mimic the brain environment and could offer valuable insight not possible with isolated vessels.

Appendix A

Table 5. Formulae to calculate seven parameters of vessel mechanics[224]

Vessel Mechanics Parameter	Formula	Legend
Media stress (δ)	$\delta = \frac{PD}{2WT}$	P – intraluminal pressure (converted to mmHg, where 1mmHg = 1.334×10^3 dyn/cm2) D – lumen diameter WT – media thickness
Media strain (ε)	$\varepsilon = \frac{(D - Do)}{Do}$	D – observed lumen diameter D_o – baseline diameter at 3 mmHg
Elastic modulus (δ)	$(y = ae^{bx})$: $\delta = \delta_\theta e^{\beta\varepsilon}$	Exponential curve of the stress-strain data δ_θ – stress at baseline diameter β – a constant related to the rate of increase in the stress-strain curve
Media CSA	$CSA = \pi\frac{(D_e^2 - D_i^2)}{4}$	D_e – external diameter D_i – lumen diameter
Remodeling index[53]	Remodeling index = $100 \times \frac{(D_i)_n - (D_i)_{remodel}}{(D_i)_n - (D_i)_h}$ $(D_i)_{remodel} = \left((D_e)_h^{\,2} - 4 \times \frac{CSA_n}{\pi}\right)^{0.5}$	$(D_i)_n$ – mean lumen diameter of normotensive rats $(D_i)h$ – mean lumen diameter of hypertensive rats $(D_e)_h$ – mean external diameter of hypertensive rats CSA_n– CSA of normotensive vessels
Growth index[10]	Growth index = $\frac{(CSA_h - CSA_n)}{CSA_n}$	CSA_h– mean media CSA of hypertensive vessels CSA_n– mean media CSA of normotensive vessels

Appendix B

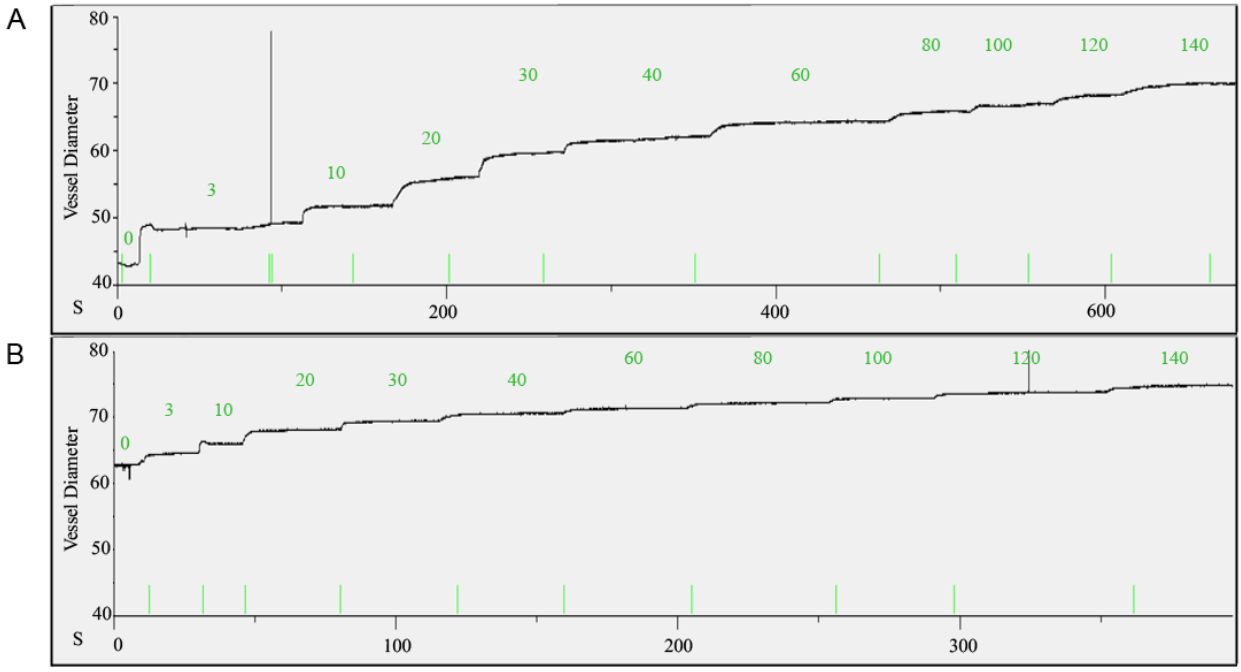

Figure 22. Representative pressure myography traces. Incremental increase in diameter of penetrating arteriole from SD (A) and SHHF (B) with step-wise increase in pressure. Pressures indicated in green.

Appendix C

MCA		Penetrating arterioles	
SHHF		SHHF	SHR
↓	Remodeling	Eutrophic	Eutrophic
↓ =	Compliance	↓	↑
= =	Stiffness	↑	↓
↑ ↓	Wall component stiffness	↑	=
	Collagen-elastin ratio	↑	=
	Glu/D-ser	↓	=
	Ach	=	↑
	SNP	↓	↓

Stilbenoid treatment

Table 6. Summary of vascular changes observed in MCA and penetrating arterioles during hypertension alone and with risk for heart failure.

Appendix D

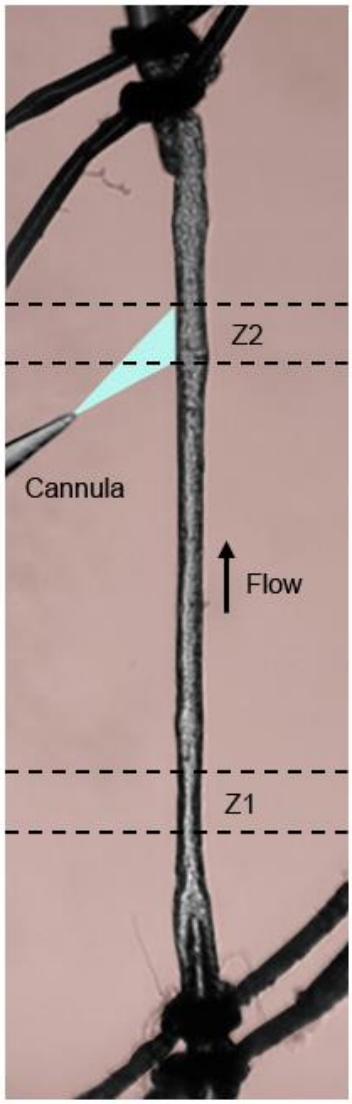

Figure 23. Global vs. local application of agonist to cannulated penetrating arterioles. Area in pink shows global application of an agonist via bath perfusion. In contrast, local application to study conducted functional responses are focally applied (blue area). Arteriole segments are first tested for functional viability by focal application of agonist at zones 1 and 2. Afterwards, agonist is applied at zone 2, but diameter is measured at zone 1 to quantify conducted responses.

Appendix E

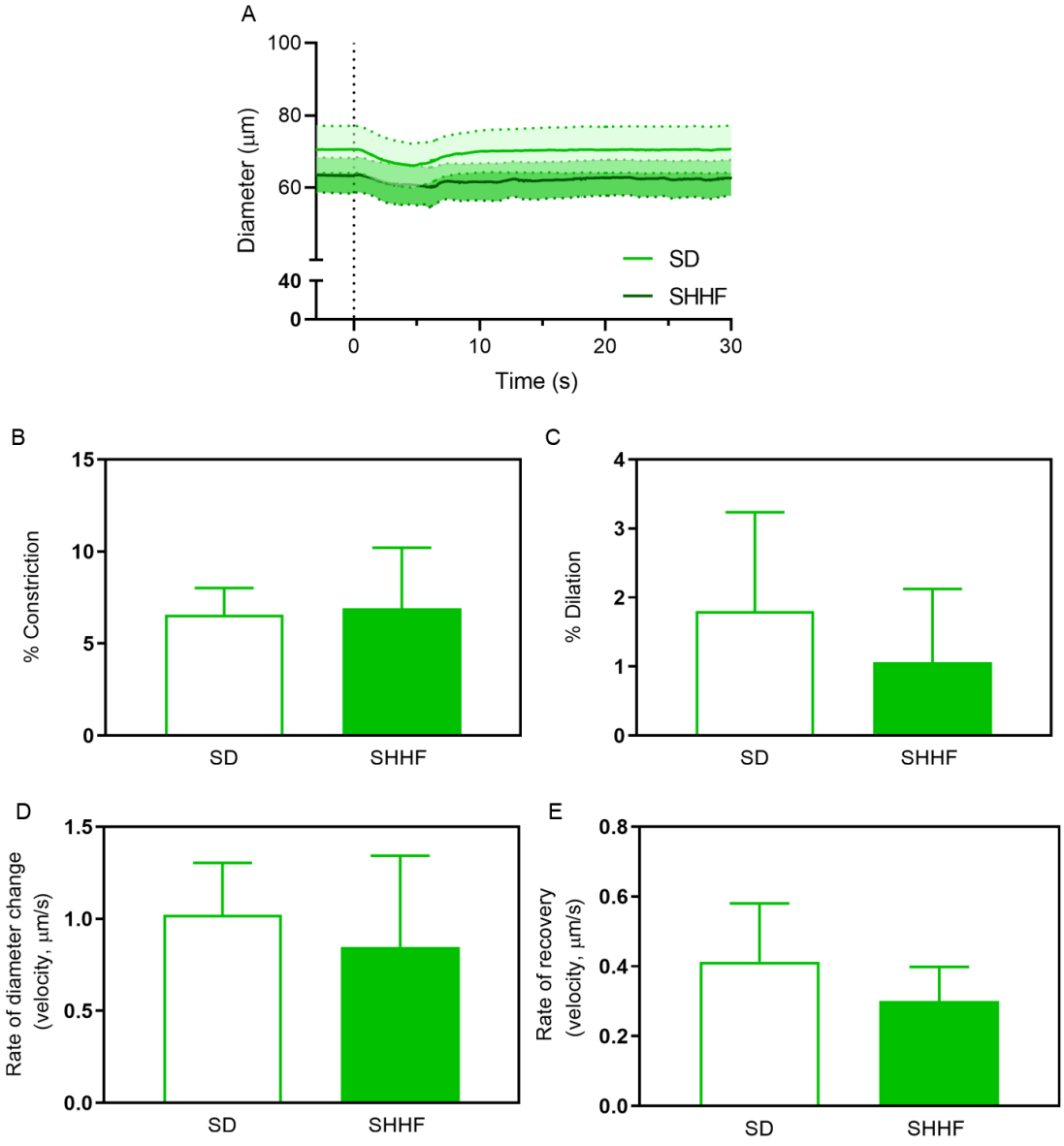

Figure 24. Conducted vasomotor responses to acetylcholine in penetrating arterioles from SHHF rats. (A) Mean diameter changes over time 400-500 µm downstream from site of local application of 1M acetylcholine. Vertical dotted line represents time at which acetylcholine was

administered. Percent constriction (B), percent dilation (C), rate of response (D), and rate of recovery (E) (to acetylcholine is similar in SD and SHHF. n = 4-6. Error bars represent SEM.

Appendix F

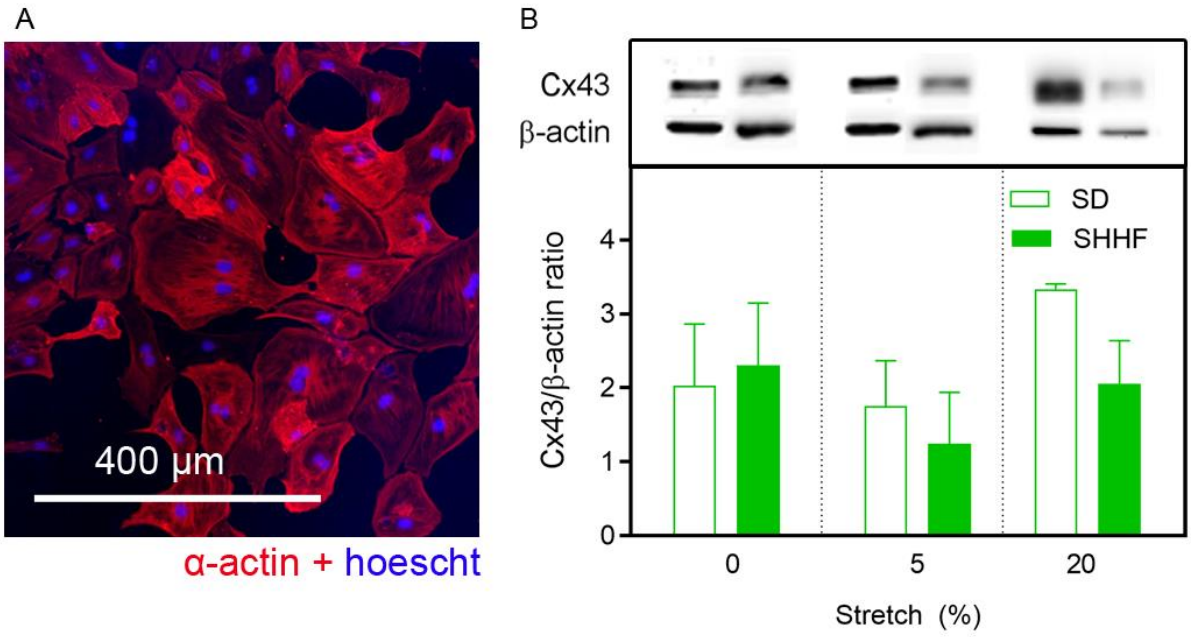

Figure 25. Effects of mechanical strain on brain VSMC isolated from SD and SHHF rats. (A) Cultured VSMC isolated from brain vessels. Red: α actin. Blue: Hoescht nucleic acid stain. (B) Cx43 was upregulated in SD rat VSMC subjected to ~20% strain (hypertensive state) vs. ~5% strain (physiological stretch). Cx43 expression was lower in SHHF rat during physiological stretch compared to SD rat. Levels of Cx43 increased during hypertensive stretch but remained lower than SD rat. n = 2-3. Error bars represent SEM.

Appendix G

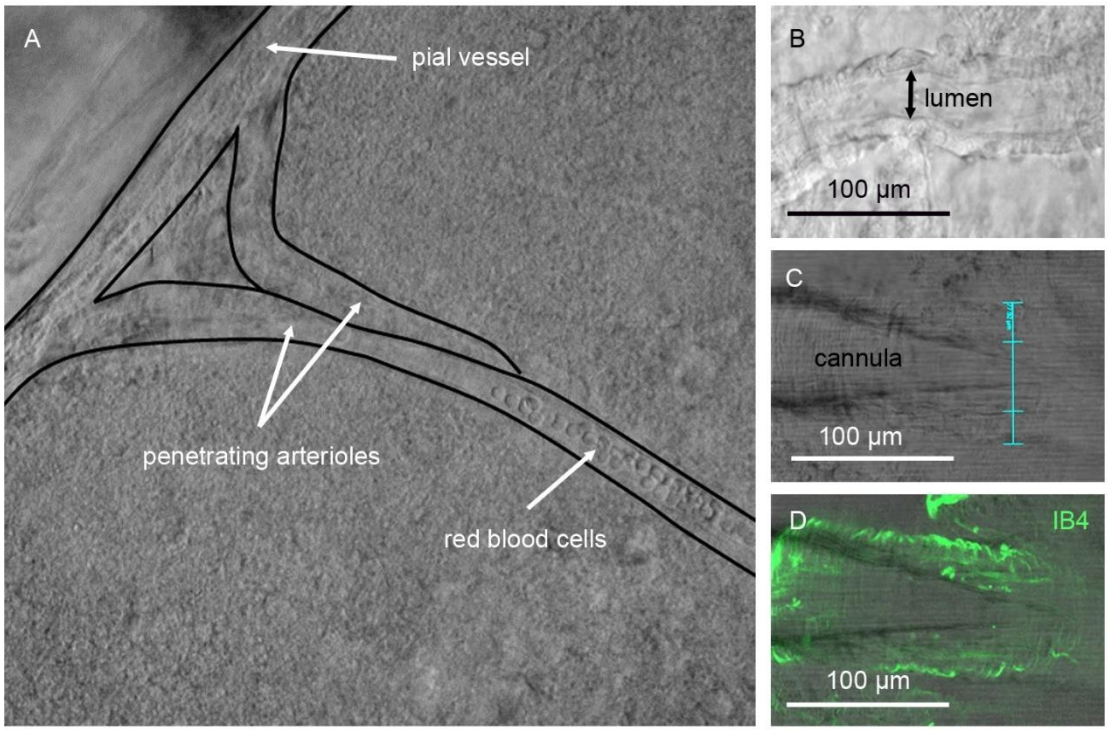

Figure 26. Observation of penetrating arterioles in brain slices under 2-Photon microscopy. (A) A brain slice showing penetrating vessels coming off a pial vessel. (B) Penetrating arteriole with visible lumen and wall. (C) Lumen of cannulated arteriole can be measured, (D) which is facilitated by isolectin B4 (IB4) labelling of the endothelium.

1. Touzani O, MacKenzie, E.T. Cerebrovascular Disease. In: A. H. V. Schapira, ed. *Neurology and Clinical Neuroscience* Philadelphia, PA: Mosby, Inc. ; 2007.
2. Jain V, Langham MC and Wehrli FW. MRI estimation of global brain oxygen consumption rate. *J Cereb Blood Flow Metab*. 2010;30:1598-607.
3. Weber MA, Schiffrin EL, White WB, Mann S, Lindholm LH, Kenerson JG, Flack JM, Carter BL, Materson BJ, Ram CV, Cohen DL, Cadet JC, Jean-Charles RR, Taler S, Kountz D, Townsend RR, Chalmers J, Ramirez AJ, Bakris GL, Wang J, Schutte AE, Bisognano JD, Touyz RM, Sica D and Harrap SB. Clinical practice guidelines for the management of hypertension in the community: a statement by the American Society of Hypertension and the International Society of Hypertension. *J Clin Hypertens (Greenwich)*. 2014;16:14-26.
4. Dasgupta K, Quinn RR, Zarnke KB, Rabi DM, Ravani P, Daskalopoulou SS, Rabkin SW, Trudeau L, Feldman RD, Cloutier L, Prebtani A, Herman RJ, Bacon SL, Gilbert RE, Ruzicka M, McKay DW, Campbell TS, Grover S, Honos G, Schiffrin EL, Bolli P, Wilson TW, Lindsay P, Hill MD, Coutts SB, Gubitz G, Gelfer M, Vallee M, Prasad GV, Lebel M, McLean D, Arnold JM, Moe GW, Howlett JG, Boulanger JM, Larochelle P, Leiter LA, Jones C, Ogilvie RI, Woo V, Kaczorowski J, Burns KD, Petrella RJ, Hiremath S, Milot A, Stone JA, Drouin D, Lavoie KL, Lamarre-Cliche M, Tremblay G, Hamet P, Fodor G, Carruthers SG, Pylypchuk GB, Burgess E, Lewanczuk R, Dresser GK, Penner SB, Hegele RA, McFarlane PA, Khara M, Pipe A, Oh P, Selby P, Sharma M, Reid DJ, Tobe SW, Padwal RS and Poirier L. The 2014 Canadian Hypertension Education Program recommendations for blood pressure measurement, diagnosis, assessment of risk, prevention, and treatment of hypertension. *Can J Cardiol*. 2014;30:485-501.
5. Lund-Johansen P. Haemodynamics in essential hypertension. *Clin Sci (Lond)*. 1980;59 Suppl 6:343s-354s.
6. Mayet J and Hughes A. Cardiac and vascular pathophysiology in hypertension. *Heart*. 2003;89:1104-1109.
7. Weber KT and Brilla CG. Pathological hypertrophy and cardiac interstitium. Fibrosis and renin-angiotensin-aldosterone system. *Circulation*. 1991;83:1849-65.
8. Roger VL, Go AS, Lloyd-Jones DM, Adams RJ, Berry JD, Brown TM, Carnethon MR, Dai S, de Simone G, Ford ES, Fox CS, Fullerton HJ, Gillespie C, Greenlund KJ, Hailpern SM, Heit JA, Ho PM, Howard VJ, Kissela BM, Kittner SJ, Lackland DT, Lichtman JH, Lisabeth LD, Makuc DM, Marcus GM, Marelli A, Matchar DB, McDermott MM, Meigs JB, Moy CS, Mozaffarian D, Mussolino ME, Nichol G, Paynter NP, Rosamond WD, Sorlie PD, Stafford RS, Turan TN, Turner MB, Wong ND and Wylie-Rosett J. Heart disease and stroke statistics--2011 update: a report from the American Heart Association. *Circulation*. 2011;123:e18-e209.
9. Levy D, Larson MG, Vasan RS, Kannel WB and Ho KK. The progression from hypertension to congestive heart failure. *JAMA*. 1996;275:1557-62.
10. Heagerty AM, Aalkjaer C, Bund SJ, Korsgaard N and Mulvany MJ. Small artery structure in hypertension. Dual processes of remodeling and growth. *Hypertension*. 1993;21:391-7.
11. Heagerty AM, Heerkens EH and Izzard AS. Small artery structure and function in hypertension. *J Cell Mol Med*. 2010;14:1037-43.
12. Tzourio C. Hypertension, cognitive decline, and dementia: an epidemiological perspective. *Dialogues Clin Neurosci*. 2007;9:61-70.

13. Walker KA, Power MC and Gottesman RF. Defining the Relationship Between Hypertension, Cognitive Decline, and Dementia: a Review. *Curr Hypertens Rep*. 2017;19:24.
14. Iadecola C. Hypertension and dementia. *Hypertension*. 2014;64:3-5.
15. Jimenez-Balado J, Riba-Llena I, Abril O, Garde E, Penalba A, Ostos E, Maisterra O, Montaner J, Noviembre M, Mundet X, Ventura O, Pizarro J and Delgado P. Cognitive Impact of Cerebral Small Vessel Disease Changes in Patients With Hypertension. *Hypertension*. 2019;73:342-349.
16. Trojano L, Antonelli Incalzi R, Acanfora D, Picone C, Mecocci P and Rengo F. Cognitive impairment: a key feature of congestive heart failure in the elderly. *J Neurol*. 2003;250:1456-63.
17. Qiu C, Winblad B, Marengoni A, Klarin I, Fastbom J and Fratiglioni L. Heart failure and risk of dementia and Alzheimer disease: a population-based cohort study. *Arch Intern Med*. 2006;166:1003-8.
18. Schiffrin EL. Reactivity of small blood vessels in hypertension: relation with structural changes. State of the art lecture. *Hypertension*. 1992;19:II1-9.
19. Mulvany MJ and Aalkjaer C. Structure and function of small arteries. *Physiol Rev*. 1990;70:921-61.
20. Rizzoni D and Agabiti-Rosei E. Structural abnormalities of small resistance arteries in essential hypertension. *Intern Emerg Med*. 2012;7:205-12.
21. Mulvany MJ, Baumbach GL, Aalkjaer C, Heagerty AM, Korsgaard N, Schiffrin EL and Heistad DD. Vascular remodeling. *Hypertension*. 1996;28:505-6.
22. Laurent S and Boutouyrie P. The structural factor of hypertension: large and small artery alterations. *Circ Res*. 2015;116:1007-21.
23. Levy BI, Ambrosio G, Pries AR and Struijker-Boudier HA. Microcirculation in hypertension: a new target for treatment? *Circulation*. 2001;104:735-40.
24. Cho YI, Cho DJ and Rosenson RS. Endothelial shear stress and blood viscosity in peripheral arterial disease. *Curr Atheroscler Rep*. 2014;16:404.
25. Lenz C, Frietsch T, Futterer C, van Ackern K, Kuschinsky W and Waschke KF. Influence of blood viscosity on blood flow in the forebrain but not hindbrain after carotid occlusion in rats. *J Cereb Blood Flow Metab*. 2000;20:947-55.
26. Klabunde RE. Determinants of Resistance to Flow (Poiseuille's Equation). *Cardiovascular Physiology Concepts*. 2017.
27. Falloon BJ and Heagerty AM. In vitro perfusion studies of human resistance artery function in essential hypertension. *Hypertension*. 1994;24:16-23.
28. Schiffrin EL, Deng LY and Larochelle P. Morphology of resistance arteries and comparison of effects of vasoconstrictors in mild essential hypertensive patients. *Clin Invest Med*. 1993;16:177-86.
29. Rosei EA, Rizzoni D, Castellano M, Porteri E, Zulli R, Muiesan ML, Bettoni G, Salvetti M, Muiesan P and Giulini SM. Media: lumen ratio in human small resistance arteries is related to forearm minimal vascular resistance. *J Hypertens*. 1995;13:341-7.
30. Intengan HD, Deng LY, Li JS and Schiffrin EL. Mechanics and composition of human subcutaneous resistance arteries in essential hypertension. *Hypertension*. 1999;33:569-74.
31. Intengan HD, Thibault G, Li JS and Schiffrin EL. Resistance artery mechanics, structure, and extracellular components in spontaneously hypertensive rats : effects of angiotensin receptor antagonism and converting enzyme inhibition. *Circulation*. 1999;100:2267-75.

32. Zanchi A, Wiesel P, Aubert JF, Brunner HR and Hayoz D. Time course changes of the mechanical properties of the carotid artery in renal hypertensive rats. *Hypertension*. 1997;29:1199-203.
33. Schiffrin EL, Park JB, Intengan HD and Touyz RM. Correction of arterial structure and endothelial dysfunction in human essential hypertension by the angiotensin receptor antagonist losartan. *Circulation*. 2000;101:1653-9.
34. Davies PF. Hemodynamic shear stress and the endothelium in cardiovascular pathophysiology. *Nat Clin Pract Cardiovasc Med*. 2009;6:16-26.
35. Davies PF, Robotewskyj A and Griem ML. Quantitative studies of endothelial cell adhesion. Directional remodeling of focal adhesion sites in response to flow forces. *J Clin Invest*. 1994;93:2031-8.
36. Anwar MA, Shalhoub J, Lim CS, Gohel MS and Davies AH. The effect of pressure-induced mechanical stretch on vascular wall differential gene expression. *J Vasc Res*. 2012;49:463-78.
37. Baumbach GL and Heistad DD. Cerebral circulation in chronic arterial hypertension. *Hypertension*. 1988;12:89-95.
38. Mulvany MJ. Small artery structure: time to take note? *Am J Hypertens*. 2007;20:853-4.
39. Feihl F, Liaudet L, Levy BI and Waeber B. Hypertension and microvascular remodelling. *Cardiovasc Res*. 2008;78:274-85.
40. Rizzoni D, Porteri E, Boari GE, De Ciuceis C, Sleiman I, Muiesan ML, Castellano M, Miclini M and Agabiti-Rosei E. Prognostic significance of small-artery structure in hypertension. *Circulation*. 2003;108:2230-5.
41. Sandoo A, van Zanten JJ, Metsios GS, Carroll D and Kitas GD. The endothelium and its role in regulating vascular tone. *Open Cardiovasc Med J*. 2010;4:302-12.
42. Dingemans KP, Teeling P, Lagendijk JH and Becker AE. Extracellular matrix of the human aortic media: an ultrastructural histochemical and immunohistochemical study of the adult aortic media. *Anat Rec*. 2000;258:1-14.
43. Green EM, Mansfield JC, Bell JS and Winlove CP. The structure and micromechanics of elastic tissue. *Interface Focus*. 2014;4:20130058.
44. Shinaoka A, Momota R, Shiratsuchi E, Kosaka M, Kumagishi K, Nakahara R, Naito I and Ohtsuka A. Architecture of the subendothelial elastic fibers of small blood vessels and variations in vascular type and size. *Microsc Microanal*. 2013;19:406-14.
45. Rizzoni D, Porteri E, Guefi D, Piccoli A, Castellano M, Pasini G, Muiesan ML, Mulvany MJ and Rosei EA. Cellular hypertrophy in subcutaneous small arteries of patients with renovascular hypertension. *Hypertension*. 2000;35:931-5.
46. Korsgaard N and Mulvany MJ. Cellular hypertrophy in mesenteric resistance vessels from renal hypertensive rats. *Hypertension*. 1988;12:162-7.
47. Rizzoni D, Rodella L, Porteri E, Rezzani R, Guelfi D, Piccoli A, Castellano M, Muiesan ML, Bianchi R and Rosei EA. Time course of apoptosis in small resistance arteries of spontaneously hypertensive rats. *J Hypertens*. 2000;18:885-91.
48. Intengan HD and Schiffrin EL. Structure and mechanical properties of resistance arteries in hypertension: role of adhesion molecules and extracellular matrix determinants. *Hypertension*. 2000;36:312-8.

49. Mulvany MJ, Baandrup U and Gundersen HJ. Evidence for hyperplasia in mesenteric resistance vessels of spontaneously hypertensive rats using a three-dimensional disector. *Circ Res*. 1985;57:794-800.
50. Brown IAM, Diederich L, Good ME, DeLalio LJ, Murphy SA, Cortese-Krott MM, Hall JL, Le TH and Isakson BE. Vascular Smooth Muscle Remodeling in Conductive and Resistance Arteries in Hypertension. *Arterioscler Thromb Vasc Biol*. 2018;38:1969-1985.
51. Savoia C, Sada L, Zezza L, Pucci L, Lauri FM, Befani A, Alonzo A and Volpe M. Vascular inflammation and endothelial dysfunction in experimental hypertension. *Int J Hypertens*. 2011;2011:281240.
52. Briones AM, Arribas SM and Salaices M. Role of extracellular matrix in vascular remodeling of hypertension. *Curr Opin Nephrol Hypertens*. 2010;19:187-94.
53. Baumbach GL and Heistad DD. Remodeling of cerebral arterioles in chronic hypertension. *Hypertension*. 1989;13:968-72.
54. Rizzoni D, Porteri E, Castellano M, Bettoni G, Muiesan ML, Muiesan P, Giulini SM and Agabiti-Rosei E. Vascular hypertrophy and remodeling in secondary hypertension. *Hypertension*. 1996;28:785-90.
55. Deng LY and Schiffrin EL. Morphological and functional alterations of mesenteric small resistance arteries in early renal hypertension in rats. *Am J Physiol*. 1991;261:H1171-7.
56. Faraco G and Iadecola C. Hypertension: a harbinger of stroke and dementia. *Hypertension*. 2013;62:810-7.
57. Touyz RM, He G, El Mabrouk M and Schiffrin EL. p38 Map kinase regulates vascular smooth muscle cell collagen synthesis by angiotensin II in SHR but not in WKY. *Hypertension*. 2001;37:574-80.
58. Chiang HY, Korshunov VA, Serour A, Shi F and Sottile J. Fibronectin is an important regulator of flow-induced vascular remodeling. *Arterioscler Thromb Vasc Biol*. 2009;29:1074-9.
59. Mulvany MJ. Small artery remodelling in hypertension. *Basic Clin Pharmacol Toxicol*. 2012;110:49-55.
60. Hein M, Fischer J, Kim DK, Hein L and Pratt RE. Vascular smooth muscle cell phenotype influences glycosaminoglycan composition and growth effects of extracellular matrix. *J Vasc Res*. 1996;33:433-41.
61. Castro CM, Cruzado MC, Miatello RM and Risler NR. Proteoglycan production by vascular smooth muscle cells from resistance arteries of hypertensive rats. *Hypertension*. 1999;34:893-6.
62. Alexander MR and Owens GK. Epigenetic control of smooth muscle cell differentiation and phenotypic switching in vascular development and disease. *Annu Rev Physiol*. 2012;74:13-40.
63. Jaminon A, Reesink K, Kroon A and Schurgers L. The Role of Vascular Smooth Muscle Cells in Arterial Remodeling: Focus on Calcification-Related Processes. *Int J Mol Sci*. 2019;20.
64. Rensen SS, Doevendans PA and van Eys GJ. Regulation and characteristics of vascular smooth muscle cell phenotypic diversity. *Neth Heart J*. 2007;15:100-8.
65. Qi YX, Jiang J, Jiang XH, Wang XD, Ji SY, Han Y, Long DK, Shen BR, Yan ZQ, Chien S and Jiang ZL. PDGF-BB and TGF-{beta}1 on cross-talk between endothelial and smooth muscle cells in vascular remodeling induced by low shear stress. *Proc Natl Acad Sci U S A*. 2011;108:1908-13.

66. Cecchettini A, Rocchiccioli S, Boccardi C and Citti L. Vascular smooth-muscle-cell activation: proteomics point of view. *Int Rev Cell Mol Biol*. 2011;288:43-99.
67. Bennett MR. Apoptosis of vascular smooth muscle cells in vascular remodelling and atherosclerotic plaque rupture. *Cardiovasc Res*. 1999;41:361-8.
68. Zhang L, Xie P, Wang J, Yang Q, Fang C, Zhou S and Li J. Impaired peroxisome proliferator-activated receptor-gamma contributes to phenotypic modulation of vascular smooth muscle cells during hypertension. *J Biol Chem*. 2010;285:13666-77.
69. Gerthoffer WT. Mechanisms of vascular smooth muscle cell migration. *Circ Res*. 2007;100:607-21.
70. Willis AI, Pierre-Paul D, Sumpio BE and Gahtan V. Vascular smooth muscle cell migration: current research and clinical implications. *Vasc Endovascular Surg*. 2004;38:11-23.
71. Duca L, Blaise S, Romier B, Laffargue M, Gayral S, El Btaouri H, Kawecki C, Guillot A, Martiny L, Debelle L and Maurice P. Matrix ageing and vascular impacts: focus on elastin fragmentation. *Cardiovasc Res*. 2016;110:298-308.
72. Qin H, Ishiwata T, Wang R, Kudo M, Yokoyama M, Naito Z and Asano G. Effects of extracellular matrix on phenotype modulation and MAPK transduction of rat aortic smooth muscle cells in vitro. *Exp Mol Pathol*. 2000;69:79-90.
73. Laurent S, Boutouyrie P and Lacolley P. Structural and genetic bases of arterial stiffness. *Hypertension*. 2005;45:1050-5.
74. Chi C, Li DJ, Jiang YJ, Tong J, Fu H, Wu YH and Shen FM. Vascular smooth muscle cell senescence and age-related diseases: State of the art. *Biochim Biophys Acta Mol Basis Dis*. 2019;1865:1810-1821.
75. Panza JA, Quyyumi AA, Brush JE, Jr. and Epstein SE. Abnormal endothelium-dependent vascular relaxation in patients with essential hypertension. *N Engl J Med*. 1990;323:22-7.
76. Rizzoni D, Porteri E, Castellano M, Bettoni G, Muiesan ML, Tiberio G, Giulini SM, Rossi G, Bernini G and Agabiti-Rosei E. Endothelial dysfunction in hypertension is independent from the etiology and from vascular structure. *Hypertension*. 1998;31:335-41.
77. Willems C, Astaldi GC, De Groot PG, Janssen MC, Gonsalvez MD, Zeijlemaker WP, Van Mourik JA and Van Aken WG. Media conditioned by cultured human vascular endothelial cells inhibit the growth of vascular smooth muscle cells. *Exp Cell Res*. 1982;139:191-7.
78. Baker AB, Ettenson DS, Jonas M, Nugent MA, Iozzo RV and Edelman ER. Endothelial cells provide feedback control for vascular remodeling through a mechanosensitive autocrine TGF-beta signaling pathway. *Circ Res*. 2008;103:289-97.
79. Rudic RD, Shesely EG, Maeda N, Smithies O, Segal SS and Sessa WC. Direct evidence for the importance of endothelium-derived nitric oxide in vascular remodeling. *J Clin Invest*. 1998;101:731-6.
80. Brandes RP. Endothelial dysfunction and hypertension. *Hypertension*. 2014;64:924-8.
81. Reneman RS, Meinders JM and Hoeks AP. Non-invasive ultrasound in arterial wall dynamics in humans: what have we learned and what remains to be solved. *Eur Heart J*. 2005;26:960-6.
82. Vegas MR and Martin del Yerro JL. Stiffness, compliance, resilience, and creep deformation: understanding implant-soft tissue dynamics in the augmented breast: fundamentals based on materials science. *Aesthetic Plast Surg*. 2013;37:922-30.

83. Vlachopoulos C, Aznaouridis K and Stefanadis C. Prediction of cardiovascular events and all-cause mortality with arterial stiffness: a systematic review and meta-analysis. *J Am Coll Cardiol*. 2010;55:1318-27.
84. Laurent S, Boutouyrie P, Asmar R, Gautier I, Laloux B, Guize L, Ducimetiere P and Benetos A. Aortic stiffness is an independent predictor of all-cause and cardiovascular mortality in hypertensive patients. *Hypertension*. 2001;37:1236-41.
85. Lee YB, Park JH, Kim E, Kang CK and Park HM. Arterial stiffness and functional outcome in acute ischemic stroke. *J Cerebrovasc Endovasc Neurosurg*. 2014;16:11-9.
86. Rabkin SW. Arterial stiffness: detection and consequences in cognitive impairment and dementia of the elderly. *J Alzheimers Dis*. 2012;32:541-9.
87. AlGhatrif M, Strait JB, Morrell CH, Canepa M, Wright J, Elango P, Scuteri A, Najjar SS, Ferrucci L and Lakatta EG. Longitudinal trajectories of arterial stiffness and the role of blood pressure: the Baltimore Longitudinal Study of Aging. *Hypertension*. 2013;62:934-41.
88. Rosenbloom J, Abrams WR and Mecham R. Extracellular matrix 4: the elastic fiber. *FASEB J*. 1993;7:1208-18.
89. Shirwany NA and Zou MH. Arterial stiffness: a brief review. *Acta Pharmacol Sin*. 2010;31:1267-76.
90. Clark JM and Glagov S. Transmural organization of the arterial media. The lamellar unit revisited. *Arteriosclerosis*. 1985;5:19-34.
91. Wagenseil JE and Mecham RP. Elastin in large artery stiffness and hypertension. *J Cardiovasc Transl Res*. 2012;5:264-73.
92. Armentano RL, Levenson J, Barra JG, Fischer EI, Breitbart GJ, Pichel RH and Simon A. Assessment of elastin and collagen contribution to aortic elasticity in conscious dogs. *Am J Physiol*. 1991;260:H1870-7.
93. Wilkinson IB and McEniery CM. Arterial stiffness, endothelial function and novel pharmacological approaches. *Clin Exp Pharmacol Physiol*. 2004;31:795-9.
94. Lee HW, Karam J, Hussain B and Winer N. Vascular compliance in hypertension: therapeutic implications. *Curr Diab Rep*. 2008;8:208-13.
95. Keeley FW. The synthesis of soluble and insoluble elastin in chicken aorta as a function of development and age. Effect of a high cholesterol diet. *Can J Biochem*. 1979;57:1273-80.
96. Li Z, Froehlich J, Galis ZS and Lakatta EG. Increased expression of matrix metalloproteinase-2 in the thickened intima of aged rats. *Hypertension*. 1999;33:116-23.
97. Briones AM, Gonzalez JM, Somoza B, Giraldo J, Daly CJ, Vila E, Gonzalez MC, McGrath JC and Arribas SM. Role of elastin in spontaneously hypertensive rat small mesenteric artery remodelling. *J Physiol*. 2003;552:185-95.
98. Li DY, Brooke B, Davis EC, Mecham RP, Sorensen LK, Boak BB, Eichwald E and Keating MT. Elastin is an essential determinant of arterial morphogenesis. *Nature*. 1998;393:276-80.
99. Jiao Y, Li G, Korneva A, Caulk AW, Qin L, Bersi MR, Li Q, Li W, Mecham RP, Humphrey JD and Tellides G. Deficient Circumferential Growth Is the Primary Determinant of Aortic Obstruction Attributable to Partial Elastin Deficiency. *Arterioscler Thromb Vasc Biol*. 2017;37:930-941.
100. Intengan HD and Schiffrin EL. Vascular remodeling in hypertension: roles of apoptosis, inflammation, and fibrosis. *Hypertension*. 2001;38:581-7.

101. Lacolley P, Regnault V, Segers P and Laurent S. Vascular Smooth Muscle Cells and Arterial Stiffening: Relevance in Development, Aging, and Disease. *Physiol Rev*. 2017;97:1555-1617.
102. Safar ME, Asmar R, Benetos A, Blacher J, Boutouyrie P, Lacolley P, Laurent S, London G, Pannier B, Protogerou A, Regnault V and French Study Group on Arterial S. Interaction Between Hypertension and Arterial Stiffness. *Hypertension*. 2018;72:796-805.
103. Kinlay S, Creager MA, Fukumoto M, Hikita H, Fang JC, Selwyn AP and Ganz P. Endothelium-derived nitric oxide regulates arterial elasticity in human arteries in vivo. *Hypertension*. 2001;38:1049-53.
104. Levy BI, Benessiano J, Poitevin P and Safar ME. Endothelium-dependent mechanical properties of the carotid artery in WKY and SHR. Role of angiotensin converting enzyme inhibition. *Circ Res*. 1990;66:321-8.
105. Davis MJ and Hill MA. Signaling mechanisms underlying the vascular myogenic response. *Physiol Rev*. 1999;79:387-423.
106. Feihl F, Liaudet L, Waeber B and Levy BI. Hypertension: a disease of the microcirculation? *Hypertension*. 2006;48:1012-7.
107. MJ. C. Control of Cerebral Blood Flow. *The Cerebral Circulation*. 2009
108. Osol G, Brekke JF, McElroy-Yaggy K and Gokina NI. Myogenic tone, reactivity, and forced dilatation: a three-phase model of in vitro arterial myogenic behavior. *Am J Physiol Heart Circ Physiol*. 2002;283:H2260-7.
109. Phillips SJ and Whisnant JP. Hypertension and the brain. The National High Blood Pressure Education Program. *Arch Intern Med*. 1992;152:938-45.
110. Kontos HA, Wei EP, Navari RM, Levasseur JE, Rosenblum WI and Patterson JL, Jr. Responses of cerebral arteries and arterioles to acute hypotension and hypertension. *Am J Physiol*. 1978;234:H371-83.
111. Davis MJ. Perspective: physiological role(s) of the vascular myogenic response. *Microcirculation*. 2012;19:99-114.
112. Touyz RM, Alves-Lopes R, Rios FJ, Camargo LL, Anagnostopoulou A, Arner A and Montezano AC. Vascular smooth muscle contraction in hypertension. *Cardiovasc Res*. 2018;114:529-539.
113. Ren Y, D'Ambrosio MA, Liu R, Pagano PJ, Garvin JL and Carretero OA. Enhanced myogenic response in the afferent arteriole of spontaneously hypertensive rats. *Am J Physiol Heart Circ Physiol*. 2010;298:H1769-75.
114. Falcone JC and Meininger GA. Endothelin mediates a component of the enhanced myogenic responsiveness of arterioles from hypertensive rats. *Microcirculation*. 1999;6:305-13.
115. Shibuya J, Ohyanagi M and Iwasaki T. Enhanced myogenic response in resistance small arteries from spontaneously hypertensive rats: relationship to the voltage-dependent calcium channel. *Am J Hypertens*. 1998;11:767-73.
116. Izzard AS, Bund SJ and Heagerty AM. Myogenic tone in mesenteric arteries from spontaneously hypertensive rats. *Am J Physiol*. 1996;270:H1-6.
117. Bund SJ. Spontaneously hypertensive rat resistance artery structure related to myogenic and mechanical properties. *Clin Sci (Lond)*. 2001;101:385-93.
118. Dunn WR, Wallis SJ and Gardiner SM. Remodelling and enhanced myogenic tone in cerebral resistance arteries isolated from genetically hypertensive Brattleboro rats. *J Vasc Res*. 1998;35:18-26.

119. Pires PW, Jackson WF and Dorrance AM. Regulation of myogenic tone and structure of parenchymal arterioles by hypertension and the mineralocorticoid receptor. *Am J Physiol Heart Circ Physiol*. 2015;309:H127-36.
120. Osol G and Halpern W. Myogenic properties of cerebral blood vessels from normotensive and hypertensive rats. *Am J Physiol*. 1985;249:H914-21.
121. Vallance P, Collier J and Moncada S. Effects of endothelium-derived nitric oxide on peripheral arteriolar tone in man. *Lancet*. 1989;2:997-1000.
122. Hermann M, Flammer A and Luscher TF. Nitric oxide in hypertension. *J Clin Hypertens (Greenwich)*. 2006;8:17-29.
123. Huang A, Sun D and Koller A. Endothelial dysfunction augments myogenic arteriolar constriction in hypertension. *Hypertension*. 1993;22:913-21.
124. Huang A and Koller A. Endothelin and prostaglandin H2 enhance arteriolar myogenic tone in hypertension. *Hypertension*. 1997;30:1210-5.
125. Huang A and Koller A. Both nitric oxide and prostaglandin-mediated responses are impaired in skeletal muscle arterioles of hypertensive rats. *J Hypertens*. 1996;14:887-95.
126. Peng X, Haldar S, Deshpande S, Irani K and Kass DA. Wall stiffness suppresses Akt/eNOS and cytoprotection in pulse-perfused endothelium. *Hypertension*. 2003;41:378-81.
127. Zieman SJ, Melenovsky V and Kass DA. Mechanisms, pathophysiology, and therapy of arterial stiffness. *Arterioscler Thromb Vasc Biol*. 2005;25:932-43.
128. Matsumoto T, Watanabe S, Iguchi M, Ando M, Oda M, Nagata M, Yamada K, Taguchi K and Kobayashi T. Mechanisms Underlying Enhanced Noradrenaline-Induced Femoral Arterial Contractions of Spontaneously Hypertensive Rats: Involvement of Endothelium-Derived Factors and Cyclooxygenase-Derived Prostanoids. *Biol Pharm Bull*. 2016;39:384-93.
129. Bakker EN, van der Meulen ET, van den Berg BM, Everts V, Spaan JA and VanBavel E. Inward remodeling follows chronic vasoconstriction in isolated resistance arteries. *J Vasc Res*. 2002;39:12-20.
130. Rosenblum WI and Kontos HA. The importance and relevance of studies of the pial microcirculation. *Stroke*. 1974;5:425-8.
131. Faraci FM and Heistad DD. Regulation of large cerebral arteries and cerebral microvascular pressure. *Circ Res*. 1990;66:8-17.
132. Faraci FM. Protecting against vascular disease in brain. *Am J Physiol Heart Circ Physiol*. 2011;300:H1566-82.
133. Baumbach GL, Sigmund CD and Faraci FM. Cerebral arteriolar structure in mice overexpressing human renin and angiotensinogen. *Hypertension*. 2003;41:50-5.
134. Iadecola C. Neurovascular regulation in the normal brain and in Alzheimer's disease. *Nat Rev Neurosci*. 2004;5:347-60.
135. Cipolla MJ and Bullinger LV. Reactivity of brain parenchymal arterioles after ischemia and reperfusion. *Microcirculation*. 2008;15:495-501.
136. Iadecola C and Nedergaard M. Glial regulation of the cerebral microvasculature. *Nat Neurosci*. 2007;10:1369-76.
137. Filosa JA. Vascular tone and neurovascular coupling: considerations toward an improved in vitro model. *Front Neuroenergetics*. 2010;2.
138. Hamel E. Perivascular nerves and the regulation of cerebrovascular tone. *J Appl Physiol (1985)*. 2006;100:1059-64.

139. Zonta M, Angulo MC, Gobbo S, Rosengarten B, Hossmann KA, Pozzan T and Carmignoto G. Neuron-to-astrocyte signaling is central to the dynamic control of brain microcirculation. *Nat Neurosci*. 2003;6:43-50.
140. Mulligan SJ and MacVicar BA. Calcium transients in astrocyte endfeet cause cerebrovascular constrictions. *Nature*. 2004;431:195-9.
141. Metea MR and Newman EA. Glial cells dilate and constrict blood vessels: a mechanism of neurovascular coupling. *J Neurosci*. 2006;26:2862-70.
142. Takano T, Tian GF, Peng W, Lou N, Libionka W, Han X and Nedergaard M. Astrocyte-mediated control of cerebral blood flow. *Nat Neurosci*. 2006;9:260-7.
143. Stobart JL, Lu L, Anderson HD, Mori H and Anderson CM. Astrocyte-induced cortical vasodilation is mediated by D-serine and endothelial nitric oxide synthase. *Proc Natl Acad Sci U S A*. 2013;110:3149-54.
144. MacVicar BA and Newman EA. Astrocyte regulation of blood flow in the brain. *Cold Spring Harb Perspect Biol*. 2015;7.
145. Iadecola C, Yaffe K, Biller J, Bratzke LC, Faraci FM, Gorelick PB, Gulati M, Kamel H, Knopman DS, Launer LJ, Saczynski JS, Seshadri S, Zeki Al Hazzouri A, American Heart Association Council on H, Council on Clinical C, Council on Cardiovascular Disease in the Y, Council on C, Stroke N, Council on Quality of C, Outcomes R and Stroke C. Impact of Hypertension on Cognitive Function: A Scientific Statement From the American Heart Association. *Hypertension*. 2016;68:e67-e94.
146. Mitchell GF. Cerebral small vessel disease: role of aortic stiffness and pulsatile hemodynamics. *J Hypertens*. 2015;33:2025-8.
147. Yang Y, Kimura-Ohba S, Thompson J and Rosenberg GA. Rodent Models of Vascular Cognitive Impairment. *Transl Stroke Res*. 2016;7:407-14.
148. Liu Y, Dong YH, Lyu PY, Chen WH and Li R. Hypertension-Induced Cerebral Small Vessel Disease Leading to Cognitive Impairment. *Chin Med J (Engl)*. 2018;131:615-619.
149. Birns J and Kalra L. Cognitive function and hypertension. *J Hum Hypertens*. 2009;23:86-96.
150. Iadecola C and Davisson RL. Hypertension and cerebrovascular dysfunction. *Cell Metab*. 2008;7:476-84.
151. Waldstein SR, Rice SC, Thayer JF, Najjar SS, Scuteri A and Zonderman AB. Pulse pressure and pulse wave velocity are related to cognitive decline in the Baltimore Longitudinal Study of Aging. *Hypertension*. 2008;51:99-104.
152. Hajjar I, Goldstein FC, Martin GS and Quyyumi AA. Roles of Arterial Stiffness and Blood Pressure in Hypertension-Associated Cognitive Decline in Healthy Adults. *Hypertension*. 2016;67:171-5.
153. Muela HC, Costa-Hong VA, Yassuda MS, Moraes NC, Memoria CM, Machado MF, Macedo TA, Shu EB, Massaro AR, Nitrini R, Mansur AJ and Bortolotto LA. Hypertension Severity Is Associated With Impaired Cognitive Performance. *J Am Heart Assoc*. 2017;6.
154. Beason-Held LL, Moghekar A, Zonderman AB, Kraut MA and Resnick SM. Longitudinal changes in cerebral blood flow in the older hypertensive brain. *Stroke*. 2007;38:1766-73.
155. Jennings JR, Muldoon MF, Ryan C, Price JC, Greer P, Sutton-Tyrrell K, van der Veen FM and Meltzer CC. Reduced cerebral blood flow response and compensation among patients with untreated hypertension. *Neurology*. 2005;64:1358-65.

156. Cannon JA, McMurray JJ and Quinn TJ. 'Hearts and minds': association, causation and implication of cognitive impairment in heart failure. *Alzheimers Res Ther*. 2015;7:22.
157. Woo MA, Kumar R, Macey PM, Fonarow GC and Harper RM. Brain injury in autonomic, emotional, and cognitive regulatory areas in patients with heart failure. *J Card Fail*. 2009;15:214-23.
158. Roy B, Woo MA, Wang DJJ, Fonarow GC, Harper RM and Kumar R. Reduced regional cerebral blood flow in patients with heart failure. *Eur J Heart Fail*. 2017;19:1294-1302.
159. Pini L, Pievani M, Bocchetta M, Altomare D, Bosco P, Cavedo E, Galluzzi S, Marizzoni M and Frisoni GB. Brain atrophy in Alzheimer's Disease and aging. *Ageing Res Rev*. 2016;30:25-48.
160. Cai Z, Liu Z, Xiao M, Wang C and Tian F. Chronic Cerebral Hypoperfusion Promotes Amyloid-Beta Pathogenesis via Activating beta/gamma-Secretases. *Neurochem Res*. 2017;42:3446-3455.
161. Thomas T, Miners S and Love S. Post-mortem assessment of hypoperfusion of cerebral cortex in Alzheimer's disease and vascular dementia. *Brain*. 2015;138:1059-69.
162. Hansson O, Palmqvist S, Ljung H, Cronberg T, van Westen D and Smith R. Cerebral hypoperfusion is not associated with an increase in amyloid beta pathology in middle-aged or elderly people. *Alzheimers Dement*. 2018;14:54-61.
163. Rouch L, Cestac P, Hanon O, Cool C, Helmer C, Bouhanick B, Chamontin B, Dartigues JF, Vellas B and Andrieu S. Antihypertensive drugs, prevention of cognitive decline and dementia: a systematic review of observational studies, randomized controlled trials and meta-analyses, with discussion of potential mechanisms. *CNS Drugs*. 2015;29:113-30.
164. Jaiswal A, Bhavsar V, Jaykaran and Kantharia ND. Effect of antihypertensive therapy on cognitive functions of patients with hypertension. *Ann Indian Acad Neurol*. 2010;13:180-3.
165. Murray MD, Lane KA, Gao S, Evans RM, Unverzagt FW, Hall KS and Hendrie H. Preservation of cognitive function with antihypertensive medications: a longitudinal analysis of a community-based sample of African Americans. *Arch Intern Med*. 2002;162:2090-6.
166. Yasar S, Xia J, Yao W, Furberg CD, Xue QL, Mercado CI, Fitzpatrick AL, Fried LP, Kawas CH, Sink KM, Williamson JD, DeKosky ST, Carlson MC and Ginkgo Evaluation of Memory Study I. Antihypertensive drugs decrease risk of Alzheimer disease: Ginkgo Evaluation of Memory Study. *Neurology*. 2013;81:896-903.
167. Hoffman LB, Schmeidler J, Lesser GT, Beeri MS, Purohit DP, Grossman HT and Haroutunian V. Less Alzheimer disease neuropathology in medicated hypertensive than nonhypertensive persons. *Neurology*. 2009;72:1720-6.
168. Lipsitz LA, Gagnon M, Vyas M, Iloputaife I, Kiely DK, Sorond F, Serrador J, Cheng DM, Babikian V and Cupples LA. Antihypertensive therapy increases cerebral blood flow and carotid distensibility in hypertensive elderly subjects. *Hypertension*. 2005;45:216-21.
169. Limas C, Westrum B and Limas CJ. Effect of antihypertensive therapy on the vascular changes of spontaneously hypertensive rats. *Am J Pathol*. 1983;111:380-93.
170. Ram CV. Beta-blockers in hypertension. *Am J Cardiol*. 2010;106:1819-25.
171. Itskovitz HD. Alpha 1 blockers. Safe, effective treatment for hypertension. *Postgrad Med*. 1991;89:89-92, 95-8, 103-6, passim.
172. James PA, Oparil S, Carter BL, Cushman WC, Dennison-Himmelfarb C, Handler J, Lackland DT, LeFevre ML, MacKenzie TD, Ogedegbe O, Smith SC, Jr., Svetkey LP, Taler SJ, Townsend RR, Wright JT, Jr., Narva AS and Ortiz E. 2014 evidence-based guideline for the

management of high blood pressure in adults: report from the panel members appointed to the Eighth Joint National Committee (JNC 8). *Jama*. 2014;311:507-20.
173. Calhoun DA, Jones D, Textor S, Goff DC, Murphy TP, Toto RD, White A, Cushman WC, White W, Sica D, Ferdinand K, Giles TD, Falkner B, Carey RM and American Heart Association Professional Education C. Resistant hypertension: diagnosis, evaluation, and treatment: a scientific statement from the American Heart Association Professional Education Committee of the Council for High Blood Pressure Research. *Circulation*. 2008;117:e510-26.
174. Calhoun DA, Jones D, Textor S, Goff DC, Murphy TP, Toto RD, White A, Cushman WC, White W, Sica D, Ferdinand K, Giles TD, Falkner B and Carey RM. Resistant hypertension: diagnosis, evaluation, and treatment. A scientific statement from the American Heart Association Professional Education Committee of the Council for High Blood Pressure Research. *Hypertension*. 2008;51:1403-19.
175. Akinwumi BC, Bordun KM and Anderson HD. Biological Activities of Stilbenoids. *Int J Mol Sci*. 2018;19.
176. Siemann EH and Creasy LL. Concentration of the Phytoalexin Resveratrol in Wine. *American Journal of Enology and Viticulture*. 1992;43:49-52.
177. Renaud S and de Lorgeril M. Wine, alcohol, platelets, and the French paradox for coronary heart disease. *Lancet*. 1992;339:1523-6.
178. Cooper KA, Chopra M and Thurnham DI. Wine polyphenols and promotion of cardiac health. *Nutr Res Rev*. 2004;17:111-30.
179. Xia N, Daiber A, Forstermann U and Li H. Antioxidant effects of resveratrol in the cardiovascular system. *Br J Pharmacol*. 2017;174:1633-1646.
180. Wang Z, Zou J, Cao K, Hsieh TC, Huang Y and Wu JM. Dealcoholized red wine containing known amounts of resveratrol suppresses atherosclerosis in hypercholesterolemic rabbits without affecting plasma lipid levels. *Int J Mol Med*. 2005;16:533-40.
181. Dolinsky VW, Chakrabarti S, Pereira TJ, Oka T, Levasseur J, Beker D, Zordoky BN, Morton JS, Nagendran J, Lopaschuk GD, Davidge ST and Dyck JR. Resveratrol prevents hypertension and cardiac hypertrophy in hypertensive rats and mice. *Biochim Biophys Acta*. 2013;1832:1723-33.
182. Jang M, Cai L, Udeani GO, Slowing KV, Thomas CF, Beecher CW, Fong HH, Farnsworth NR, Kinghorn AD, Mehta RG, Moon RC and Pezzuto JM. Cancer chemopreventive activity of resveratrol, a natural product derived from grapes. *Science*. 1997;275:218-20.
183. Timmers S, Hesselink MK and Schrauwen P. Therapeutic potential of resveratrol in obesity and type 2 diabetes: new avenues for health benefits? *Ann N Y Acad Sci*. 2013;1290:83-9.
184. Baur JA and Sinclair DA. Therapeutic potential of resveratrol: the in vivo evidence. *Nat Rev Drug Discov*. 2006;5:493-506.
185. Li F, Gong Q, Dong H and Shi J. Resveratrol, a neuroprotective supplement for Alzheimer's disease. *Curr Pharm Des*. 2012;18:27-33.
186. la Porte C, Voduc N, Zhang G, Seguin I, Tardiff D, Singhal N and Cameron DW. Steady-State pharmacokinetics and tolerability of trans-resveratrol 2000 mg twice daily with food, quercetin and alcohol (ethanol) in healthy human subjects. *Clin Pharmacokinet*. 2010;49:449-54.
187. Trela BC and Waterhouse AL. Resveratrol: Isomeric Molar Absorptivities and Stability. *Journal of Agricultural and Food Chemistry*. 1996;44:1253-1257.

188. Moreno A, Castro M and Falqué E. Evolution of trans- and cis-resveratrol content in red grapes (Vitis vinifera L. cv Mencía, Albarello and Merenzao) during ripening. *European Food Research and Technology*. 2008;227:667-674.
189. Cvejic JM, Djekic SV, Petrovic AV, Atanackovic MT, Jovic SM, Brceski ID and Gojkovic-Bukarica LC. Determination of trans- and cis-resveratrol in Serbian commercial wines. *J Chromatogr Sci*. 2010;48:229-34.
190. Orallo F. Comparative studies of the antioxidant effects of cis- and trans-resveratrol. *Curr Med Chem*. 2006;13:87-98.
191. Vian MA, Tomao V, Gallet S, Coulomb PO and Lacombe JM. Simple and rapid method for cis- and trans-resveratrol and piceid isomers determination in wine by high-performance liquid chromatography using chromolith columns. *J Chromatogr A*. 2005;1085:224-9.
192. Figueiras TS, Neves-Petersen MT and Petersen SB. Activation energy of light induced isomerization of resveratrol. *J Fluoresc*. 2011;21:1897-906.
193. Robinson K, Mock C and Liang D. Pre-formulation studies of resveratrol. *Drug Dev Ind Pharm*. 2015;41:1464-9.
194. Goldberg DM, Yan J and Soleas GJ. Absorption of three wine-related polyphenols in three different matrices by healthy subjects. *Clin Biochem*. 2003;36:79-87.
195. Walle T, Hsieh F, DeLegge MH, Oatis JE, Jr. and Walle UK. High absorption but very low bioavailability of oral resveratrol in humans. *Drug Metab Dispos*. 2004;32:1377-82.
196. Kapetanovic IM, Muzzio M, Huang Z, Thompson TN and McCormick DL. Pharmacokinetics, oral bioavailability, and metabolic profile of resveratrol and its dimethylether analog, pterostilbene, in rats. *Cancer Chemother Pharmacol*. 2011;68:593-601.
197. Boocock DJ, Faust GE, Patel KR, Schinas AM, Brown VA, Ducharme MP, Booth TD, Crowell JA, Perloff M, Gescher AJ, Steward WP and Brenner DE. Phase I dose escalation pharmacokinetic study in healthy volunteers of resveratrol, a potential cancer chemopreventive agent. *Cancer Epidemiol Biomarkers Prev*. 2007;16:1246-52.
198. Weiskirchen S and Weiskirchen R. Resveratrol: How Much Wine Do You Have to Drink to Stay Healthy? *Adv Nutr*. 2016;7:706-18.
199. Chimento A, De Amicis F, Sirianni R, Sinicropi MS, Puoci F, Casaburi I, Saturnino C and Pezzi V. Progress to Improve Oral Bioavailability and Beneficial Effects of Resveratrol. *Int J Mol Sci*. 2019;20.
200. Johnson JJ, Nihal M, Siddiqui IA, Scarlett CO, Bailey HH, Mukhtar H and Ahmad N. Enhancing the bioavailability of resveratrol by combining it with piperine. *Mol Nutr Food Res*. 2011;55:1169-76.
201. Liang L, Liu X, Wang Q, Cheng S, Zhang S and Zhang M. Pharmacokinetics, tissue distribution and excretion study of resveratrol and its prodrug 3,5,4'-tri-O-acetylresveratrol in rats. *Phytomedicine*. 2013;20:558-63.
202. Patel KR, Andreadi C, Britton RG, Horner-Glister E, Karmokar A, Sale S, Brown VA, Brenner DE, Singh R, Steward WP, Gescher AJ and Brown K. Sulfate metabolites provide an intracellular pool for resveratrol generation and induce autophagy with senescence. *Sci Transl Med*. 2013;5:205ra133.
203. Azachi M, Yatuv R, Katz A, Hagay Y and Danon A. A novel red grape cells complex: health effects and bioavailability of natural resveratrol. *Int J Food Sci Nutr*. 2014;65:848-55.
204. de Vries K, Strydom M and Steenkamp V. Bioavailability of resveratrol: Possibilities for enhancement. *Journal of Herbal Medicine*. 2018;11:71-77.

205. Rimando AM, Kalt W, Magee JB, Dewey J and Ballington JR. Resveratrol, pterostilbene, and piceatannol in vaccinium berries. *J Agric Food Chem*. 2004;52:4713-9.
206. Chan EWCW, C. W.; Tan, Y. H.; Foo, J. P. Y.; Wong, S.K.; Chan, H. T. Resveratrol and pterostilbene: A comparative overview of their chemistry, biosynthesis, plant sources and pharmacological properties. *J Appl Pharm Sci*. 9:124–129.
207. Asensi M, Medina I, Ortega A, Carretero J, Bano MC, Obrador E and Estrela JM. Inhibition of cancer growth by resveratrol is related to its low bioavailability. *Free Radic Biol Med*. 2002;33:387-98.
208. Riche DM, McEwen CL, Riche KD, Sherman JJ, Wofford MR, Deschamp D and Griswold M. Analysis of safety from a human clinical trial with pterostilbene. *J Toxicol*. 2013;2013:463595.
209. Riche DM, Riche KD, Blackshear CT, McEwen CL, Sherman JJ, Wofford MR and Griswold ME. Pterostilbene on metabolic parameters: a randomized, double-blind, and placebo-controlled trial. *Evid Based Complement Alternat Med*. 2014;2014:459165.
210. Remsberg CM, Martinez SE, Akinwumi BC, Anderson HD, Takemoto JK, Sayre CL and Davies NM. Preclinical Pharmacokinetics and Pharmacodynamics and Content Analysis of Gnetol in Foodstuffs. *Phytotherapy research : PTR*. 2015;29:1168-79.
211. McCormack D and McFadden D. Pterostilbene and cancer: current review. *The Journal of surgical research*. 2012;173:e53-61.
212. Uson-Lopez RA, Kataoka S, Mukai Y, Sato S and Kurasaki M. Melinjo (Gnetum gnemon) Seed Extract Consumption during Lactation Improved Vasodilation and Attenuated the Development of Hypertension in Female Offspring of Fructose-Fed Pregnant Rats. *Birth Defects Res*. 2018;110:27-34.
213. Sermboonpaisarn T and Sawasdee P. Potent and selective butyrylcholinesterase inhibitors from Ficus foveolata. *Fitoterapia*. 2012;83:780-4.
214. Baumbach GL, Walmsley JG and Hart MN. Composition and mechanics of cerebral arterioles in hypertensive rats. *Am J Pathol*. 1988;133:464-71.
215. Baumbach GL, Dobrin PB, Hart MN and Heistad DD. Mechanics of cerebral arterioles in hypertensive rats. *Circ Res*. 1988;62:56-64.
216. Winquist RJ and Bohr DF. Structural and functional changes in cerebral arteries from spontaneously hypertensive rats. *Hypertension*. 1983;5:292-7.
217. Toda N, Okunishi H and Miyazaki M. Length-passive tension relationships in cerebral and peripheral arteries isolated from spontaneously hypertensive and normotensive rats. *Jpn Circ J*. 1982;46:1088-94.
218. Brayden JE, Halpern W and Brann LR. Biochemical and mechanical properties of resistance arteries from normotensive and hypertensive rats. *Hypertension*. 1983;5:17-25.
219. Izzard AS, Horton S, Heerkens EH, Shaw L and Heagerty AM. Middle cerebral artery structure and distensibility during developing and established phases of hypertension in the spontaneously hypertensive rat. *J Hypertens*. 2006;24:875-80.
220. Hart MN, Heistad DD and Brody MJ. Effect of chronic hypertension and sympathetic denervation on wall/lumen ratio of cerebral vessels. *Hypertension*. 1980;2:419-23.
221. Harper SL and Bohlen HG. Microvascular adaptation in the cerebral cortex of adult spontaneously hypertensive rats. *Hypertension*. 1984;6:408-19.

222. Izzard AS, Graham D, Burnham MP, Heerkens EH, Dominiczak AF and Heagerty AM. Myogenic and structural properties of cerebral arteries from the stroke-prone spontaneously hypertensive rat. *Am J Physiol Heart Circ Physiol*. 2003;285:H1489-94.
223. Heyen JR, Blasi ER, Nikula K, Rocha R, Daust HA, Frierdich G, Van Vleet JF, De Ciechi P, McMahon EG and Rudolph AE. Structural, functional, and molecular characterization of the SHHF model of heart failure. *Am J Physiol Heart Circ Physiol*. 2002;283:H1775-84.
224. Behbahani J, Thandapilly SJ, Louis XL, Huang Y, Shao Z, Kopilas MA, Wojciechowski P, Netticadan T and Anderson HD. Resveratrol and small artery compliance and remodeling in the spontaneously hypertensive rat. *Am J Hypertens*. 2010;23:1273-8.
225. Gerdes AM, Onodera T, Wang X and McCune SA. Myocyte remodeling during the progression to failure in rats with hypertension. *Hypertension*. 1996;28:609-14.
226. Doggrell SA and Brown L. Rat models of hypertension, cardiac hypertrophy and failure. *Cardiovasc Res*. 1998;39:89-105.
227. Akinwumi BC, Raj P, Lee DI, Acosta C, Yu L, Thomas SM, Nagabhushanam K, Majeed M, Davies NM, Netticadan T and Anderson HD. Disparate Effects of Stilbenoid Polyphenols on Hypertrophic Cardiomyocytes In Vitro vs. in the Spontaneously Hypertensive Heart Failure Rat. *Molecules*. 2017;22.
228. Lee DI, Acosta C, Anderson CM and Anderson HD. Peripheral and Cerebral Resistance Arteries in the Spontaneously Hypertensive Heart Failure Rat: Effects of Stilbenoid Polyphenols. *Molecules*. 2017;22.
229. Mathiassen ON, Buus NH, Sihm I, Thybo NK, Morn B, Schroeder AP, Thygesen K, Aalkjaer C, Lederballe O, Mulvany MJ and Christensen KL. Small artery structure is an independent predictor of cardiovascular events in essential hypertension. *J Hypertens*. 2007;25:1021-6.
230. Fogacci F, Tocci G, Presta V, Fratter A, Borghi C and Cicero AFG. Effect of resveratrol on blood pressure: A systematic review and meta-analysis of randomized, controlled, clinical trials. *Crit Rev Food Sci Nutr*. 2019;59:1605-1618.
231. Theodotou M, Fokianos K, Mouzouridou A, Konstantinou C, Aristotelous A, Prodromou D and Chrysikou A. The effect of resveratrol on hypertension: A clinical trial. *Exp Ther Med*. 2017;13:295-301.
232. Likhitwitayawuid K, Sawasdee K and Kirtikara K. Flavonoids and stilbenoids with COX-1 and COX-2 inhibitory activity from Dracaena loureiri. *Planta Med*. 2002;68:841-3.
233. Touyz RM. The role of angiotensin II in regulating vascular structural and functional changes in hypertension. *Curr Hypertens Rep*. 2003;5:155-64.
234. Virdis A, Colucci R, Neves MF, Rugani I, Aydinoglu F, Fornai M, Ippolito C, Antonioli L, Duranti E, Solini A, Bernardini N, Blandizzi C and Taddei S. Resistance artery mechanics and composition in angiotensin II-infused mice: effects of cyclooxygenase-1 inhibition. *Eur Heart J*. 2012;33:2225-34.
235. Kang SS, Cuendet M, Endringer DC, Croy VL, Pezzuto JM and Lipton MA. Synthesis and biological evaluation of a library of resveratrol analogues as inhibitors of COX-1, COX-2 and NF-kappaB. *Bioorg Med Chem*. 2009;17:1044-54.
236. Murias M, Handler N, Erker T, Pleban K, Ecker G, Saiko P, Szekeres T and Jager W. Resveratrol analogues as selective cyclooxygenase-2 inhibitors: synthesis and structure-activity relationship. *Bioorg Med Chem*. 2004;12:5571-8.

237. Vessieres E, Belin de Chantemele EJ, Guihot AL, Jardel A, Toutain B, Loufrani L and Henrion D. Cyclooxygenase-2-derived prostanoids reduce inward arterial remodeling induced by blood flow reduction in old obese Zucker rat mesenteric arteries. *Vascul Pharmacol*. 2013;58:356-62.
238. Rudic RD, Brinster D, Cheng Y, Fries S, Song WL, Austin S, Coffman TM and FitzGerald GA. COX-2-derived prostacyclin modulates vascular remodeling. *Circ Res*. 2005;96:1240-7.
239. Deacon K and Knox AJ. Endothelin-1 (ET-1) increases the expression of remodeling genes in vascular smooth muscle through linked calcium and cAMP pathways: role of a phospholipase A(2)(cPLA(2))/cyclooxygenase-2 (COX-2)/prostacyclin receptor-dependent autocrine loop. *J Biol Chem*. 2010;285:25913-27.
240. LaPointe MC, Mendez M, Leung A, Tao Z and Yang XP. Inhibition of cyclooxygenase-2 improves cardiac function after myocardial infarction in the mouse. *Am J Physiol Heart Circ Physiol*. 2004;286:H1416-24.
241. Plutzky J. Peroxisome proliferator-activated receptors as therapeutic targets in inflammation. *J Am Coll Cardiol*. 2003;42:1764-6.
242. Kim T and Yang Q. Peroxisome-proliferator-activated receptors regulate redox signaling in the cardiovascular system. *World J Cardiol*. 2013;5:164-74.
243. Rimando AM, Nagmani R, Feller DR and Yokoyama W. Pterostilbene, a new agonist for the peroxisome proliferator-activated receptor alpha-isoform, lowers plasma lipoproteins and cholesterol in hypercholesterolemic hamsters. *J Agric Food Chem*. 2005;53:3403-7.
244. Inoue H, Jiang XF, Katayama T, Osada S, Umesono K and Namura S. Brain protection by resveratrol and fenofibrate against stroke requires peroxisome proliferator-activated receptor alpha in mice. *Neurosci Lett*. 2003;352:203-6.
245. Calleri E, Pochetti G, Dossou KSS, Laghezza A, Montanari R, Capelli D, Prada E, Loiodice F, Massolini G, Bernier M and Moaddel R. Resveratrol and its metabolites bind to PPARs. *Chembiochem*. 2014;15:1154-1160.
246. Jinadatta P, Rajshekarappa S, Sundera Raja Rao K, Pasura Subbaiah SG and Shastri S. In silico, in vitro: antioxidant and antihepatotoxic activity of gnetol from Gnetum ula Brongn. *Bioimpacts*. 2019;9:239-249.
247. Smeets PJ, Teunissen BE, Willemsen PH, van Nieuwenhoven FA, Brouns AE, Janssen BJ, Cleutjens JP, Staels B, van der Vusse GJ and van Bilsen M. Cardiac hypertrophy is enhanced in PPAR alpha-/- mice in response to chronic pressure overload. *Cardiovasc Res*. 2008;78:79-89.
248. Chan AY, Dolinsky VW, Soltys CL, Viollet B, Baksh S, Light PE and Dyck JR. Resveratrol inhibits cardiac hypertrophy via AMP-activated protein kinase and Akt. *The Journal of biological chemistry*. 2008.
249. Chen ZP, Mitchelhill KI, Michell BJ, Stapleton D, Rodriguez-Crespo I, Witters LA, Power DA, Ortiz de Montellano PR and Kemp BE. AMP-activated protein kinase phosphorylation of endothelial NO synthase. *FEBS Lett*. 1999;443:285-9.
250. Dolinsky VW, Chan AY, Robillard Frayne I, Light PE, Des Rosiers C and Dyck JR. Resveratrol prevents the prohypertrophic effects of oxidative stress on LKB1. *Circulation*. 2009;119:1643-52.
251. Chan AY, Dolinsky VW, Soltys CL, Viollet B, Baksh S, Light PE and Dyck JR. Resveratrol inhibits cardiac hypertrophy via AMP-activated protein kinase and Akt. *J Biol Chem*. 2008;283:24194-201.

252. Ford RJ, Teschke SR, Reid EB, Durham KK, Kroetsch JT and Rush JW. AMP-activated protein kinase activator AICAR acutely lowers blood pressure and relaxes isolated resistance arteries of hypertensive rats. *J Hypertens*. 2012;30:725-33.
253. Li H, Xia N, Hasselwander S and Daiber A. Resveratrol and Vascular Function. *Int J Mol Sci*. 2019;20.
254. El Mabrouk M, Touyz RM and Schiffrin EL. Differential ANG II-induced growth activation pathways in mesenteric artery smooth muscle cells from SHR. *American journal of physiology*. 2001;281:H30-9.
255. Fremont L. Biological effects of resveratrol. *Life sciences*. 2000;66:663-73.
256. Narayanan NK, Kunimasa K, Yamori Y, Mori M, Mori H, Nakamura K, Miller G, Manne U, Tiwari AK and Narayanan B. Antitumor activity of melinjo (Gnetum gnemon L.) seed extract in human and murine tumor models in vitro and in a colon-26 tumor-bearing mouse model in vivo. *Cancer Med*. 2015;4:1767-80.
257. Gao P, Xu TT, Lu J, Li L, Xu J, Hao DL, Chen HZ and Liu DP. Overexpression of SIRT1 in vascular smooth muscle cells attenuates angiotensin II-induced vascular remodeling and hypertension in mice. *J Mol Med (Berl)*. 2014;92:347-57.
258. Li L, Gao P, Zhang H, Chen H, Zheng W, Lv X, Xu T, Wei Y, Liu D and Liang C. SIRT1 inhibits angiotensin II-induced vascular smooth muscle cell hypertrophy. *Acta Biochim Biophys Sin (Shanghai)*. 2011;43:103-9.
259. Mattagajasingh I, Kim CS, Naqvi A, Yamamori T, Hoffman TA, Jung SB, DeRicco J, Kasuno K and Irani K. SIRT1 promotes endothelium-dependent vascular relaxation by activating endothelial nitric oxide synthase. *Proc Natl Acad Sci U S A*. 2007;104:14855-60.
260. Fry JL, Al Sayah L, Weisbrod RM, Van Roy I, Weng X, Cohen RA, Bachschmid MM and Seta F. Vascular Smooth Muscle Sirtuin-1 Protects Against Diet-Induced Aortic Stiffness. *Hypertension*. 2016;68:775-84.
261. Tang Y, Xu J, Qu W, Peng X, Xin P, Yang X, Ying C, Sun X and Hao L. Resveratrol reduces vascular cell senescence through attenuation of oxidative stress by SIRT1/NADPH oxidase-dependent mechanisms. *J Nutr Biochem*. 2012;23:1410-6.
262. Touyz RM and Schiffrin EL. Reactive oxygen species in vascular biology: implications in hypertension. *Histochem Cell Biol*. 2004;122:339-52.
263. Park JB, Touyz RM and Schiffrin EL. F012: Antioxidant treatment reverses vascular remodeling, but not myogenic tone in mesenteric resistance arteries of stroke-prone spontaneously hypertensive rats (SHRSP). *American Journal of Hypertension*. 2000;13:243A-244A.
264. Lee B and Moon SK. Resveratrol inhibits TNF-alpha-induced proliferation and matrix metalloproteinase expression in human vascular smooth muscle cells. *J Nutr*. 2005;135:2767-73.
265. Ferrero ME, Bertelli AE, Fulgenzi A, Pellegatta F, Corsi MM, Bonfrate M, Ferrara F, De Caterina R, Giovannini L and Bertelli A. Activity in vitro of resveratrol on granulocyte and monocyte adhesion to endothelium. *Am J Clin Nutr*. 1998;68:1208-14.
266. Cullen JP, Morrow D, Jin Y, von Offenberg Sweeney N, Sitzmann JV, Cahill PA and Redmond EM. Resveratrol inhibits expression and binding activity of the monocyte chemotactic protein-1 receptor, CCR2, on THP-1 monocytes. *Atherosclerosis*. 2007;195:e125-33.
267. Wang HZ, L.; Wang, L.; Zhou, Q.; Wang, H.; Hou, Y.; Ma, Y. Pterostilbene suppresses vascular adhesion molecule expression in TNF-α-stimulated vascular muscle cells. *Int J Clin Exp Pathol*. 2016;9:1432-1438.

268. Akiguchi I, Pallas M, Budka H, Akiyama H, Ueno M, Han J, Yagi H, Nishikawa T, Chiba Y, Sugiyama H, Takahashi R, Unno K, Higuchi K and Hosokawa M. SAMP8 mice as a neuropathological model of accelerated brain aging and dementia: Toshio Takeda's legacy and future directions. *Neuropathology*. 2017;37:293-305.
269. Chang J, Rimando A, Pallas M, Camins A, Porquet D, Reeves J, Shukitt-Hale B, Smith MA, Joseph JA and Casadesus G. Low-dose pterostilbene, but not resveratrol, is a potent neuromodulator in aging and Alzheimer's disease. *Neurobiol Aging*. 2012;33:2062-71.
270. Danz ED, Skramsted J, Henry N, Bennett JA and Keller RS. Resveratrol prevents doxorubicin cardiotoxicity through mitochondrial stabilization and the Sirt1 pathway. *Free Radic Biol Med*. 2009;46:1589-97.
271. Hori YS, Kuno A, Hosoda R and Horio Y. Regulation of FOXOs and p53 by SIRT1 modulators under oxidative stress. *PLoS One*. 2013;8:e73875.
272. Cai YZ, Mei S, Jie X, Luo Q and Corke H. Structure-radical scavenging activity relationships of phenolic compounds from traditional Chinese medicinal plants. *Life Sci*. 2006;78:2872-88.
273. Cai YJ, Wei QY, Fang JG, Yang L, Liu ZL, Wyche JH and Han Z. The 3,4-dihydroxyl groups are important for trans-resveratrol analogs to exhibit enhanced antioxidant and apoptotic activities. *Anticancer Res*. 2004;24:999-1002.
274. Murias M, Jager W, Handler N, Erker T, Horvath Z, Szekeres T, Nohl H and Gille L. Antioxidant, prooxidant and cytotoxic activity of hydroxylated resveratrol analogues: structure-activity relationship. *Biochem Pharmacol*. 2005;69:903-12.
275. Cai YJ, Fang JG, Ma LP, Yang L and Liu ZL. Inhibition of free radical-induced peroxidation of rat liver microsomes by resveratrol and its analogues. *Biochim Biophys Acta*. 2003;1637:31-8.
276. Zuo AR, Dong HH, Yu YY, Shu QL, Zheng LX, Yu XY and Cao SW. The antityrosinase and antioxidant activities of flavonoids dominated by the number and location of phenolic hydroxyl groups. *Chin Med*. 2018;13:51.
277. O'Donnell MJ, Xavier D, Liu L, Zhang H, Chin SL, Rao-Melacini P, Rangarajan S, Islam S, Pais P, McQueen MJ, Mondo C, Damasceno A, Lopez-Jaramillo P, Hankey GJ, Dans AL, Yusoff K, Truelsen T, Diener HC, Sacco RL, Ryglewicz D, Czlonkowska A, Weimar C, Wang X and Yusuf S. Risk factors for ischaemic and intracerebral haemorrhagic stroke in 22 countries (the INTERSTROKE study): a case-control study. *Lancet*. 2010;376:112-23.
278. Dahlof B. Prevention of stroke in patients with hypertension. *Am J Cardiol*. 2007;100:17J-24J.
279. Lee RM, Owens GK, Scott-Burden T, Head RJ, Mulvany MJ and Schiffrin EL. Pathophysiology of smooth muscle in hypertension. *Canadian journal of physiology and pharmacology*. 1995;73:574-84.
280. Allen SP, Wade SS and Prewitt RL. Myogenic tone attenuates pressure-induced gene expression in isolated small arteries. *Hypertension*. 1997;30:203-8.
281. Li J, Kemp BA, Howell NL, Massey J, Minczuk K, Huang Q, Chordia MD, Roy RJ, Patrie JT, Davogustto GE, Kramer CM, Epstein FH, Carey RM, Taegtmeyer H, Keller SR and Kundu BK. Metabolic Changes in Spontaneously Hypertensive Rat Hearts Precede Cardiac Dysfunction and Left Ventricular Hypertrophy. *J Am Heart Assoc*. 2019;8:e010926.
282. Pires PW, Dams Ramos CM, Matin N and Dorrance AM. The effects of hypertension on the cerebral circulation. *Am J Physiol Heart Circ Physiol*. 2013;304:H1598-614.

283. Henning EC, Warach S and Spatz M. Hypertension-induced vascular remodeling contributes to reduced cerebral perfusion and the development of spontaneous stroke in aged SHRSP rats. *J Cereb Blood Flow Metab*. 2010;30:827-36.
284. Galis ZS and Khatri JJ. Matrix metalloproteinases in vascular remodeling and atherogenesis: the good, the bad, and the ugly. *Circ Res*. 2002;90:251-62.
285. Avolio A. Arterial Stiffness. *Pulse (Basel)*. 2013;1:14-28.
286. Onal IK, Altun B, Onal ED, Kirkpantur A, Gul Oz S and Turgan C. Serum levels of MMP-9 and TIMP-1 in primary hypertension and effect of antihypertensive treatment. *Eur J Intern Med*. 2009;20:369-72.
287. Friese RS, Rao F, Khandrika S, Thomas B, Ziegler MG, Schmid-Schonbein GW and O'Connor DT. Matrix metalloproteinases: discrete elevations in essential hypertension and hypertensive end-stage renal disease. *Clin Exp Hypertens*. 2009;31:521-33.
288. Tan J, Hua Q, Xing X, Wen J, Liu R and Yang Z. Impact of the metalloproteinase-9/tissue inhibitor of metalloproteinase-1 system on large arterial stiffness in patients with essential hypertension. *Hypertens Res*. 2007;30:959-63.
289. Rajzer M, Wojciechowska W, Kameczura T, Olszanecka A, Fedak D, Terlecki M, Kawecka-Jaszcz K and Czarnecka D. The effect of antihypertensive treatment on arterial stiffness and serum concentration of selected matrix metalloproteinases. *Arch Med Sci*. 2017;13:760-770.
290. Tayebjee MH, Nadar SK, MacFadyen RJ and Lip GY. Tissue inhibitor of metalloproteinase-1 and matrix metalloproteinase-9 levels in patients with hypertension Relationship to tissue Doppler indices of diastolic relaxation. *Am J Hypertens*. 2004;17:770-4.
291. Li H, Simon H, Bocan TM and Peterson JT. MMP/TIMP expression in spontaneously hypertensive heart failure rats: the effect of ACE- and MMP-inhibition. *Cardiovasc Res*. 2000;46:298-306.
292. Myers PR and Tanner MA. Vascular endothelial cell regulation of extracellular matrix collagen: role of nitric oxide. *Arterioscler Thromb Vasc Biol*. 1998;18:717-22.
293. Fleenor BS, Marshall KD, Rippe C and Seals DR. Replicative aging induces endothelial to mesenchymal transition in human aortic endothelial cells: potential role of inflammation. *J Vasc Res*. 2012;49:59-64.
294. An SJ, Boyd R, Wang Y, Qiu X and Wang HD. Endothelin-1 expression in vascular adventitial fibroblasts. *Am J Physiol Heart Circ Physiol*. 2006;290:H700-8.
295. An SJ, Boyd R, Zhu M, Chapman A, Pimentel DR and Wang HD. NADPH oxidase mediates angiotensin II-induced endothelin-1 expression in vascular adventitial fibroblasts. *Cardiovasc Res*. 2007;75:702-9.
296. Yue J, Zhang K and Chen J. Role of integrins in regulating proteases to mediate extracellular matrix remodeling. *Cancer Microenviron*. 2012;5:275-83.
297. Fogerty FJ, Akiyama SK, Yamada KM and Mosher DF. Inhibition of binding of fibronectin to matrix assembly sites by anti-integrin (alpha 5 beta 1) antibodies. *J Cell Biol*. 1990;111:699-708.
298. Bezie Y, Lamaziere JM, Laurent S, Challande P, Cunha RS, Bonnet J and Lacolley P. Fibronectin expression and aortic wall elastic modulus in spontaneously hypertensive rats. *Arterioscler Thromb Vasc Biol*. 1998;18:1027-34.
299. Bezie Y, Lacolley P, Laurent S and Gabella G. Connection of smooth muscle cells to elastic lamellae in aorta of spontaneously hypertensive rats. *Hypertension*. 1998;32:166-9.

300. Meng W, Tobin JR and Busija DW. Glutamate-induced cerebral vasodilation is mediated by nitric oxide through N-methyl-D-aspartate receptors. *Stroke*. 1995;26:857-62; discussion 863.
301. Knowles RG, Palacios M, Palmer RM and Moncada S. Formation of nitric oxide from L-arginine in the central nervous system: a transduction mechanism for stimulation of the soluble guanylate cyclase. *Proc Natl Acad Sci U S A*. 1989;86:5159-62.
302. Southam E, East SJ and Garthwaite J. Excitatory amino acid receptors coupled to the nitric oxide/cyclic GMP pathway in rat cerebellum during development. *J Neurochem*. 1991;56:2072-81.
303. LeMaistre JL, Sanders SA, Stobart MJ, Lu L, Knox JD, Anderson HD and Anderson CM. Coactivation of NMDA receptors by glutamate and D-serine induces dilation of isolated middle cerebral arteries. *J Cereb Blood Flow Metab*. 2011;32:537-47.
304. Qureshi I, Chen H, Brown AT, Fitzgerald R, Zhang X, Breckenridge J, Kazi R, Crocker AJ, Stuhlinger MC, Lin K, Cooke JP, Eidt JF and Moursi MM. Homocysteine-induced vascular dysregulation is mediated by the NMDA receptor. *Vasc Med*. 2005;10:215-23.
305. Shah RC, Sanker S, Wood KC, Durgin BG and Straub AC. Redox regulation of soluble guanylyl cyclase. *Nitric Oxide*. 2018;76:97-104.
306. Priviero FB, Zemse SM, Teixeira CE and Webb RC. Oxidative stress impairs vasorelaxation induced by the soluble guanylyl cyclase activator BAY 41-2272 in spontaneously hypertensive rats. *Am J Hypertens*. 2009;22:493-9.
307. Ruetten H, Zabel U, Linz W and Schmidt HH. Downregulation of soluble guanylyl cyclase in young and aging spontaneously hypertensive rats. *Circ Res*. 1999;85:534-41.
308. Gillard SE, Tzaferis J, Tsui HC and Kingston AE. Expression of metabotropic glutamate receptors in rat meningeal and brain microvasculature and choroid plexus. *J Comp Neurol*. 2003;461:317-32.
309. Liu X, Li C, Gebremedhin D, Hwang SH, Hammock BD, Falck JR, Roman RJ, Harder DR and Koehler RC. Epoxyeicosatrienoic acid-dependent cerebral vasodilation evoked by metabotropic glutamate receptor activation in vivo. *Am J Physiol Heart Circ Physiol*. 2011;301:H373-81.
310. Ohata H, Cao S and Koehler RC. Contribution of adenosine A2A and A2B receptors and heme oxygenase to AMPA-induced dilation of pial arterioles in rats. *Am J Physiol Regul Integr Comp Physiol*. 2006;291:R728-35.
311. Andras IE, Deli MA, Veszelka S, Hayashi K, Hennig B and Toborek M. The NMDA and AMPA/KA receptors are involved in glutamate-induced alterations of occludin expression and phosphorylation in brain endothelial cells. *J Cereb Blood Flow Metab*. 2007;27:1431-43.
312. Bernatova I. Endothelial dysfunction in experimental models of arterial hypertension: cause or consequence? *Biomed Res Int*. 2014;2014:598271.
313. Ghosh D, Syed AU, Prada MP, Nystoriak MA, Santana LF, Nieves-Cintron M and Navedo MF. Calcium Channels in Vascular Smooth Muscle. *Adv Pharmacol*. 2017;78:49-87.
314. RA K. Protein Kinase C. *Regulation of Vascular Smooth Muscle Function*. 2010.
315. Brozovich FV, Nicholson CJ, Degen CV, Gao YZ, Aggarwal M and Morgan KG. Mechanisms of Vascular Smooth Muscle Contraction and the Basis for Pharmacologic Treatment of Smooth Muscle Disorders. *Pharmacol Rev*. 2016;68:476-532.
316. Hutcheson IR, Chaytor AT, Evans WH and Griffith TM. Nitric oxide-independent relaxations to acetylcholine and A23187 involve different routes of heterocellular communication. Role of Gap junctions and phospholipase A2. *Circ Res*. 1999;84:53-63.

317. Fukushima S and Ohhashi T. Acetylcholine-induced endothelium-independent relaxations in monkey isolated superior and inferior caval veins. *Br J Pharmacol*. 1993;109:992-7.
318. Knight DR, Shen YT, Young MA and Vatner SF. Acetylcholine-induced coronary vasoconstriction and vasodilation in tranquilized baboons. *Circ Res*. 1991;69:706-13.
319. Armstead WM, Zuckerman SL, Shibata M, Parfenova H and Leffler CW. Different pial arteriolar responses to acetylcholine in the newborn and juvenile pig. *J Cereb Blood Flow Metab*. 1994;14:1088-95.
320. Armstead WM, Mirro R, Leffler CW and Busija DW. Acetylcholine produces cerebrovascular constriction through activation of muscarinic-1 receptors in the newborn pig. *J Pharmacol Exp Ther*. 1988;247:926-33.
321. Li J and Bukoski RD. Endothelium-dependent relaxation of hypertensive resistance arteries is not impaired under all conditions. *Circ Res*. 1993;72:290-6.
322. Jameson M, Dai FX, Luscher T, Skopec J, Diederich A and Diederich D. Endothelium-derived contracting factors in resistance arteries of young spontaneously hypertensive rats before development of overt hypertension. *Hypertension*. 1993;21:280-8.
323. Sunano S, Watanabe H, Tanaka S, Sekiguchi F and Shimamura K. Endothelium-derived relaxing, contracting and hyperpolarizing factors of mesenteric arteries of hypertensive and normotensive rats. *Br J Pharmacol*. 1999;126:709-16.
324. Diederich D, Yang ZH, Buhler FR and Luscher TF. Impaired endothelium-dependent relaxations in hypertensive resistance arteries involve cyclooxygenase pathway. *Am J Physiol*. 1990;258:H445-51.
325. Gattu M, Terry AV, Jr., Pauly JR and Buccafusco JJ. Cognitive impairment in spontaneously hypertensive rats: role of central nicotinic receptors. Part II. *Brain Res*. 1997;771:104-14.
326. Gattu M, Pauly JR, Boss KL, Summers JB and Buccafusco JJ. Cognitive impairment in spontaneously hypertensive rats: role of central nicotinic receptors. I. *Brain Res*. 1997;771:89-103.
327. Pepeu G. Mild cognitive impairment: animal models. *Dialogues Clin Neurosci*. 2004;6:369-77.
328. Wyss JM, Fisk G and van Groen T. Impaired learning and memory in mature spontaneously hypertensive rats. *Brain Res*. 1992;592:135-40.
329. Wyss JM, Chambless BD, Kadish I and van Groen T. Age-related decline in water maze learning and memory in rats: strain differences. *Neurobiol Aging*. 2000;21:671-81.
330. Krause M, Yang Z, Rao G, Houston FP and Barnes CA. Altered dendritic integration in hippocampal granule cells of spatial learning-impaired aged rats. *J Neurophysiol*. 2008;99:2769-78.
331. Menard C and Quirion R. Successful cognitive aging in rats: a role for mGluR5 glutamate receptors, homer 1 proteins and downstream signaling pathways. *PLoS One*. 2012;7:e28666.
332. Rapp PR, Stack EC and Gallagher M. Morphometric studies of the aged hippocampus: I. Volumetric analysis in behaviorally characterized rats. *J Comp Neurol*. 1999;403:459-70.
333. Driscoll I, Hamilton DA, Petropoulos H, Yeo RA, Brooks WM, Baumgartner RN and Sutherland RJ. The aging hippocampus: cognitive, biochemical and structural findings. *Cereb Cortex*. 2003;13:1344-51.

334. Tajima A, Hans FJ, Livingstone D, Wei L, Finnegan W, DeMaro J and Fenstermacher J. Smaller local brain volumes and cerebral atrophy in spontaneously hypertensive rats. *Hypertension*. 1993;21:105-11.
335. Sabbatini M, Catalani A, Consoli C, Marletta N, Tomassoni D and Avola R. The hippocampus in spontaneously hypertensive rats: an animal model of vascular dementia? *Mech Ageing Dev*. 2002;123:547-59.
336. Moulana M, Hosick K, Stanford J, Zhang H, Roman RJ and Reckelhoff JF. Sex differences in blood pressure control in SHR: lack of a role for EETs. *Physiol Rep*. 2014;2.
337. Michel MC, Brunner HR, Foster C and Huo Y. Angiotensin II type 1 receptor antagonists in animal models of vascular, cardiac, metabolic and renal disease. *Pharmacol Ther*. 2016;164:1-81.
338. de PRSF, dos Santos RA, Silva-Antonialli MM, Scavone C, Nigro D, Carvalho MH, de Cassia Tostes R and Fortes ZB. Differential effect of losartan in female and male spontaneously hypertensive rats. *Life Sci*. 2006;78:2280-5.
339. Carraway JW, Park S, McCune SA, Holycross BJ and Radin MJ. Comparison of irbesartan with captopril effects on cardiac hypertrophy and gene expression in heart failure-prone male SHHF/Mcc-fa(cp) rats. *J Cardiovasc Pharmacol*. 1999;33:451-60.
340. Sharkey LC, Holycross BJ, McCune SA and Radin MJ. Obese female SHHF/Mcc-fa(cp) rats resist antihypertensive effects of renin-angiotensin system inhibition. *Clin Exp Hypertens*. 2001;23:227-39.
341. Sharkey LC, Radin MJ, Heller L, Rogers LK, Tobias A, Matise I, Wang Q, Apple FS and McCune SA. Differential cardiotoxicity in response to chronic doxorubicin treatment in male spontaneous hypertension-heart failure (SHHF), spontaneously hypertensive (SHR), and Wistar Kyoto (WKY) rats. *Toxicol Appl Pharmacol*. 2013;273:47-57.
342. Shannahan JH, Schladweiler MC, Richards JH, Ledbetter AD, Ghio AJ and Kodavanti UP. Pulmonary oxidative stress, inflammation, and dysregulated iron homeostasis in rat models of cardiovascular disease. *J Toxicol Environ Health A*. 2010;73:641-56.
343. Khadour FH, Kao RH, Park S, Armstrong PW, Holycross BJ and Schulz R. Age-dependent augmentation of cardiac endothelial NOS in a genetic rat model of heart failure. *Am J Physiol*. 1997;273:H1223-30.
344. Holycross BJ, Summers BM, Dunn RB and McCune SA. Plasma renin activity in heart failure-prone SHHF/Mcc-facp rats. *Am J Physiol*. 1997;273:H228-33.
345. Iadecola C, Yang G, Ebner TJ and Chen G. Local and propagated vascular responses evoked by focal synaptic activity in cerebellar cortex. *J Neurophysiol*. 1997;78:651-9.
346. Nielsen MS, Axelsen LN, Sorgen PL, Verma V, Delmar M and Holstein-Rathlou NH. Gap junctions. *Comprehensive Physiology*. 2012;2:1981-2035.
347. de Wit C, Roos F, Bolz SS, Kirchhoff S, Kruger O, Willecke K and Pohl U. Impaired conduction of vasodilation along arterioles in connexin40-deficient mice. *Circulation research*. 2000;86:649-55.
348. Jobs A, Schmidt K, Schmidt VJ, Lubkemeier I, van Veen TA, Kurtz A, Willecke K and de Wit C. Defective Cx40 maintains Cx37 expression but intact Cx40 is crucial for conducted dilations irrespective of hypertension. *Hypertension*. 2012;60:1422-9.
349. Goto K, Rummery NM, Grayson TH and Hill CE. Attenuation of conducted vasodilatation in rat mesenteric arteries during hypertension: role of inwardly rectifying potassium channels. *The Journal of physiology*. 2004;561:215-31.

350. Gauthier SA, Sahoo S, Jung SS and Levy E. Murine cerebrovascular cells as a cell culture model for cerebral amyloid angiopathy: isolation of smooth muscle and endothelial cells from mouse brain. *Methods Mol Biol*. 2012;849:261-74.
351. Jung SS and Levy E. Murine cerebrovascular cells as a cell culture model for cerebral amyloid angiopathy: isolation of smooth muscle and endothelial cells from mouse brain. *Methods Mol Biol*. 2005;299:211-9.
352. Anderson HD, Wang F and Gardner DG. Role of the epidermal growth factor receptor in signaling strain-dependent activation of the brain natriuretic peptide gene. *The Journal of biological chemistry*. 2004;279:9287-97.
353. Boutouyrie P, Laurent S, Benetos A, Girerd XJ, Hoeks AP and Safar ME. Opposing effects of ageing on distal and proximal large arteries in hypertensives. *J Hypertens Suppl*. 1992;10:S87-91.
354. Kim KJ and Filosa JA. Advanced in vitro approach to study neurovascular coupling mechanisms in the brain microcirculation. *J Physiol*. 2012;590:1757-70.